Centre for Interdisciplinary Research on Micro-Nano Methods

ACTIVITY REPORT

April 2021 - March 2022

Takuji Takahashi
Professor & Director
Centre for Interdisciplinary Research on Micro-Nano Methods
IIS University of Tokyo

ACTIVITY REPORT

CONTENT

Center for Interdisciplinary Research on Micro-nano Methods (CIRMM) 3

1-1 What is CIRMM — 1-2 History of CIRMM

1-3 History of NAMIS — 1-4 Research Areas

1-5 Missions of Each Organization in CIRMM

1-6 CIRMM Offices and Oversea Laboratory

1-7 CIRMM Network — 1-8 Members

Activity Highlight (April 2020 - March 2022).. 18

Takahashi Laboratory.. 26

Toshiyoshi Laboratory... 36

Kawakatsu Laboratory 46

Kim Laboratory.. 54

Takamiya Laboratory 64

Mizoguchi Laboratory... 74

Nomura Laboratory... 84

Tixier-Mita Laboratory.. 97

Centre for Interdisciplinary Research on Micro-Nano Methods (CIRMM)

1-1. What is CIRMM

The CIRMM was established in 2000 to facilitate international collaboration on micromechatronics research, which is the study of micro miniature systems composed of mechanical, electrical, optical and bio/chemical devices. The prospect is to obtain high-performance multi-functional devices using heterogeneous integrated process over scale and materials. The first phase of CIRMM (April 2000 – March 2010) finished successfully. The second phase started for a 6-year mandate in April 2010 and come to an end in March 2016. The third phase has started in April 2016 for another 5 years. The name of the center becomes Centre for Interdisciplinary Research on Micronano Methods. Professors conducting biomedical MEMS research in CIRMM created a new center, named "Center for International Research on Integrative Biomedical Systems (CIBiS)" jointly with other professors working on bioengineering on April 1, 2015. Those two centers share the same technological base, i.e. MEMS, and will work together to continue the international activities of CIRMM.

The international activities of CIRMM date back to 1995 with the creation of Laboratory for Integrated Micro-Mechatronic Systems (LIMMS); the joint research laboratory between Institute of Industrial Science(IIS) in the University of Tokyo and Institut des sciences de l'ingènierie et des systèmes (INSIS) in Centre National de la Recherche Scientifique (CNRS). After 9 years of operation, in 2004, the LIMMS became the first Unité Mixte Internationale de Recherche (UMI 2820) of CNRS situated in Asia. International research networks on nano and micro systems (NAMIS) were organized in 2005. Using the network, LIMMS obtained an EU FP-7 project (EUJO-Limms) in 2011 to extend its activities to other European countries, namely Germany, Finland, Switzerland, and Netherlands. On July 16, 2014, SMMiL-E* laboratory, mirror site of LIMMS was founded at Centre Oscar Lambret in Lille, in North France. Bio-MEMS technology of CIRMM is applied to cancer research in SMMiL-E. IIS/UTokyo Bureau for European Collaboration (IBEC) is open in July, 2015 in Lille for both supporting the SMMiL-E project

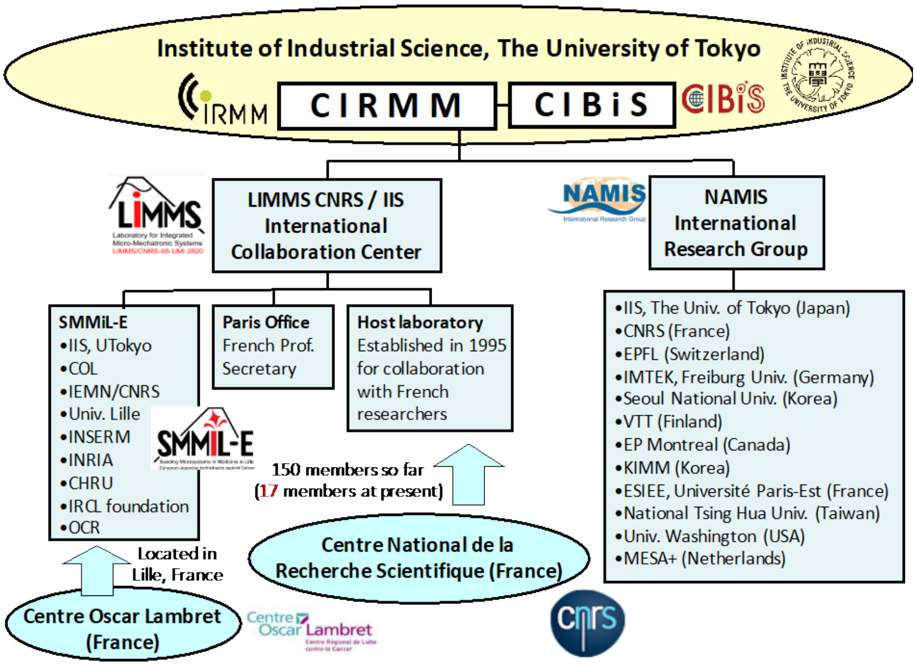

CIRMM Organization

and strengthening EU relation.

SMMiL-E stands for Seeding Microsystems in Medicine in Lille - European Japanese Technologies against Cancer; this program aims at technology transfer of state-of-the-art bioMEMS research performed in IIS/The University of Tokyo and LIMMS/CNRS-IIS towards the research against cancer conducted in Lille, France in the SIRIC ONCO-Lille program. The fusion of the BioMEMS technology and Cancer research plans to take place in a hosting platform located on the Oscar Lambret Centre site, within the hospital-university campus, in order to be in close contact with medical teams. This platform provides an experimental environment in which IIS researchers can perform joint work in France. In other word, SMMiL-E is a "mirror" structure of LIMMS to welcome researchers from Japan and to organize French/Japanese teams performing tight joint research. The program also includes IEMN/CNRS and Lille-1 University. Currently, there are experimental/office space in IRCL (Institute of Cancer Research in Lille). Laboratory for SMMiL-E will be first installed in IRCL from 2016 and then moved to a new building built by 2020 with the support from the State, Local Government, CNRS, COL, Lille University and INSERM.

In April 2016, CIRMM was renewed under a new name "Centre for Interdisciplinary Research on Micro-Nano Methods", and welcomed two new professors. The Centre named three axes of its activity, namely, "True-Nano Physics: exploitation of effects and phenomena based on nano to mesoscopic regime", "Cyber Physical Systems Implementation", and "Nano-Fabrication". As the name implies, it puts emphasis on creating new methods, in terms of detection, processing, or implementation of époque making devices. The following schematic depicts the scope of our new centre of research. In April 2021, in addition, CIRMM was renewed as an internal center of IIS, while the main mission of CIRMM has been retained.

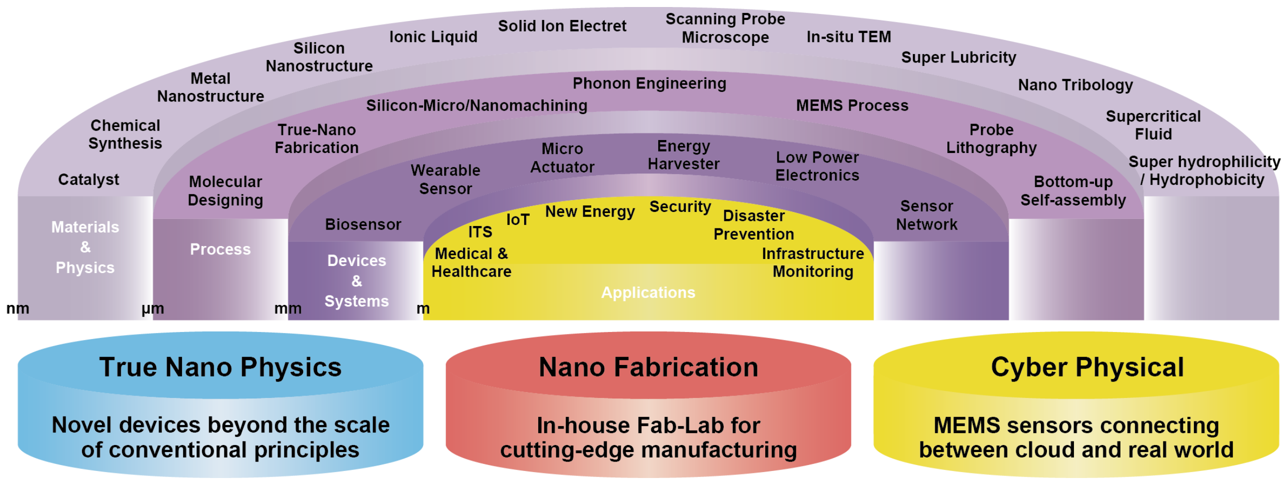

1-2. History of CIRMM

1999	CIRMM is proposed to Ministry of Education in Japan
	Preliminary discussion with CNRS/Science Pour l'Ingenieur(SPI) and positive response
Mar. 2000	Approval of the (Japanese/French) Diet
Apr. 2000	CIRMM is founded for 10-year term
Sep. 2000	CIRMM /CNRS in Paris opens in rue Capitaine Scott, LIP6/UPMC
Nov. 2000	Inauguration ceremony of CIRMM/CNRS Paris is held in CNRS/Headquarter in Paris
Oct. 2001	EPFL in Switzerland agrees to cooperate research activities with CIRMM
Mar. 2002	Twente University in the Netherlands agrees to cooperate research activities with CIRMM
Jul. 2002	Neuchatel University in Switzerland agrees to cooperate research activities with CIRMM
May 2003	KIMM in Korea agrees to cooperate research activities with CIRMM
Jul. 2003	University of Karlsruhe in Germany agrees to cooperate research activities with CIRMM
Aug. 2004	VTT Electronics and VTT Information Technology, Technical Research Center of Finland agreed to cooperate research activity with CIRMM
Apr. 2005	Seoul National University agrees to cooperate research activity with CIRMM
Nov. 2005	CIRMM contributes to establish NAMIS with CNRS, EPFL, IMTEK, SNU and VTT
Nov. 2006	National Tsing Hua University agrees to cooperate research activities with CIRMM
Jul. 2008	Initiation of Beans project founded by METI/NEDO Life-Beans Center and 3D-Beans Center are accommodated in IIS. Bio Nano Process collaboration Center was established.
Mar. 2009	CIRMM Evaluation Committee in Paris, France
Sep. 2009	CIRMM and VTT extended its Agreement of Joint Research
Apr. 2010	CIRMM is renewed for another 6 years / The official name became Center for International Research on Micronano Mechatronics
Oct. 2010	Academic Exchange Agreement signed with College of EECS in Seoul University
Dec. 2011	EU Project: EUJO-LIMMS (EUrope-Japan Opening of LIMMS) started for 4 years
Apr. 2012	Core-to-Core Program of the Japan Society for the Promotion of Science was launched by JSPS for 5 years
May 2012	EUJO-LIMMS Kick-off Meeting at IIS
Dec. 2012	JST Japanese-Taiwanese Cooperative Programme on 'Bioelectronics' started for 4 years with National Tsing Hua University: Neuron-on-CMOS-MEMS

	EUJO-LIMMS Info Day at EPFL
May 2013	LIMMS Workshop at Paris
Jun. 2013	Director General of Research & Technolgy Directorate at the European Commission, Mr. Robert Jan Smits, visited LIMMS
Sep. 2013	Workshop on Japan-Taiwan collaboration Research on Bio electronic at National TsingHuaUniversity in Hshinchu, Taiwan
Oct. 2013	EUJO LIMMS Info.Day at IMTEK in Freiburg, Germany
Dec. 2013	Workshop on Bio MEMS against Cancer at Centre Oscar Lambret in Lille, France
Jun. 2014	Inauguration Ceremony of SMMiL-E in Lille, France
	EUJO-LIMMS Workshop at VTT in Helsinki, Finland
Jul. 2014	Inauguration Symposium of CIBiS at IIS
Jan. 2015	20-year Aniversary of LIMMS at IIS
	Eujo-LIMMS Workshop at IIS
Apr. 2016	Foundation of new CIRMM (Centre for Interdisciplinary Research on Micro-Nano Methods)
Jun. 2016	Innovation show case at JST with the CNRS, LIMMS, CIBiS and the French embassy
Oct. 2016	Participation to Forum-X at the Ecole Polytechnique, Paris France
Dec. 2016	Joint Workshop of CIRMM/LIMMS/CIBiS on “International research leading to innovation and new technology bridging academics and societal demands”, at IIS
Feb. 2017	FEMO-ST Workshop “International Seminar LIMMS and FEMTO-ST and Partners”, Besancon France
Mar. 2019	LIMMS-Next PV Joint Energy Workshop at IIS
Nov. 2019	2019 NAMIS Marathon Workshop, Hsinchu, Taiwan
Nov. 2020	2020 NAMIS Marathon Workshop, Hybrid (Online and Hsinchu, Taiwan)
Apr. 2021	Renewal of CIRMM as Internal Center of IIS
Dec. 2021	2021 NAMIS Marathon Workshop, Hybrid (Online and Hsinchu, Taiwan)

1-3. History of NAMIS

Nov. 2005	CIRMM contributes to establish NAMIS with CNRS, EPFL, IMTEK, SNU and VTT
May 2006	The 1st NAMIS Workshop in IEF, Orsay and IEMN, Lille, France
Nov. 2006	The 2nd NAMIS Workshop in EPFL, Laudanne, Switzerland
Jun. 2007	The 3rd NAMIS Workshop in VTT, Oulu, Finland
Oct. 2007	International MEMS school for NAMIS students at IIS

Nov. 2007	The 4th NAMIS Workshop in Seoul, Korea
Apr. 2008	The 5th NAMIS Workshop in Freiburg, Germany
Sep. 2008	NAMIS International Autumn School 2008 at IIS, Tokyo The 6th NAMIS Workshop in Shonan Village, Japan University of Paris South and Tohoku University joined NAMIS as associated partners
Jun. 2009	The 7th NAMIS Workshop in Montreal, Canada.
Sep. 2009	NAMIS International Autumn School 2009 at Toulouse, France
Jun. 2010	The 7th NAMIS Workshop in Hsinchu Taiwan. University of Washington, Seattle, USA joined the network.
Oct. 2010	NAMIS International Autumn School 2010 at IIS, UTokyo, Japan
Jun. 2011	The 9th NAMIS Workshop in Paris, France
Sep. 2011	NAMIS International Autumn School 2011 at Neuchâtel – Arc-et-Senans - Besançon
May 2012	The 10th NAMIS Workshop at Sendai
Sep. 2012	NAMIS International Autumn School 2012 at IIS, UTokyo, Japan
Jul. 2013	The 11th NAMIS Workshop in Seattle
Sep. 2013	NAMIS International Autumn School 2013 in Seoul, Korea
Jun. 2014	The 12th NAMIS Workshop in Vietnum
Sep. 2014	NAMIS International Autumn School 2014 at National TsingHua University in Hshinchu, Taiwan
Jun. 2015	NAMIS International Autumn School 2015 in Montréal, Canada
Sep. 2015	The 13th NAMIS Workshop in Wroclaw University of Technology, Poland
Jul. 2016	The 14th NAMIS Workshop in University of Twente, The Netherlands
Sep. 2016	NAMIS International Autumn School 2016 in IIS, UTokyo, Japan
Jun. 2017	The 15th NAMIS Workshop in Daejeon, Korea
Oct. 2017	NAMIS International Autumn School 2017 in Freiburg, Germany
Jun. 2018	The 16th NAMIS Workshop in VTT-Oulu, Finland
Sep. 2018	NAMIS International Autumn School 2018 in University of Washington, Seattle, USA
Nov. 2019	2019 NAMIS Marathon Workshop, Hsinchu, Taiwan
Jan. 2020	Seoul National Univ.(SNU) / IIS, The Univ. of Tokyo Joint Workshop on Innovative Micro/Nano systems, Seoul, Korea
Nov. 2020	2020 NAMIS Marathon Workshop, Hybrid (Online and Hsinchu, Taiwan)
Dec. 2021	2021 NAMIS Marathon Workshop, Hybrid (Online and Hsinchu, Taiwan)

1-4. Research Areas

- Micro/nano 3D fabrication technologies based on silicon process, precision, mechanical machining, printing, bonding, bio coating, soft lithography and self-assembly.
- Basic components such as micro actuators, micro fluidics, mirrors/gratings and nano structures.
- Fundamantals and application of various Microscopy
- Integration and packaging technologies; evaluation methods
- Applications especially in bio/medical systems, optics, wireless communication, IoT (internet of things) and nano technologies.
- Technology transfer to industry

1-5. Missions of Each Organization in CIRMM

- ❑ CIRMM for global networking activities in Micro- and Nano-systems
  - Stimulate exchanges by workshops, meetings, visits
  - Establish joint research projects between Japanese university network and foreign Universities/Laboratories.
- ❑ LIMMS (Laboratory for Integrated Micromechatronic Systems)
  - Accept CNRS related French researchers in IIS
  - Perform state-of-the art research on MEMS and applications.
  - EUJO-LIMMS (2011-2015): Extention to 4 European partners
  - SMMiL-E (2014-): Bio MEMS installation in Cancer Hospital in France
- ❑ NAMIS (International Research Group on Nano and Microsystems)
  - Stimulate research exchanges of twelve organizations:
    CNRS (France), EPFL (Switzerland), SNU (Korea), VTT (Finland), IMTEK (Germany), IIS (Japan), EPM (Canada), KIMM (Korea), UPE (France), NTHU (Taiwan), UW (USA), MESA+ (the Netherlands)
- ❑ IBEC (IIS/UTokyo Bureau for European Collaboration)
  - Management of research projects in SMMIL-E and the support for IIS researchers visiting Lille.Technology transfer to clinical applications
  - Networking with EU committees and with EU researchers
  - Partial support of LIMMS administration in terms of CNRS related operation

1-6. CIRMM Offices and Oversea Laboratory

Tokyo Office

Address: 4-6-1 Komaba, Meguro-ku, Tokyo, 153-8505, Japan

The University of Tokyo, Institute of Industrial Science

Phone +81-3-5452-6248 at Prof. Fujita / Fax +81-3-3402-5078 (IIS main)

IIS/UTokyo Bureau for European Collaboration (IBEC)

Address: CNRS Délégation Nord Pas de Calais et Picardie, 2 rue des Canonniers CS60009, 59046 LILLE CEDEX, France

Phone: + 33 3 20 12 28 16

SMMiL-E Laboratory

Address: IRCL, Place de Verdun, 59000 Lille, France

(IRCL: Institut pour la Recherche sur le Cancer de Lille)

1-7. CIRMM Network

CIRMM's micromechatronics (MEMS) research network in Europe, Asia, US/Canada and in Japan.

Centre de la National Recherche Scientifique (CNRS) — France

http://www.cnrs.fr/

Ecole Polytechnique Federal de Lausanne (EPFL) — Switzerland

http://www.epfl.ch/

University Paris Est (UPE) — France

http://www.univ-paris-est.fr/fr/

VTT Technical Research Centre of Finland Ltd. — Finland

http://www.hydromod.de/loleif/Participants/VTT/vtt.html

Department of Microsystem Engineering, University of Freiburg (IMTEK) — Germany

http://www.imtek.mml/material

Inter-University Semiconductor Research Center (ISRC) — South Korea

http://isrc.snu.ac.kr/

Seoul National University (SNU) — South Korea

http://www.useoul.edu/

Korea Institute of Machinery and Materials (KIMM) — South Korea http://www.kimm.re.kr/main.php

Polytechnique of Montreal Canada

http://www.umontreal.ca/

National Tsing Hua University (NTHU) Republic of China (Taiwan)

http://www.nthu.edu.tw/english/index.php

Tohoku University (TU) Japan

http://www.tohoku.ac.jp

University of Washington (UW) USA

http://www.washington.edu/

MESA+, Twente University the Netherlands

http:// http://www.utwente.nl/mesaplus/

Centre Oscar Lambret (COL) France

http://www. centreoscarlambret.fr/

Other Related Organizations

Korea Institute of Industrial Technology South Korea

http://english.itep.re.kr/

Research Center for Advanced Science and Technology, The University of Tokyo Japan

http://www.rcast.u-tokyo.ac.jp/ja/

VLSI Design and Education Center (VDEC), The University of Tokyo Japan

http://www.vdec.u-tokyo.ac.jp/English/index.html

Nanofabrication Platform, The Nanotechnology Platform Japan Program Japan

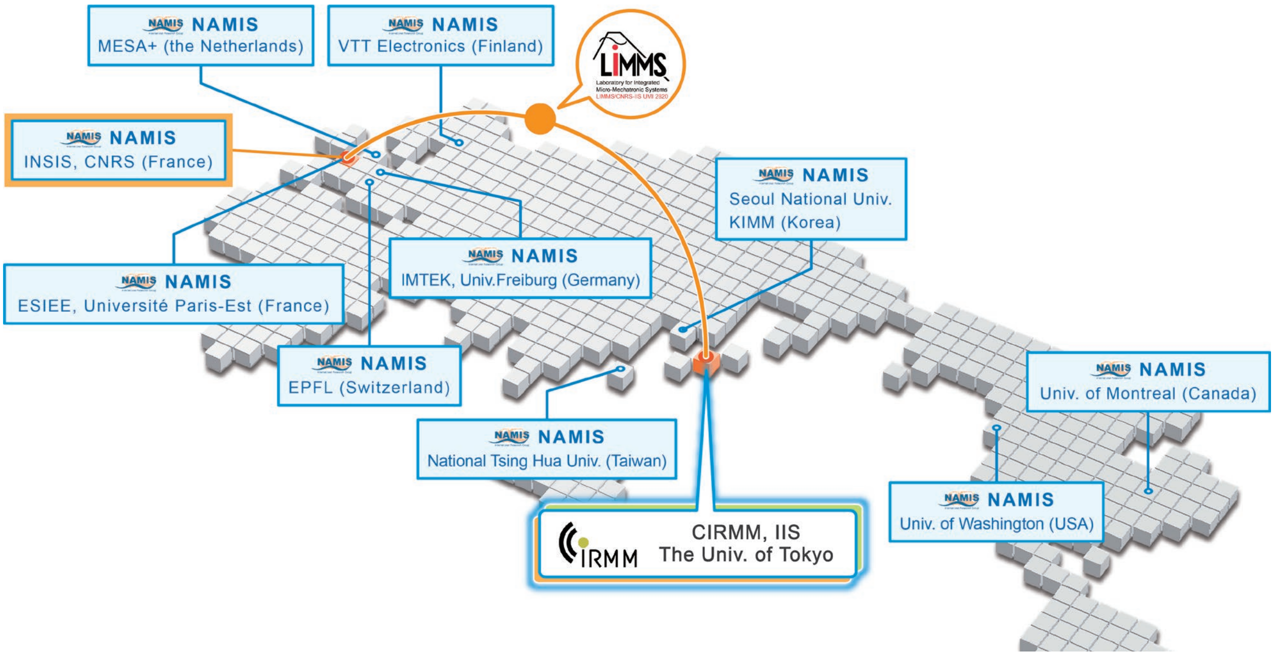

CIRMM International Network

1-8. Members

Name	Position	Research Field
TAKAHASHI, Takuji	Director and Professor	Nano-probing Technologies
TOSHIYOSHI, Hiroshi	Deputy Director and Professor	Optical MEMS & RF-MEMS
KAWAKATSU, Hideki	Professor	Coupling to the Nano Regime
KIM, Beomjoon	Professor	Micro Components & Systems
TAKAMIYA, Makoto	Professor	Integrated Power Management Circuits
MIZOGUCHI, Teruyasu	Professor	Understanding Role of Atom and Electron in Material
NOMURA, Masahiro	Associate Professor	Nanoscale Heat Transfer and Thermoelectrics
TIXIER-MITA, Agnes	Associate Professor	Bio CMOS-MEMS Platforms

-Takahashi Laboratory Members:
SHIMADA, Yuuji (Technical Support Specialist)
FUKUZAWA, Ryota (Graduate Student)
YAMADA, Ayaka (Graduate Student)
KUROIWA, Tomoe (Graduate Student)
LI, Shenwei (Graduate Student)
KOBAYASHI, Daichi (Graduate Student)
SATO, Jo (Graduate Student)
YOGI, Naomi (Assistant)

-Toshiyoshi Laboratory Members:
ATAKA, Manabu (Research Associate)
TAKAHASHI, Takuya (Technical Support Specialist)
HASHIGUCHI, Gen (Research Fellow)
SASAKI, Naruo (Research Fellow)
ONO, Shinpei (Research Fellow)
YOKOKAWA, Ryuji (Research Fellow)
KAKUSHIMA, Kuniyuki (Research Fellow)
SEKIYA, Hidehiko (Research Fellow)
ISHIDA, Tadashi (Research Fellow)
KUMEMUEA, Momoko (Research Fellow)
YAMANE, Daisuke (Research Fellow)
MITA, Makoto (Associate Research Fellow)
HIGO, Akio (Associate Research Fellow)
NAGAI, Moeto (Associate Research Fellow)
CHIU Wan-Ting (Associate Research Fellow)
YAMADA, Shunsuke (Associate Research Fellow)
HONMA, Hiroaki (Project Research Associate)
IHIDA, Satoshi (Private Sector Collaborative Researcher)
ISAMOTO, Keiji (Private Sector Collaborative Researcher)
YI, Xiao (Private Sector Collaborative Researcher)
MITSUYA, Hiroyuki (Private Sector Collaborative Researcher)
ODA, Yutaro(Private Sector Collaborative Researcher)
TOHYAMA, Yukiya (Graduate Student)
SUGAHARA, Junpei (Graduate Student)
PUTRA, Refaldi Intro Dwi (Graduate Student)
AKAI, Yuto ((Graduate Student)
HU, Xingzhuo (Graduate Student)
FAURE, Gabriel (Graduate Student)

KOIZUMI, Hiroko (Assistant)

-Kawakatsu Laboratory Members:
KOBAYASHI, Dai (Research Associate)
SHIOZAKI, Yuriko (Assistant)
KATAYAMA Ryo (Graduate Student)
ZHU Zhenyan (Research Student)

-Kim Laboratory Members:
TAKAMA, Nobuyuki (Senior Technical Support Specialist)
PARK, JongHo (Assistant Professor)
SALLES, Vincent (Visiting Research Fellow)
HWANG, Gilgueng (Visiting Research Fellow)
TAKEUCHI, Kai (Private Sector Collaborative Researcher)
KOMA, Yosuke (Private Sector Collaborative Researcher)
WU, Li-Bo (Graduate student)
LEE, Hak-Jae (Graduate student)
BAO, LeiLei (Graduate student)
WU, Xiaobin (Graduate student)
HAYAKAWA, Kiyotaka (Graduate student)
KAMAKI, Yuto (Graduate student)
NISHIDA, Kohei(Graduate student))
JING, Heyi (Graduate student)
SHOBAYASHI, Kotaro (Graduate student)
KUDO, Kota (Graduate student)
QIN, Boyu (Graduate student)
KINOSHITA Rie (Technical assistant)
OKUDAIRA, Kazuko (Assistant)
KOIZUMI, Hiroko (Assistant)

-Takamiya Laboratory Members:
HATA, Katsuhiro (Research Associate)
SAI, Toru (Research Fellow)
INUMA, Toshiaki (Project Academic Specialist)
IBARAKI, Ryotaro (Graduate Student)
WANG, Ruizhi (Graduate Student)
YAMASAKI, Hiromu (Graduate Student)
HORII, Kohei (Graduate Student)
ZHANG, Dibo (Graduate Student)

ZHANG, Haifeng (Graduate Student)
AOKI, Noel (Internship Student)
AMANO, Ayako (Assistant)

-Mizoguchi Laboratory Members:
SHIBATA, Kiyou (Assitant Professor)
FUKUDA, Atsushi (Technical staff)
XIE, Yaoshu(Postdoctral researcher)
KAWAGUCHI, Naoto (Graduate student)
HATA, Yuki (Graduate student)
CHEN, Poyen (Graduate student)
TAKAHARA, Izumi (Graduate student)
NISHIO, Kento (Graduate student)
LEE, Yebin (Graduate student)

-Nomura Laboratory Members:
ANUFRIEV, Roman (Project Associate Professor)
VOLZ, Sebastian (Visiting Research Fellow)
JALABERT, Laurent (Visiting Research Fellow)
ORDONEZ-MIRANDA, Jose (Visiting Research Fellow)
KIM, Byunggi (Project Research Associate)
WU, Yunhui (Project Researcher)
YANAGISAWA, Ryoto (Project Researcher)
ZHANG, Zhongwei (Project Researcher)
TACHIKAWA, Saeko (Graduate student)
HUANG, Xin (Graduate student)
KOIKE, Souta (Graduate student)
SHI, Hongyuan (Graduate student)
SIDO, Eldar (Graduate student)
NAWAE, Tomoki (Graduate student)
SINGH, Dhanishtha (Graduate student)
OGAWARA, Youhei (Graduate student)
AGIN, Diyar（Internship student）
TOYODA, Satoshi (Collaborative Researcher)
NAKAOKA, Toshihiro (Research Fellow)
INADA, Yuta (Associate Research Fellow)
GUO, Yangyu (Associate Research Fellow)
HARASHIMA, Junichi (Associate Research Fellow)
KINUMURA, Takashi (Associate Research Fellow）

SATO, Takaaki (Associate Research Fellow)

YAMASHITA, Yuichiro (Associate Research Fellow)

YOSHIDA, Yoshifumi (Associate Research Fellow)

OKOCHI, Erina (Assistant)

-Tixier-Mita Laboratory Members:

FAURE, Pierre-Marie (Internship Student)

EILER, Anne-Claire (PhD Student)

XU Tieying (IIS Postdoctoral Fellow)

KOIZUMI, Hiroko (Assistant)

Affiliated members:

HIRAKAWA, Kazuhiko (Professor)
The University of Tokyo, Institute of Industrial Science
Research Area: Quantum Semiconductor Electronics

SAKAI, Yasuyuki (Professor)
The University of Tokyo, Graduate School of Engineering
Research Area: Organs and Biosystems Engineering

MITA, Yoshio (Associate Professor)
The University of Tokyo, School of Engineering
Research Area: Intelligent Electron Devices by MEMS Technology

SOMEYA, Takao (Professor)
The University of Tokyo, School of Engineering
Research Area: Flexible Electronics

SUGIYAMA, Masakazu (Professor)
The University of Tokyo, Research Center for Advanced Science and Technology
Research Area: Novel Micro-nano Fabrication Processes for Next-generation MEMS, Crystal Growth of III-V Semiconductors for High-efficiency Solar Cells

HIBARA, Akihide (Professor)
Tohoku University, Institute of Multidisciplinary Research for Advanced Materials
Research Area: Nano/Micro Chemical Measurements

HANE, Kazuhiro (Professor)
Tohoku University, Department of Nanomechanics
Research Area: Optical MEMS, especially Optical Micro-sensors and Integrated Optical Systems for Telecom

HASHIGUCHI, Gen (Professor)
Shizuoka University, Research Institute of Electronics
Research Area: Micromachining, Electret-based Energy Harvester

KONISHI, Satoshi (Professor)
Ritsumeikan University
Research Area: Microelectromechanical Systems (MEMS), Microrobotics, Biomedical Engineering

NOJI, Hiroyuki (Professor)
The University of Tokyo, School of Engineering
Research Area: Single Molecular Biophysics

Activity Highlight
April 2020 - March 2022

April 1st, 2020
Institute of Electrical Engineers of Japan 2020 Excellent Presentation Award

Dr. Hiroaki Honma won the 2020 IEEJ Excellent Presentation Award for his paper "A 1.3 mW Electrostatic Vibrational Energy Harvester and Charging of Large Storage Capacitance for IoT Applications" presented at the IEEJ (Institute of Electrical Engineers of Japan) Sensor Symposium in Hamamatsu (Nov. 19 – 20, 2019). This paper also won the 2019 Igarashi Award, which is given to a researcher younger than 35 years old.

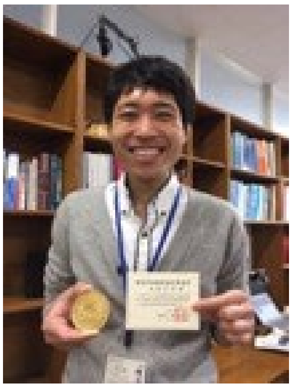

Octoboer 19th, 2020
MEMS Energy Harvester Wins the CEATEC 2020 Grand-Prix Award

The MEMS vibrational energy harvester co-developed with Saginomiya Seisakusho, Inc. and the NMEMS Technological Research Association won the Grand-Prix Award (open competition chapter) of the CEATEC 2020 Exhibition. This work has been performed as a project (JPNP16007) commissioned by the New Energy and Industrial Technology Development Organization (NEDO).

December 25st, 2020
On-line Joint Ideathon between the iCenter of Tsinghua University and UTokyo

Amid near lock-down conditions, an on-line joint Ideathon was held for a month between the iCenter of Tsinghua University and UTokyo. Some of the ideas and prototypes that came out from the meeting were, (i) parcel sterilizer with anions, (ii) computer desktop avatar to keep you smart during on-line work, (iii) smart linked footware to make your outings and walks more enjoyable. We are greatful to Professor Meng and Professor Woody for their continued support.

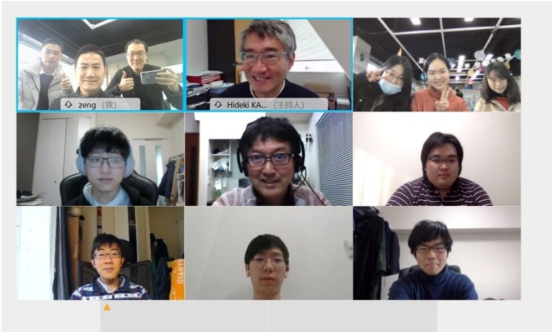

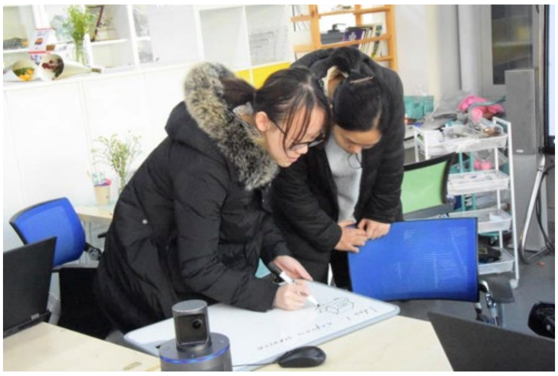

March 23rd, 24th and April 28th, 2021
Development of Microneedles patch for COVID-19 antibody detection as well as vaccination delivery

TV Ashahi "Good Morning", TV TBS"Asa-tyan", TV BS-TBS"報道1930", Development of Microneedle patch to detect COVID-19 antibodies painless from Prof. BJ Kimlab., was introduced in several Broadcasting TV news. The MEMS vibrational energy harvester co-developed with Saginomiya Seisakusho, Inc. and the NMEMS Technological Research Association won the Grand-Prix Award (open competition chapter) of the CEATEC 2020 Exhibition. This work has been performed as a project (JPNP16007) commissioned by the New Energy and Industrial Technology Development Organization (NEDO).

April 19th , 2021
The 53rd Ichimura Prize in Science for Distinguished Achievement

Prof. Hiroshi Toshiyoshi (IIS, UTokyo) and Prof. Gen Hashiguchi (Shizuoka University) won the 53rd Ichimura Prize for their recent work on MEMS vibrational energy harvester. Prof. Hiroyuki Fujita joined the award ceremony.

April 28th , 2021
An IEEJ Award for Advancement of Technology

An IEEJ (Institute of Electrical Engineers of Japan) presented an award to Prof. H. Toshiyoshi for his contribution to the advanced technology on MEMS vibrational energy harvester.

October 18th , 2021
Kyodo News, etc, Development of microneedles patch for COVID-19 detection

The research conducted by the team of Prof.BJ. Kim was introduced in Kyodo News and several news media. Small needles with a tip diameter of 50 micrometers (1/20 of 1 mm) or less and a length of 1 mm or less, called "microneedle", are lined up on a sheet of paper and processed. When this is attached to the arm, the needle extracts up "interstitial fluid" from under the skin, and when it reaches the sensor, the amount of antibody is known.

新型コロナ

自分でできる ◆ 痛みもなし

針のシートで抗体検査

実用化へ 東大で研究

November 12th , 2021
The Best paper Award on 10th. IEEE CPMT Symposium Japan 2021 (ICSJ 2021)

The best paper award was presented to Ms. Leilei Bao, who is a Ph.D. student in Prof. Beomjoon Kim's group, for her presentation on "A rapid COVID-19 diagnostic device integrating porous microneedles and the paper-based immunoassay biosensor" at the 10th. IEEE CPMT Symposium Japan (ICSJ 2021) in Kyoto Univ. Clock Tower Centennial Hall. This international conference is the leading international symposium about components, packaging and manufacturing technology. Prof. BJ Kim will be a general chair of this conference at 2022 (ICSJ2022). Moreover, Prof. Agnes Tixier -Mita gave an invited talk on the same ICSJ 2021 conference.

November 16th , 2021
New Frontiers with Corona Lectures Series - 1st - SNU-IIS/UTokyo

Between Seoul National University (SNU), Korea and Institute of Industrial Science, The University of Tokyo (IIS, UTokyo), the first online seminar through ZOOM meeting on November 16th., in 2021 was organized. This workshop was supported by Super Global SP Program of Univ. of Tokyo. 4 young professors from SNU (Dept. of mechanical Eng. and Electrical and computer Eng.) and 2 professors from IIS, gave lectures and totally 46 people including graduate students and researchers attended this one day workshop and exchanged fruitful scientific discussions.

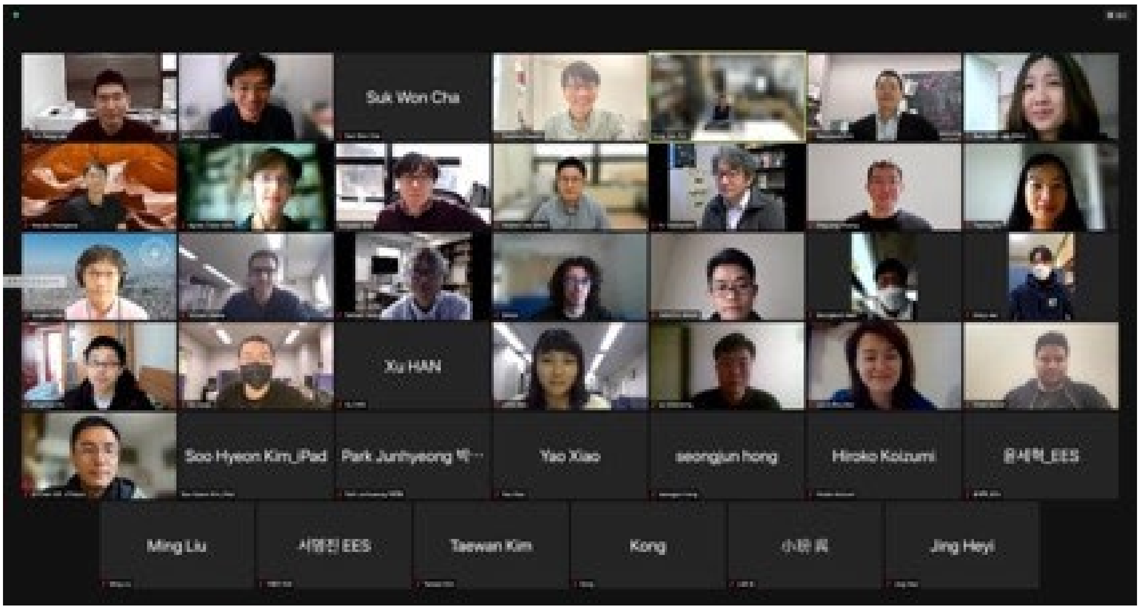

November 27th , 2021
International Event on Innovation "Hit Innovation, Hit the Future" at the iCenter Design Workshop 2021

Professor Hideki Kawakatsu gave an invited talk(on-line) at an International event on innovation "Hit Innovation, Hit the Future" held at the iCenter Design Workshop 2021, Tsinghua University, Beijing, China. The quality and scale of the workshop was overwhelming with gigantic full wall screens and organisers in panda outfits.

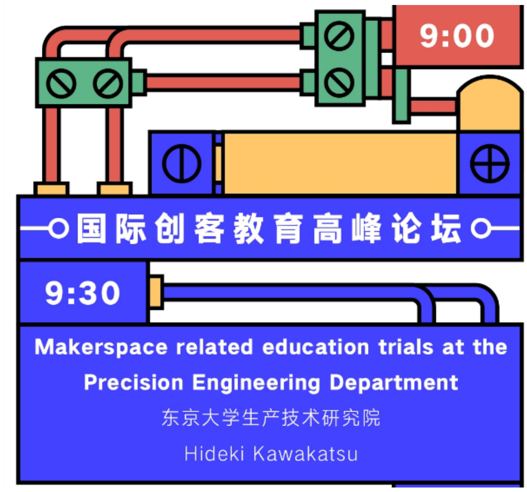

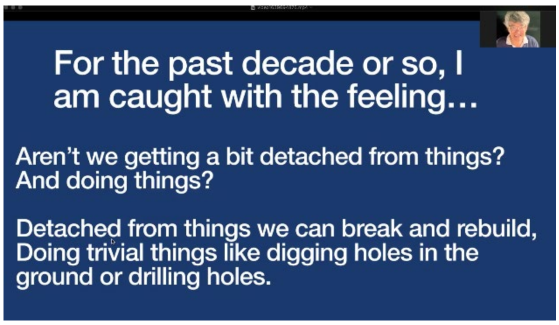

December 20th , 2021
2021 NAMIS Marathon Workshop

2021 NAMIS Marathon Workshop organized by the National TsingHua University, Taiwan. An On-line Workshop was held between the National Tsinghua University and members of IIS following last year's successful event. Three professors, Professor Andrew Yeh, Professor Hiroshi Toshiyoshi and Professor Hideki Kawakatsu, together with thirteen young researchers presented their work. We are once again very grateful for the organization by Professor Yeh and his team.

March 7th-11th 2022
CIRMM Open Laboratory

To promote exchange among young researchers and students in CIRMM, the open laboratory was held, and 5 laboratories (Nomura, Toshiyoshi/Tixier-Mita, Takamiya, Takahashi, and Kim Laboratories) were open in turn for the visitors.

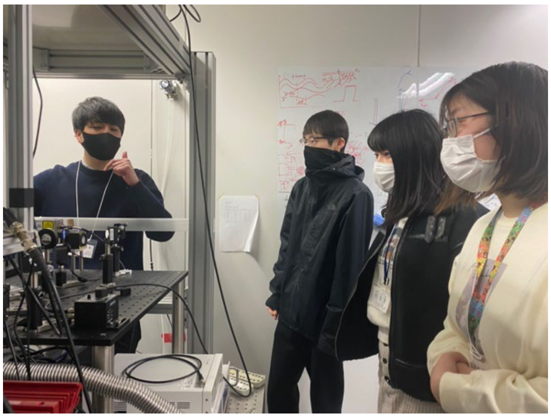

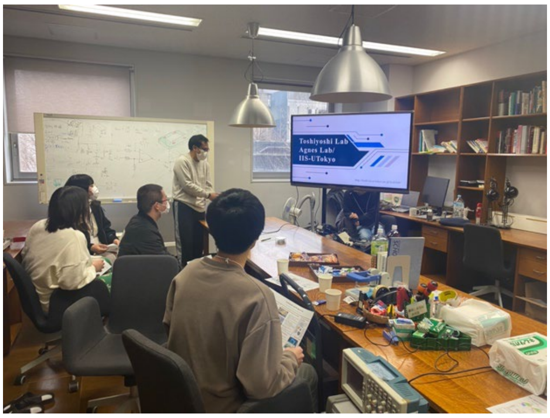

Research Activities

April 2021 - March 2022

TAKAHASHI Laboratory

Current Research Activities 2020-2021

Takahashi Laboratory

1. Research Topics

1.1 Time-resolved Photo-assisted Kelvin Probe Microscopy on Solar Cells

Photo-assisted Kelvin probe force microscopy (P-KFM) allows us to investigate photovoltaic properties especially in solar cells, and if a temporal change in photovoltage can be observed by P-KFM, photocarrier dynamics will be analyzed in further detail. In order to realize a time-resolved measurement of photovoltage, we have combined the intermittent bias application method and the pump-probe method for P-KFM. In the intermittent bias application method for KFM, we apply the bias pulse train, synchronized at the bottom in the cantilever oscillation, with a sinusoidal envelope at a certain frequency, and an electrostatic force at this frequency is used to determine a surface potential. For the time-resolved P-KFM, a sample is illuminated by light pulses with the same repetition period as that of the electrical bias pulses, and the light pulses are slowly swept to acquire a time-resolved waveform of photovoltage, regarded as the pump-probe method.

Figure shows time-resolved waveforms of photovoltage observed by P-KFM on $Cu(In,Ga)Se_2$ solar cells with different Ga contents, and the results indicate that rise and decay rates of photovoltage were clearly different between the two samples.

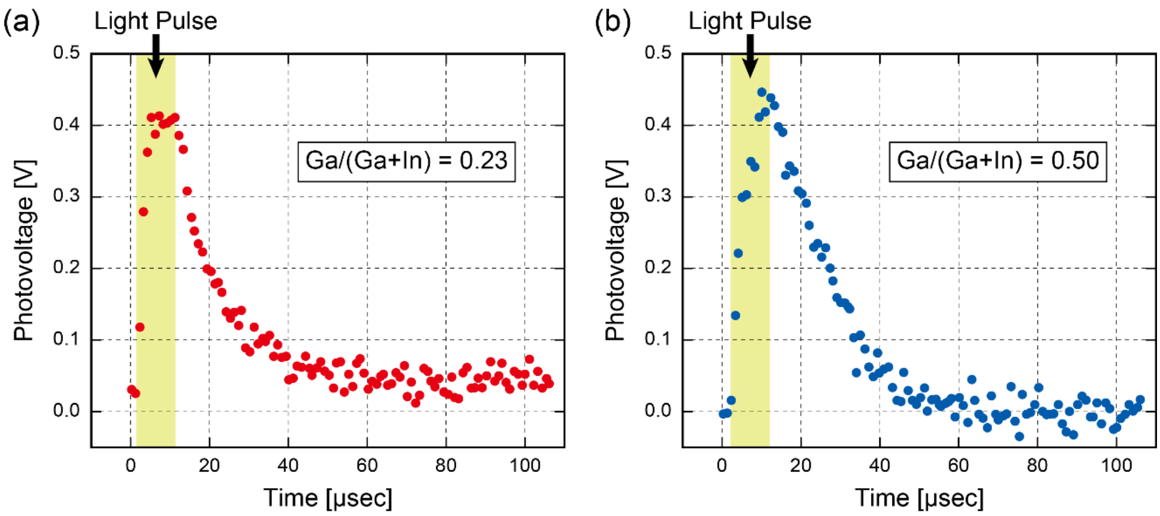

1.2 Photothermal Atomic Force Microscopy on Solar Cells

We performed the photothermal atomic force microscopy (PT-AFM), in which the periodical thermal expansion induced by the intermittent light illumination was detected by AFM, on the $Cu(In,Ga)(S,Se)_2$ [CIGSSe] materials to examine non-radiative recombination properties very locally.

In particular, we have proposed a multi-pulse (MP) modulation method, where the duration for light illumination is divided into multiple light pulses and their period is varied in order to realize variable frequency modulation of incident light in PT-AFM. To assess the capability of this method, we first examined the frequency characteristics of our detection system and confirmed the nearly flat frequency response. Then we observed some PT signal images on CdS/CIGSSe samples with or without the CsF-treatment and found that the PT signals at a modulation frequency of 800 kHz decreased only on the CsF-treated sample. The result is very consistent with the expectation that the CdS/CIGSSe interface was well passivated by the CsF treatment and consequently the non-radiative recombination was well suppressed there.

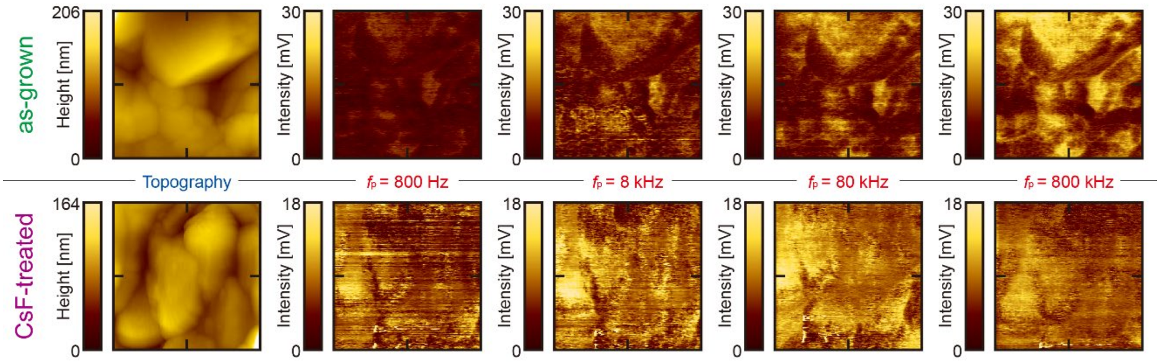

1.3 Electrostatic Force Microscopy for Investigation of Surface Depletion Capacitance

Scanning capacitance force microscopy (SCFM) is a good method for capacitance measurements using electrostatic force detection. However, to obtain an entire capacitance–voltage (C–V) curve by SCFM, a sweep of a direct current (DC) bias voltage is required at a certain fixed point on a sample surface during scan suspension, and thus the measurements become very time-consuming when we want to observe some types of images related with C–V characteristics. So, we have proposed peak-tracking scanning capacitance force microscopy (PT-SCFM) for the purpose of extracting the main feature of the C–V curve without DC voltage sweep. In PT-SCFM, alternating current voltages at three different angular frequencies, ω_1, ω_2, and ω_m, are applied together with DC voltage, V_{DC}, to generate an electrostatic force, and high-order components at the angular frequencies of $\omega_2 - 2\omega_1$ and $\omega_2 - 2\omega_1 - \omega_m$, which represent a voltage derivative of a capacitance ($\partial C/\partial V$) and a second-order derivative of the capacitance ($\partial^2 C/\partial V^2$), respectively, are extracted from the electrostatic force. Then, a DC voltage, V_p, giving the peak of $\partial C/\partial V$ is determined from V_{DC} to be adjusted to nullify the $\omega_2 - 2\omega_1 - \omega_m$ component using a feedback controller. From the obtained values of V_p and $\partial C/\partial V$ at V_p, the C–V curve can be outlined. In PT-SCFM, the distributions of those values are simultaneously imaged together with a topography without V_{DC} sweep, and when we operate PT-SCFM under various modulation frequency conditions, analyses similar to those based on the frequency dependence of the C–V property are realized. We have applied the PT-SCFM to a microcrystalline Cu(In, Ga)Se_2 material to discuss the effects of surface depletion and deep-level states, from which the validity of PT-SCFM has been examined.

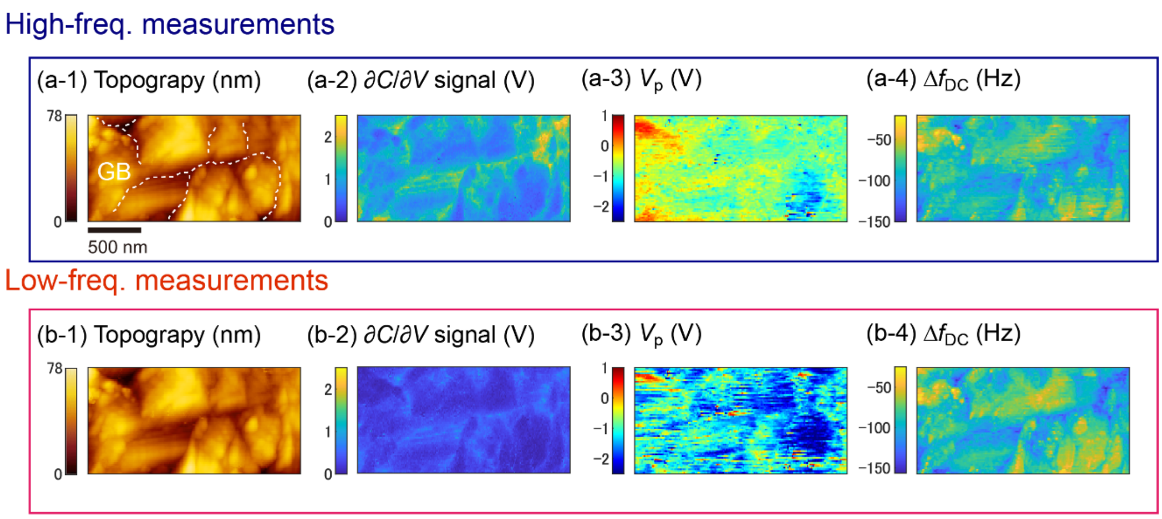

2. Research Achievements

2.1 Number of original journal papers: 3

2.2 International conference: 11

2.3 Domestic conference: 11

2.4 Number of patents: 0

3. List of awards

- none

4. Research Grants

4.1 Total number of research grants: 1

4.2 Number of collaboration research with industries: 1

4.3 List of major research grants (serving as Principal Investigator)

- Grant-in-Aid for Scientific Research "Dynamics of photo-generated carriers in multinary compound semiconductor solar cells investigated by photo-assisted nanoprobes" from JSPS

5. Education

5.1 Number of Ph.D. students (including current students): 2

5.2 Number of master students (including current students): 4

5.3 Number of other students: None

6. Publication list

Journal Papers

1. Karumuri Sriharsha, Le Duc Anh, Yuuji Shimada, Takuji Takahashi, and Masaaki Tanaka, "Growth and Characterization of Ferromagnetic Fe-doped GaSb Quantum Dots with High Curie Temperature", *APL Materials*, **8**, 091107 (2020).
2. A. Yamada and T. Takahashi, "Multi-pulse Modulation Method in Photothermal Atomic Force Microscopy for Variable Frequency Modulation of Incident Light", *Japanese Journal of Applied Physics*, **60**, SE1003 (2021).
3. R. Fukuzawa and T. Takahashi, "Peak-tracking scanning capacitance force microscopy with multibias modulation technique", *Measurement Science and Technology*, **33**, 065405 (2022).

Conference Presentations

1. Ryota Ishibashi and Takuji Takahashi, "Time-resolved Measurements by Kelvin Probe Force Microscopy with Intermittent Bias Application", *2020 NAMIS Marathon Workshop*, Online, November (2020).
2. Ayaka Yamada and Takuji Takahashi, "Investigation on Non-radiative Recombination Local Property in $Cu(In,Ga)(S,Se)_2$ by Photothermal AFM", *2020 NAMIS Marathon Workshop*, Online, November (2020).

3. Ryota Ishibashi and Takuji Takahashi, "Time-resolved Kelvin Probe Force Microscopy with Intermittent Bias Application Method", *The 28th International Colloquium on Scanning Probe Microscopy (ICSPM28)*, S8-1, Online, December (2020).
4. Ayaka Yamada and Takuji Takahashi, "Multi-pulse Modulation Method in Photothermal Atomic Force Microscopy", *The 28th International Colloquium on Scanning Probe Microscopy (ICSPM28)*, S8-3, Online, December (2020).
5. Takuji Takahashi, "Photo-assisted Scanning Probe Methods on Solar Cells", *AMU/CNRS-IIS/UTokyo Energy Workshop*, Online, Oct. (2021).
6. Kosuke Takiguchi, Le Duc Anh, Takahiro Chiba, Ryota Fukuzawa, Takuji Takahashi, and Masaaki Tanaka, "Giant Gate-controlled Odd-parity Magnetoresistance in One-dimensional Channels with a Magnetic Proximity Effect", *2021 International Conference on Solid State Devices and Materials (SSDM 2021)*, I-5-05, Sep. (2021).
7. Takuji Takahashi, "Time-resolved Photovoltaic Measurements by Photo-assisted Kelvin Probe Force Microscopy", *The 4th International Symposium on "Elucidation of Property of Next Generation Functional Materials and Surface/Interface"*, 60, Online, Oct. (2021). [Invited]
8. Kosuke Takiguchi, Le Duc Anh, Takahiro Chiba, Kyosuke Okamura, Harunori Shiratani, Ryota Fukuzawa, Takuji Takahashi, and Masaaki Tanaka, "Gate-controlled Giant Proximity Magnetoresistance and Odd-parity Magnetoresistance in Semiconductor-based Nonmagnetic (InAs) / Ferromagnetic (GaFeSb) Heterostructures", *Joint Conference on 24th International Conference on Electronic Properties of Two-Dimensional Systems and 20th International Conference on Modulated Semiconductor Structures (EP2DS-24/MSS-20)*, M-1-03, Online, Nov. (2021).
9. Ryota Fukuzawa and Takuji Takahashi, "Quantitative Capacitance Measurements in Frequency Modulation Electrostatic Force Microscopy", *The 29th International Colloquium on Scanning Probe Microscopy (ICSPM29)*, S6-6, Online, Dec. (2021).
10. Tomoe Kuroiwa and Takuji Takahashi, "Time-resolved Photo-assisted Kelvin Probe Force Microscopy on Cu(In,Ga)Se_2 Solar Cells", *The 29th International Colloquium on Scanning Probe Microscopy (ICSPM29)*, S7-3, Online, Dec. (2021).
11. Tomoe Kuroiwa and Takuji Takahashi, "Time-resolved Photovoltaic Measurements on Cu(In,Ga)Se_2 Solar Cells by Photo-assisted Kelvin Probe Force Microscopy", *2021 NAMIS Marathon Workshop*, Online, Dec. (2021).

IOP Publishing | Measurement Science and Technology

Meas. Sci. Technol. 33 (2022) 065405 (6pp) https://doi.org/10.1088/1361-6501/ac5e62

Peak-tracking scanning capacitance force microscopy with multibias modulation technique

Ryota Fukuzawa[1,*] and **Takuji Takahashi**[1,2,*]

[1] Institute of Industrial Science, The University of Tokyo, 4-6-1 Komaba, Meguro, Tokyo 153-8505, Japan
[2] Institute for Nano Quantum Information Electronics, The University of Tokyo, 4-6-1 Komaba, Meguro, Tokyo, 153-8505, Japan

E-mail: fkryota@iis.u-tokyo.ac.jp and takuj@iis.u-tokyo.ac.jp

Received 19 January 2022, revised 14 March 2022
Accepted for publication 16 March 2022
Published 30 March 2022

Abstract

Scanning capacitance force microscopy (SCFM) is a good method for capacitance measurements using electrostatic force detection. However, to obtain an entire capacitance–voltage (*C*–*V*) curve by SCFM, a sweep of a direct current (DC) bias voltage is required at a certain fixed point on a sample surface during scan suspension, and thus the measurements become very time-consuming when we want to observe some types of image related with *C*–*V* characteristics. In this paper, we propose peak-tracking scanning capacitance force microscopy (PTSCFM) for the purpose of extracting the main feature of the *C*–*V* curve without DC voltage sweep. In PT-SCFM, alternating current voltages at three different angular frequencies, ω_1, ω_2, and ω_m, are applied together with DC voltage, V_DC, to generate an electrostatic force, and high-order components at the angular frequencies of $\omega_2 - 2\omega_1$ and $\omega_2 - 2\omega_1 - \omega_\mathrm{m}$, which represent a voltage derivative of a capacitance ($\partial C/\partial V$) and a second-order derivative of the capacitance ($\partial^2 C/\partial V^2$), respectively, are extracted from the electrostatic force. Then, a DC voltage, V_p, giving the peak of $\partial C/\partial V$ is determined from V_DC to be adjusted to nullify the $\omega_2 - 2\omega_1 - \omega_\mathrm{m}$ component using a feedback controller. From the obtained values of V_p and $\partial C/\partial V$ at V_p, the *C*–*V* curve can be outlined. In PT-SCFM, the distributions of those values are simultaneously imaged together with a topography without V_DC sweep, and when we operate PT-SCFM under various modulation frequency conditions, analyses similar to those based on the frequency dependence of the *C*–*V* property are realized. We have applied the PT-SCFM to a microcrystalline $\mathrm{Cu(In,Ga)Se_2}$ material to discuss the effects of surface depletion and deep-level states, from which the validity of PT-SCFM has been examined.

Keywords: *C*–*V*, atomic force microscopy, electrostatic force microscopy, deep-level investigation, scanning capacitance microscopy, dopant profile

(Some figures may appear in colour only in the online journal)

1. Introduction

Atomic force microscopy (AFM) [1] enables us to investigate a local surface structure with atomic resolution [2, 3], and various applications of AFM have been developed to evaluate the local electrical properties of a sample. By electrostatic force microscopy (EFM) [4] and Kelvin probe force microscopy [5], distributions of charge, capacitance, and surface potential can be imaged through electrostatic force measurements, and scanning spreading resistance microscopy [6, 7] can be used to measure spreading resistance in a sample through local current detection. Scanning capacitance microscopy (SCM) [8] and

* Authors to whom any correspondence should be addressed.

Time-resolved Kelvin Probe Force Microscopy with Intermittent Bias Application Method

R. Ishibashi[1] and T. Takahashi[1,2]
[1]Institute of Industrial Science/[2] Institute for Nano Quantum Information Electronics,
The University of Tokyo, 4-6-1 Komaba, Meguro-ku, Tokyo 153-8505, Japan.

Kelvin probe force microscopy (KFM) is very useful to investigate surface potentials on various samples, but its time resolution is typically limited by response time of potential feedback. By combining the intermittent bias application method [1] that we have proposed for the purpose of improvement of a spatial resolution in KFM with the pump-probe method [2] proposed by Murawski, et al., both spatial and time resolutions in KFM are expected to be improved.

In the intermittent bias application method, a series of voltage pulses with a sinusoidal envelope are applied at every instant when the tip end reaches the most vicinity to the sample surface during the oscillation, instead of a continuous sinusoidal bias voltage generally used in KFM, as shown in Fig. 1(a). Now, we presume the cyclic potential change, mostly induced by external electrical or optical excitation, synchronized with the cantilever oscillation. Then the time-resolved measurement is realized by changing the time interval between the potential change and the voltage pulse, as illustrated in Fig. 1(b). In this method, the voltage pulse width should be a key parameter to determine the time resolution: a narrower pulse is more preferable.

In the present study, we assessed this method through the surface potential measurements on an Au thin film evaporated on a Cu plate with application of a series of the triangular-shaped bias voltage between the sample and tip, which simulate the cyclic surface potential change. The acquired potential waveforms using the voltage pulses with a width of 6 μs or 2 μs are shown in Fig. 2. From these results, we have confirmed that our method achieves a time resolution of at least 2 μs.

This work was partially supported by JSPS KAKENHI Grant Number 17H02783.

[1] S. Ono and T. Takahashi, *Jpn. J. Appl. Phys.* **45**, 1931 (2006).
[2] J. Murawski, et al., *J. Appl. Phys*. **118**, 154302 (2015).

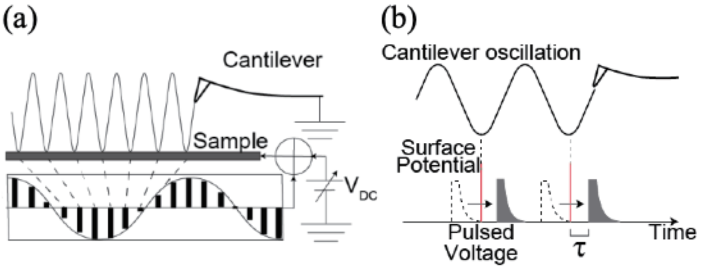

Fig. 1 Schematic diagram of (a) principle of KFM with intermittent bias application method and (b) time resolved measurement by it.

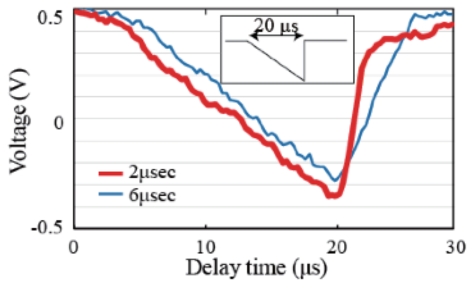

Fig. 2 The potential waveforms acquired with different voltage pulse widths. The inset shows the ideal waveform to be observed.

S6-6

Quantitative Capacitance Measurements in Frequency Modulation Electrostatic Force Microscopy

R. Fukuzawa[1] and T. Takahashi[1,2]
[1]Institute of Industrial Science/ [2]Institute for Nano Quantum Information Electronics,
The University of Tokyo 4-6-1, Meguro-ku Komaba, Tokyo, 153-8505, Japan.

Electrostatic force microscopy (EFM) is a good method to analyze electrical property such as capacitance, charge and permittivity at high spatial resolution. On a semiconductor, however, quantitative estimation of capacitance in EFM is very difficult because formulation between the tip-sample capacitance, C, and frequency shift of the cantilever is not well established when C includes a surface depletion layer capacitance. From S. Hudlet et al. [1], the electrostatic force, F^{ele}, between metallic tip and semiconductor can be expressed as equation (1), where V and z are the voltage and the distance between the tip and sample and S and $Q_{\mathrm{t}}(V,z)$ are the area of capacitor and induced charge, respectively. In frequency modulation EFM (FM-EFM) with small amplitude oscillation, on the other hand, a frequency shift, Δf, induced by the electrostatic force, is proportional to force gradient, $\partial F^{\mathrm{ele}}/\partial z$. In this study, we have derived translation formula from Δf to C, and performed quantitative measurements of the capacitance on a n-type Si substrate (provided by prof. Shigekawa at Osaka city University) using dual bias modulation EFM (DEFM) [2].

To to express Δf under the FM operation in AFM, in which the cantilever is oscillated at its resonant frequency ω_0, we derived equation (2) by calculating $\partial Q_{\mathrm{t}}/\partial z$, where k is a spring constant of the cantilever. Here, we consider that rates for charge trap to and escape from deep levels, such as surface and interface states, depend on the cantilever oscillation frequency ω_0, as represented by $C(\omega_0)$. In DEFM, DC and AC voltages $V_{\mathrm{DC}} + V_1 \sin\omega_1 t + V_2 \sin\omega_2 t$ were applied, and we assume that the charge response is approximable as equation (3) and that $\omega_{\mathrm{d}}(\equiv \omega_2 - \omega_1)$ component in Δf, $\Delta f_{\omega_{\mathrm{d}}}$, is given by equation (4) when both ω_1 and ω_2 are close to ω_0. Using equation (4), the capacitance value can be evaluated from $\Delta f_{\omega_{\mathrm{d}}}$. Figure 1 shows the capacitance – voltage characteristics on the n-type Si evaluated using equation (4). We found that the capacitance gradually decreased in the positive direction of the DC bias voltage where the surface was more depleted, and values of capacitance around aF is considered reasonable for the tip-sample capacitance. Thus, the validity of quantitative measurements by our method has been well confirmed.

[1] S. Hudlet, et al, *J. Appl. Phys.*, **77**, 3308 (1995).
[2] R. Fukuzawa and T. Takahashi, *Rev. Sci. Instrum.*, **91**, 023702 (2020)

$$F^{\mathrm{ele}} = -\frac{Q_{\mathrm{t}}^2(V,z)}{2\epsilon_0 S} \qquad (1)$$

$$\Delta f = -\frac{\omega_0}{2k} C(\omega_0) \frac{Q_{\mathrm{t}}^2(V,z_0)}{\epsilon_0^2 S^2} \qquad (2)$$

$$Q_{\mathrm{t}} \approx Q(V_{\mathrm{DC}}) + \sum_{i=1}^{2} C(\omega_i) V_i \sin\omega_i t \qquad (3)$$

$$\Delta f_{\omega_{\mathrm{d}}} \approx \frac{\omega_0 V_1 V_2}{2k\epsilon_0^2 S^2} C^3(\omega_0) \qquad (4)$$

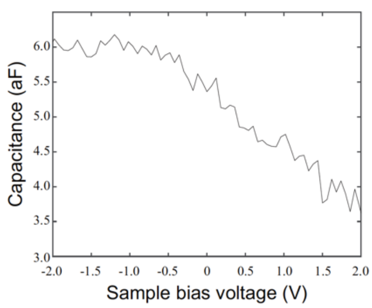

Fig.1：Capacitance-voltage characteristic on a n-type Si substrate evaluated using Eq. (4).

Time-resolved Photo-assisted Kelvin Probe Force Microscopy on $Cu(In,Ga)Se_2$ Solar Cells

T. Kuroiwa[1] and T. Takahashi[1,2]

[1]Institute of Industrial Science / [2] Institute for Nano Quantum Information Electronics,

The University of Tokyo, 4-6-1 Komaba, Meguro-ku, Tokyo 153-8505, Japan.

Photo-assisted Kelvin probe force microscopy (P-KFM) [1] allows us to investigate photovoltaic properties especially in solar cells, and if a temporal change in photovoltage can be observed by P-KFM, photocarrier dynamics will be analyzed in further detail. In this study, the intermittent bias application method which was originally proposed for the purpose to improve the spatial resolution in KFM [2] has been adopted to realize time-resolved measurements [3] by P-KFM, being similar to the pump-probe method [4]. Then we successfully observed waveforms of photovoltage on $Cu(In,Ga)Se_2$ [CIGS] solar cells under pulsed light illumination.

For KFM itself, we apply the bias pulse train, synchronized at the bottom in the cantilever oscillation, with a sinusoidal envelope at a certain frequency, and an electrostatic force at this frequency is used to determine a surface potential. For the time-resolved P-KFM, a sample is illuminated by light pulses with the same repetition period as that of the electrical bias pulses, and the light pulses are slowly swept to acquire a time-resolved waveform of photovoltage.

Figure 1 shows time-resolved waveforms of photovoltage observed by P-KFM on CIGS solar cells with different Ga contents, where the samples were illuminated by a monochromatic laser light with 800 nm in wavelength and 45 mW/cm^2 in intensity. A width of the intermittent bias pulse was 2 µsec, which limited a time resolution in the measurements.

The results indicate that rise and decay rates of photovoltage were clearly different between the two samples. A slow decay rate in Sample B is consistent with our previous results obtained by the temporally-averaged photovoltaic measurements [5]. On the other hand, a fast rise rate in Sample A is attributed to good quality in the CIGS layer, being consistent with high conversion efficiency compared with Sample B.

The samples used in this work were provided by Prof. T. Minemoto of Ritsumeikan University. This work was partially supported by JSPS KAKENHI Grant Number 17H02783.

[1] T. Takahashi, *Jpn. J. Appl. Phys.*, **50**, 08LA05 (2011).
[2] T. Takahashi, T. Matsumoto and S. Ono, *Ultramicroscopy*, **109**, 963-967 (2009).
[3] R. Ishibashi and T. Takahashi, *ICSPM28*, S8-1 (2020).
[4] J. Murawski, et al., *J. Appl. Phys.*, **118**, 154302 (2015).
[5] H. Yong, T. Minemoto and T. Takahashi, *IEEE J. Photovolt.*, **9**, 483-491 (2019).

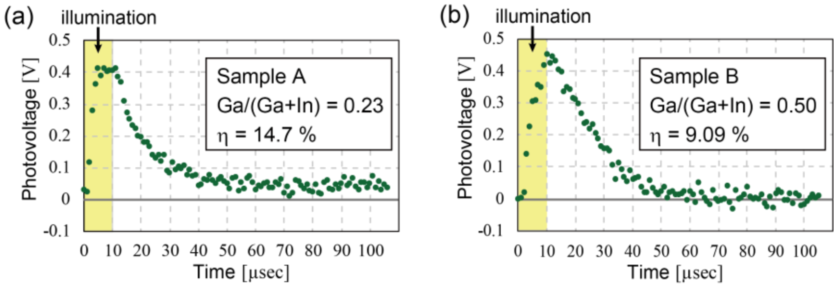

Fig. 1 Waveforms of photovoltage observed by P-KFM on two CIGS solar cells with different Ga contents.

Japanese Journal of Applied Physics 60, SE1003 (2021)
https://doi.org/10.35848/1347-4065/abf07b

REGULAR PAPER

Multi-pulse modulation method in photothermal atomic force microscopy for variable frequency modulation of incident light

Ayaka Yamada[1*] and Takuji Takahashi[1,2]

[1]Institute of Industrial Science,The University of Tokyo, Meguro-ku, Tokyo 153-8505, Japan
[2]Institute for Nano Quantum Information Electronics, The University of Tokyo, Meguro-ku, Tokyo 153-8505, Japan

*E-mail: ayaka-y@iis.u-tokyo.ac.jp

Received February 2, 2021; revised March 1, 2021; accepted March 19, 2021; published online April 14, 2021

Photothermal atomic force microscopy (PT-AFM) enables us to examine non-radiative recombination property with high spatial resolution. In order to realize variable frequency modulation of incident light in PT-AFM, we have proposed a multi-pulse modulation method, where the duration for light illumination is divided into multiple light pulses and their period is varied. We have assessed the validity of the proposed method through acquisition of photothermal signal images on microcrystalline materials under various modulation frequencies.

1. Introduction

Carrier recombination is very important dynamics in a semiconductor, and radiative recombination property of photo-generated electrons and holes can be investigated through photoluminescence (PL) measurements. In particular, local PL measurements have been realized by the scanning near-field optical microscopy[1–4] which is one application of scanning probe methods. When, on the other hand, the photo-generated carriers recombine non-radiatively, heat is generated and consequently thermal expansion of a sample occurs. In most semiconductor devices, the non-radiative recombination degrades their performance because of the loss of carrier and the rise in temperature. Although straightforward evaluation of the non-radiative recombination is difficult, the thermal expansion originating from the non-radiative recombination can be experimentally examined. For such purposes, some photothermal spectroscopic methods like a photoacoustic method[5] and a photothermal divergence method[6] were performed. Especially for the local photothermal measurements, in addition, atomic force microscopy (AFM) has been utilized in infrared spectroscopy,[7,8] local probing of photothermally induced megahertz surface vibrations,[9] and direct measurements of thermal expansion by photothermal AFM (PT-AFM) using dual sampling method.[10–14] Furthermore, the principle of micro-drivers based on photo-thermal expansion was examined by AFM,[15] where high sensitivity for height change detection in AFM was utilized. Besides the above methods, it is desirable that a method to evaluate the thermal expansion in time domain is realized because such measurements will enable us to investigate a time constant or probability of the non-radiative recombination. The PT-AFM at variable frequency modulation of the incident light in a sufficiently high frequency region will be one candidate to realize it, but it is still challenging at present.

In this study, we have adopted a multi-pulse modulation method, referred to as a MP method, in order to realize the variable frequency measurements in PT-AFM, and assessed its capability through the measurements of frequency response of the detection system and through the observation of PT-AFM images on microcrystalline $Cu(In,Ga)(S,Se)_2$ [CIGSSe] materials.

2. Experimental methods

2.1. Photothermal atomic force microscopy [PT-AFM]

Our PT-AFM system, outlined in Fig. 1, is based on a commercial AFM system (SPA-300HV/SPI4000; Hitachi High-Tech Science Corporation, Japan) operated in the intermittent contact mode to observe topography in high-vacuum ($\sim 10^{-5}$ Pa) at room temperature. In order to avoid stray light illumination onto a sample surface, a piezoresistive cantilever (PRC-DF40P; Hitachi High-Tech Science Corporation, Japan), whose typical values of a spring constant, resonance frequency and quality factor at the resonance were around 40 N m^{-1}, 400 kHz and 3000, respectively, was used, instead of the optical beam deflection method which is widely used in AFM. As a light source, a tunable $Ti{:}Al_2O_3$ laser in continuous wave mode was used, and a power of a monochromatic light was regulated by a laser power controller (LPC). Then the light was modulated by an acoustic optical modulator (AOM), guided by an optical fiber and focused on a sample surface by an optical lens. A wavelength of the incident light was 800 nm, and a spot area and light intensity at the sample surface were approximately 1 mm^2 and on the order of 100 mW cm^{-2}, respectively.

In the previous works by our group,[10–14] the incident light was simply modulated intermittently in a square waveform, referred to as a SW method here, as illustrated in Fig. 2(a), and a value of thermal expansion was extracted from a periodical change of cantilever oscillation amplitude using the dual sampling method, where a signal-to-noise (S/N) ratio was not sufficiently high because typical values of thermal expansion were on the order of 1 or 10 pm, while the oscillation amplitude of the cantilever was estimated to be several tens nm. In order to improve the S/N ratio for the measurements, in this study, a cantilever oscillation phase was detected by a phase locked loop (PLL) equipment (easyPLL; Nanosurf, Switzerland) because the oscillation phase sensitively varies according to the height change of the sample surface, compared with the oscillation amplitude.[21] In addition, a response time in the phase change of the cantilever oscillation is given by $\sim 1/f_{osc}$,[21] where f_{osc} is an oscillation frequency near the resonance of the cantilever,

TOSHIYOSHI Laboratory

Current Research Activities 2021-2022

Toshiyoshi Laboratory

1. Research Topics

1.1 MEMS Vibrational Energy Harvester System

Compared with the microelectronics integrated within an IoT device, power source has been left far behind the trend of miniaturization. To make an IoT device as small as a crop grain size, we have developed a method to produce a compact electrical power source that perpetually delivers power from the ambient vibrations. Figure 1 illustrates the concept of such powerpack using a MEMS vibrational energy harvester that creates electrical current through the electrostatic induction. An electrical rectifier and a storage capacity are integrated with the harvester chip to self-manage the output at a constant voltage level. The harvester system is co-developed with an industrial partner Saginomiya Seisakusho, Inc. and the NMEMS Technological Research Association. The device presented at the CEATEC 2020 has won the Grand-Prix Award (open competition chapter). This work has been performed as a project (JPNP16007) commissioned by the New Energy and Industrial Technology Development Organization (NEDO).

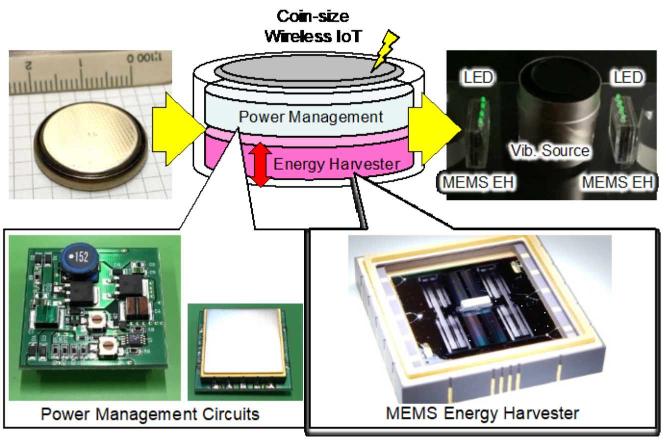

Figure 1. MEMS vibrational energy harvester [C4].

1.2 MEMS Vibrational Energy Harvester with a Wide Frequency Bandwidth

IoT sensors for a practical use requires a power source that delivers power around the clock but solar cells cannot producer power during night or in the dark. Besides, most MEMS vibrational energy harvesters ever reported are of mechanical resonant type, limiting the effective bandwidth as narrow as a few percent around the eigen frequency. The recent theoretical study of ours has predicted an enormous expansion of the bandwidth by increasing the charge potential of the electret that is used on the surface of electrodes for mechano-electric conversion. Figure 2 (right) shows an example of such vibrational energy harvester that has a bandwidth as wide as 64 Hz around its resonance of 150 Hz. Compared with the resonant type harvester, the new device has small vibration stroke on the suspended mass but the electrodes fixed on the chip frame move at a rather large stroke by the external vibration. For this reason, we call the new design scheme as the short-stroke vibrational (SSV) energy harvester with respect to the conventional long-stroke vibrational (LSV) harvesters.

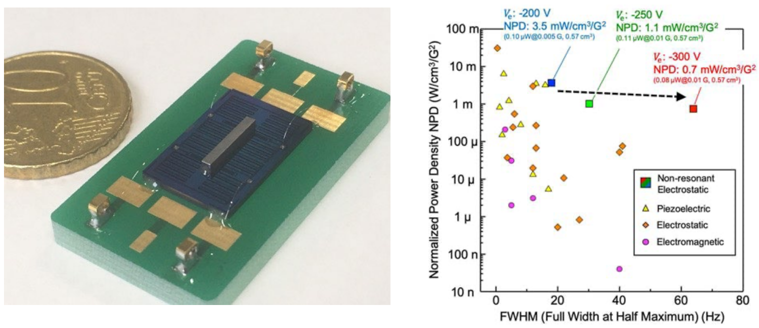

Figure 2. A MEMS vibrational energy harvester of a wide frequency bandwidth [C5].

1.3 MEMS Wavelength-Tunable VCSEL (Vertical Cavity Surface Emitting Laser) for High-Speed OCT (Optical Coherence Tomography)

We developed a wavelength tunable vertical-cavity surface-emitting laser (VCSEL) constructed by die-bonding a half-cavity InGaAs laser diode (LD) chip onto a silicon-on-insulator chip with a microelectromechanical system (MEMS) electrostatic diaphragm mirror that functions as a Fabry-Perot interferometer. As a result of the short cavity length, the integrated tunable LD has single-mode lasing characteristics with an extremely large coherence length of 150 m or more. The developed wavelength tunable LD is used to perform swept-source optical coherence tomography (SS-OCT) with a large scan depth, which is applicable to ophthalmic observation for the diagnosis of pathologic nearsightedness based on the measurement of the axial length of an eye.

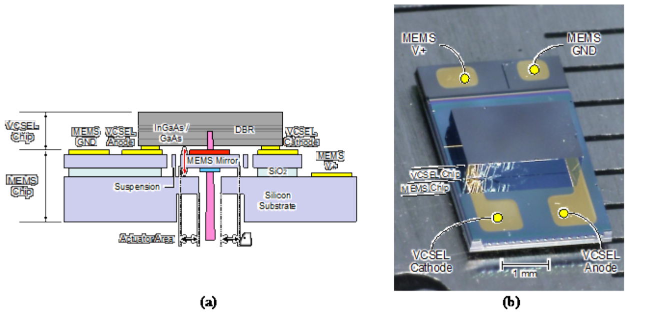

Figure 3. Cross-section of a wavelength-tunable VCSEL with an electrostatic MEMS Fabry-Perot interferometer mirror [J9].

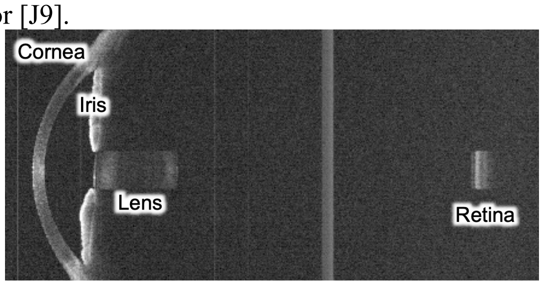

Figure 4. Cross-section of the human eye observed by the ophthalmologic OCT [J9].

1.4 Electrostatic Microelectromechanical Logic Device

An adaptive driving beam (ADM) for vehicle's headlight has been developed using a microelectromechanical systems (MEMS) optical scanner. A piezoelectric scanner is constructed using thin film lead-zirconate-titanate oxide (PbZrTiO3, PZT) on a bonded silicon-on-insulator (SOI) wafer, respectively processed by ion-milling and deep reactive ion etching (DRIE). The PZT layer is laminated in metal films on the SOI layer to form a piezoelectric unimorph actuator, which are then arranged as a pair of twisting suspensions to drive the scanner at resonance. The same piezoelectric actuators are also arranged into another form of meandering suspensions to generate a large deflection angle. By the combination of these two mechanisms, two-dimensional optical scanner is constructed in a single chip. The scanner is used to draw a Lissajous pattern of a blue laser light on a phosphor material to create a structured light source that is projected forward for illumination. The lighting patterns and positions are electronically controlled and reconfigured depending upon the location of leading/oncoming vehicles, pedestrians, road signs, and the cruising speed of the vehicle. The paper discusses on the design of the piezoelectrically driven optical scanner along with the optomechanical performances. We also report on the road-test result of the developed on-vehicle ADB module.

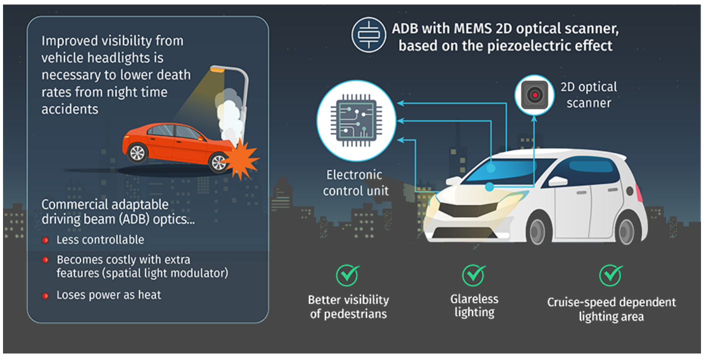

Figure 5. A cartoon introduction to ADB (adaptive driving beam) used in the cover page of Journal of Microoptics [J6].

2. Research Achievements (in 2020 and 2021)

2.1 Number of original journal papers: 18 + 12

2.2 International conference: 8 + 13 (including 1 + 5 invited presentation)

2.3 Domestic conference: 17 + 11 (including 1 + 3 invited presentations)

2.4 Number of patents: 2 + 3

3. List of awards

1. C. Sano, Excellent Paper Award, IEEJ Annual Meeting, 2020-11-12
2. H. Honma et al., IEEJ Excellent Presentation Award, IEEJ, 2020-04-01
3. M. Mita et al, Excellent Paper Award, IEEJ Trans. SM., 2020-05-01
4. NMEMS Technological Research Association, CEATEC Award 2020 Grand-Prix, 2020-10-19
5. H. Toshiyoshi and G. Hashiguchi, The 53rd Ichimura Prize in Science for Distinguished Achievement, 2021-04-19
6. H. Toshiyoshi, IEEJ Award for Advanced Technology, 2021-04-28
7. M. Goto et al., 2022 Arnaud Darmont Award for Best Paper, 2022-01-22

4. Research Grants

4.1 Total number of research grants: 3

4.2 Number of collaboration research with industries: 4

4.3 List of major research grants (serving as Principal Investigator)

- JST CREST Number JPMJCR19Q2, “Perpetual Electronics”
- JSPS Grant in Aid 21H01271, “Electret Degradation Mechanism”

5. Education

5.1 Number of Ph.D. students (including current students): 1

5.2 Number of master students (including current students): 6

5.3 Number of other students: 1

6. Publication list

Journal Paper (selected, *attached)

J1. * Hiroyuki Mitsuya, Hisayuki Ashizawa, Noriko Shimomura, Hiroaki Homma, Gen Hashiguchi, and Hiroshi Toshiyoshi, “A Method to Determine the Electret Charge Potential of MEMS Vibrational Energy Harvester using Pure-White Noise,” IEEE Transactions on Semiconductor Manufacturing, vol. 33, no. 2, 2020, pp. 180-186.

J2. Hiroaki Honma, Yukiya Tohyama, Sho Ikeno, and Hiroshi Toshiyoshi, “Equivalent Circuit Model for MEMS Vibrational Energy Harvester Compatible with Sinusoidal and Non-sinusoidal Vibrations,” Sensors and Materials, vol. 32, no. 7, 2020, pp. 2475-2492.

J3. * S. Yamada and H. Toshiyoshi, “A Temperature Sensor with A Water-Dissolvable Ionic Gel for Ionic Skin,” ACS Applied Materials & Interfaces, vol. 12, no. 32, 2020, pp. 36449–36457.

J4. Xufeng Liu, Takuya Takahashi, Masahiro Konishi, Kentaro Motohara, and Hiroshi Toshiyoshi, “Random Access Addressing of MEMS Electrostatic Shutter Array for Multi-object Astronomical Spectroscopy,” MDPI Micromachines, vol. 11, no. 8, 2020, pp. 782-798.

J5. * Toru Nakanishi, Takeshi Miyajima, Kenta Chokawa, Masaaki Araidai, Hiroshi Toshiyoshi, Tatsuhiko Sugiyama, Gen Hashiguchi, and Kenji Shiraishi, “Negative-charge-storing mechanism of potassium-ion electrets used for vibration-powered generators: Microscopic study of a-SiO_2 with and without potassium atoms,” Applied Physics Letters, vol. 117, no. 10, 2020, p. 193902.

J6. Tomotaka Asari, Mamoru Miyachi, Yutaro Oda, Takaaki Koyama, Hiroaki Kurosu, Makoto

Sakurai, Masanao Tani, Yoshiaki Yasuda, and Hiroshi Toshiyoshi, “Adaptive Driving Beam System with MEMS Optical Scanner for Reconfigurable Vehicle Headlight,” SPIE J. Optical Microsystems, vol. 1, no. 1, 2021, pp. 014501-1~9.

J7. Wan–Ting Chiu, Tso-Fu Mark Chang, Masato Sone, Hideki Hosoda, Agnès Tixier–Mita, Hiroshi Toshiyoshi, “Developments of the electroactive materials for non–enzymatic glucose sensing and their mechanisms,” MDPI Electrochem, vol. 2, no. 2, 2021, pp. 347-389.

J8. * Spyridon Bakas, Deepak Uttamchandani, Hiroshi Toshiyoshi, and Ralf Bauer, “MEMS enabled miniaturized light-sheet microscopy with all optical control,” Scientific Reports, vol. 11, 2021, Article number: 14100.

J9. Mohammed S. Khan, Changdae Keum, Yi Xiao, Keiji Isamoto, Nobuhiko Nishiyama, Hiroshi Toshiyoshi, “MEMS-VCSEL as a tunable light source for OCT imaging of long working distance,” J. Opt. Microsyst. 1(3), 034503 (2021).

J10. * Hiroaki Honma, Yukiya Tohyama, Hiroyuki Mitsuya, Gen Hashiguchi, Hiroyuki Fujita, and Hiroshi Toshiyoshi, “Power Enhancement of MEMS Vibrational Electrostatic Energy Harvester by Stray Capacitance Reduction,” Journal of Micromechanics and Microengineering, vol. 31, no. 12, 2021, p.125008 (11pp).

International Conference (selected)

C1. Hiroyuki Mitsuya, Hisayuki Ashizawa, Noriko Shimomura, Hiroaki Honma, Gen Hashiguchi, and Hiroshi Toshiyoshi, “A Method for Optimizing the Output Power of MEMS Vibrational Energy Harvester,” Design, Test, Integration & Packaging of MEMS/MOEMS (DTIP 2020), June 15-26, 2020.

C2. Hiroaki Honma and Hiroshi Toshiyoshi, “A Double-Deck Structured MEMS Electrostatic Vibrational Energy Harvester for Minimal Footprint,” in Proc. 32nd Int. Conf. on Micro Electro Mechanical Systems (MEMS 2019), Seoul, Korea, Jan. 27-31, 2019, pp. 1017-1020.

C3. Masahide Goto, Naoki Nakatani, Yuki Honda, Toshihisa Watabe, Masakazu Nanba1, Yoshinori Iguchi, Takuya Saraya, Masaharu Kobayashi, Eiji Higurashi, Hiroshi Toshiyoshi, and Toshiro Hiramoto, “Fabrication of 3-Layer Stacked Pixel for Pixel-Parallel CMOS Image Sensors by Au/SiO2 Hybrid Bonding of SOI Wafers,” Pacific Rim Meeting on Electrochemical and Solid-State Science (PRiME 2020), Oct. 4-9, 2020, Honolulu, Hawaii.

C4. Hiroshi Toshiyoshi, “MEMS Vibrational Energy Harvester for IoT Wireless Sensors,” IEEE 66th International Electron Devices Meeting (IEDM 2020), Dec. 12-16, San Francisco, US. (invited)

C5. Hiroaki Honma, Yukiya Tohyama, and Hiroshi Toshiyoshi, “A SHORT-STROKE ELECTROSTSTIC VIBRATIONAL ENERGY HARVESTER WITH EXTENDED BANDWIDTH AND SENSITIVITY,” in Proc. 21st International Conference on Solid-State Sensors, Actuators and Microsystems (Transducers 2021), June 20-24, 2021, Orland, FL, USA, pp. 132-135.

C6. Tomoya Miyoshi, Hiroyuki Mitsuya, Hiroshi Toshiyoshi, and Yuji Suzuki, “Proposal of A Unified Design of Broadband Two-Degree-of-Freedom Vibration Energy Harvesting System for High-Quality Factor Generators,” in Proc. 21st International Conference on Solid-State Sensors, Actuators and Microsystems (Transducers 2021), June 20-24, 2021, Orland, FL, USA, pp. 972-175.

C7. Hiroshi Toshiyoshi, “MEMS Energy Harvester Adaptable to Environmental Vibrations,” in Proc. 2020 International Conference on Solid State Devices and Materials (SSDM 2021), Sept. 6-9, 2021. (invited)

C8. Hiroshi Toshiyoshi and Gen Hashiguchi, “Silicon Oxide Electret for MEMS Vibrational Energy Harvester,” International Conference on Materials and Systems for Sustainability 2021 (ICMaSS 2021), Nov. 4-6, 2001, pp. 91-94. (invited)

A Method to Determine the Electret Charge Potential of MEMS Vibrational Energy Harvester Using Pure-White Noise

Hiroyuki Mitsuya, Hisayuki Ashizawa, Noriko Shimomura, Hiroaki Homma, Gen Hashiguchi, and Hiroshi Toshiyoshi, *Member, IEEE*

***Abstract*—A high-speed measurement method has been developed to electrically determine the potential voltage of the permanent charge or electret formed in a MEMS (microelectromechanical systems) vibrational energy harvester. While the conventional admittance method requires long time to observe the waveforms of the output power in time domain that diminishes when the built-in electret potential is compensated by an external voltage, this work proposes a new method to uniquely and promptly determine the electret potential by using the FFT (fast Fourier transform) analysis on the vibrational energy harvester excited by the white-noise voltage; the resonant peak in the frequency domain diminishes when the electret potential is compensated by the applied external bias voltage. White noise has been used in conventional method to measure the frequency response of devices of linear characteristics. However, due to the randomness of the input signal, random noise is inherently introduced to the measurement result, which urges us to repeat the measurement and to perform time-averaging to smooth out the noise. Therefore we used a newly developed white noise so-called "pure" white noise, which has a totally flat power spectrum, as it is synthesized from waveforms of a constant magnitude and random phases. We compute the inverse Fourier transform of such pure-white noises to instantly obtain the power spectrum without using mathematical averaging, and thus the throughput of measurement is enhanced ten-times faster.**

***Index Terms*—Electrostatic devices, microelectromechanical devices, electrets, white noise.**

I. Introduction

The CONVERGENCE of emerging Internet-of-Things (IoT) technology [1] and big-data analysis has enhanced the replacement of manual and visual inspection of utilities and infrastructures with automatic monitoring systems based on the wireless sensor network. As an autonomous power source for such systems that operate around the clock, ever-lasing energy sources or the energy harvesters are being intensively studied to harvest electrical power from the environment without the aid of battery cells or power cables. There are a few known principles for mechano-electric power conversion such as electromagnetic force [2], piezoelectricity [3] and triboelectricity [4]. Amongst of all, we have chosen the permanent charge or so-called "electret" [5] and have developed a theory to maximize the output by tailoring the damping losses though the electrostatic induction current [6].

Typical MEMS (microelectromechanical systems) energy harvester mechanism consists of a pair of opposing silicon electrodes with a narrow gap as shown in Figure 1(a). Compared with the electrets made by other processes such as corona discharge [7], ion implantation [8], electron beam injection [9], and molecule ionization by soft X-ray radiation [10], the potassium ion-doping by thermal oxidation of silicon [11] is known to store high-density electrical charges in the dielectric film that is conformally grown on the surface of the comb-like electrodes of a high aspect ratio silicon, thereby creating the strong electrostatic fields across the narrow air gap, as illustrated in Figure 1(b). The high-density electret makes a large induction current but with a penalty of strong electrostatic constraint force, which hampers the mechanical motion of the electrodes in a small vibration range. As schematically shown in Figure 2, therefore, we have designed the harvester structures to be symmetric so that the electrostatic constraint forces on the left- and right-hand sides are cancelled. As a result, we have achieved power generation of more than 1 mW at a high-power density with respect to the device volume and the excitation accelerations [12]. Electret potential must be precisely and swiftly monitored in the fabrication steps of a vibrational energy harvester because the device performances are heavily dependent on it. However, measurement of electret potential is not straightforward with a conventional surface electrometer primarily because of the poor spatial resolution to visualize the local potential distribution in a small gap between the comb electrodes, and secondarily because of its slow throughput of measurement. In this work, therefore, we have developed a new method to determine the electret potential with a high degree of accuracy and a high

Manuscript received December 14, 2019; revised February 17, 2020; accepted March 20, 2020. Date of publication March 26, 2020; date of current version May 5, 2020. This work was supported in part by the New Energy and Industrial Technology Development Organization, and in part by the Japan Science and Technology Agency Core Research for Evolutional Science and Technology under Grant JPMJCR15Q4. *(Corresponding author: Hiroyuki Mitsuya.)*

Hiroyuki Mitsuya, Hisayuki Ashizawa, and Noriko Shimomura are with R&D Center, Saginomiya Seisakusho, Inc., Saitama 350-1395, Japan (e-mail: hiro-mitsuya@saginomiya.co.jp).

Hiroaki Homma and Hiroshi Toshiyoshi are with the Institute of Industrial Science, University of Tokyo, Tokyo 153-8505, Japan (e-mail: hiro@iis.u-tokyo.ac.jp).

Gen Hashiguchi is with Mechanical Engineering, Shizuoka University, Hamamatu 432-8011, Japan (e-mail: hashiguchi.gen@shizuoka.ac.jp).

Color versions of one or more of the figures in this article are available online at http://ieeexplore.ieee.org.

Digital Object Identifier 10.1109/TSM.2020.2983442

ACS APPLIED MATERIALS & INTERFACES

www.acsami.org

Research Article

Temperature Sensor with a Water-Dissolvable Ionic Gel for Ionic Skin

Shunsuke Yamada* and Hiroshi Toshiyoshi

Cite This: ACS Appl. Mater. Interfaces 2020, 12, 36449−36457

Read Online

ABSTRACT: In the era of a trillion sensors, a tremendous number of sensors will be consumed to collect information for big data analysis. Once they are installed in a harsh environment or implanted in a human/animal body, we cannot easily retrieve the sensors; the sensors for these applications are left unattended but expected to decay after use. In this paper, a disposable temperature sensor that disappears with contact with water is reported. The gel electrolyte based on an ionic liquid and a water-soluble polymer, so-called ionic gel, exhibits a Young's modulus of 96 kPa, which is compatible with human muscle, skin, and organs, and can be a wearable device or in soft robotics. A study on electrical characteristics of the sensor with various temperatures reveals that the ionic conductivity and capacitance increased by 12 times and 4.8 times, respectively, when the temperature varies from 30 to 80 °C. The temperature sensor exhibits a short response time of 1.4 s, allowing real-time monitoring of temperature change. Furthermore, sensors in an array format can obtain the spatial distribution of temperature. The developed sensor was found to fully dissolve in water in 16 h. The water-dissolvability enables practical applications including healthcare, artificial intelligence, and environmental sensing.

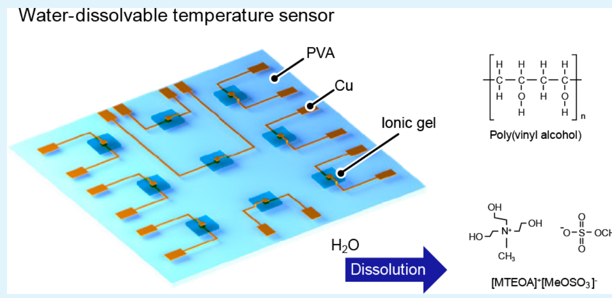

KEYWORDS: *temperature sensor, ionic liquid, poly(vinyl alcohol), electrical double layer, water dissolvable*

1. INTRODUCTION

In the era of a trillion sensors, a tremendous number of sensors will be consumed to collect information for big data analysis, including tactile,[1−5] temperature,[6−10] and biomimetic sensors.[11−13] Once they are installed in a harsh environment or implanted in a human/animal body, we cannot easily retrieve the sensors; the sensors for the above applications are required to be left unattended but disappear after use. One of the advantages of such a sensor is reduction of waste and cost. The self-disappearance is essential as well in terms of the elimination of the sensor retrieval from the human body to reduce the physical damage by the surgery. The biodegradable devices have been proposed by using organic and inorganic hybrid devices to obtain high functionality;[14−18] for instance, G. A. Salvatore et al. reported a temperature sensor based on biodegradable materials.[14] Such a sensor should disappear immediately after the prescribed time for data acquisition.[14,15] Water is abundant in the human body and the environment and can work as a trigger to decompose materials. One of the potential applications is agriculture. Environmental monitoring enables us to control the growth of vegetables and predict the time to harvest. Biodegradable temperature sensor embedded into the soil could eliminate the sensor retrieval because of self-dissolution. S. W. Hwang et al. utilized silicon, silicon dioxide, and magnesium to develop a biodegradable and bioresorbable implantable sensing system,[15] which gradually decomposed after contact with water. A chemical sensor and biosensor are crucial to detect chemical substances in a human body. Temperature sensor is also essential to calibrate the response of the sensors because the chemical sensors and biosensors shows temperature dependency.[19] Nevertheless, the conventional biodegradable temperature sensors show the small change of the resistance with respect to temperature owing to the small temperature coefficient for resistivity. Furthermore, a lack of the mechanical flexibility prevents the temperature sensors from applications to flexible and stretchable electronics.

Recently, researchers employed ions as a carrier for flexible devices, so-called ionic skin (i-skin).[20] Typical i-skin consists of a hydrogel and exhibits large mechanical deformation under a physical stimulus. Furthermore, most hydrogels are biocompatible in the human body, thereby enabling us to develop an implantable device for health monitoring. The conventional i-skin adopted hydrogel was subject to the evaporation of

Received: June 5, 2020
Accepted: July 7, 2020
Published: July 7, 2020

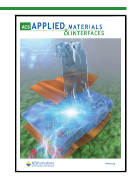

https://dx.doi.org/10.1021/acsami.0c10229
ACS Appl. Mater. Interfaces 2020, 12, 36449−36457

Negative-charge-storing mechanism of potassium-ion SiO_2-based electrets for vibration-powered generators

Cite as: Appl. Phys. Lett. **117**, 193902 (2020); doi: 10.1063/5.0029012
Submitted: 9 September 2020 · Accepted: 1 November 2020 ·
Published Online: 10 November 2020

Toru Nakanishi,[1,a)] Takeshi Miyajima,[1] Kenta Chokawa,[2,b)] Masaaki Araidai,[1,2] Hiroshi Toshiyoshi,[3] Tatsuhiko Sugiyama,[4] Gen Hashiguchi,[4] and Kenji Shiraishi[1,2]

AFFILIATIONS

[1]Graduate School of Engineering, Nagoya University, Nagoya 464-8603, Japan
[2]Institute of Materials and Systems for Sustainability, Nagoya University, Nagoya 464-8601, Japan
[3]Institute of Industrial Science, The University of Tokyo, 4-6-1 Komaba, Meguro-ku, Tokyo 153-8505, Japan
[4]Research Institute of Electronics, Shizuoka University, 3-5-1 Johoku, Naka-ku, Hamamatsu, Shizuoka 432-8011, Japan

[a)]Electronic mail: nakanishi.toru@e.mbox.nagoya-u.ac.jp
[b)]Author to whom correspondence should be addressed: chokawa@fluid.cse.nagoya-u.ac.jp

ABSTRACT

A potassium-ion electret, which is a key element of vibration-powered microelectromechanical generators, can store negative charge almost permanently. However, the mechanism by which this negative charge is stored is still unclear. We theoretically study the atomic and electronic structures of amorphous silica (a-SiO_2) with and without potassium atoms using first-principles molecular-dynamics calculations. Our calculations show that a fivefold-coordinated Si atom with five Si–O bonds (an SiO_5 structure) is the characteristic local structure of a-SiO_2 with potassium atoms, which becomes negatively charged and remains so even after removal of the potassium atoms. These results indicate that this SiO_5 structure is the physical origin of the robust negative charge observed in potassium-ion electrets. We also find that the SiO_5 structure has a Raman peak at 1000 cm^{-1}.

Energy-harvesting technology, which converts energy in the environment from sources such as light, heat, and vibration into electrical power, is a key element in meeting energy demands.[1–4] Many types of energy-harvesting devices have been proposed, and these include thermoelectric devices and vibration-powered generators. Such devices tend to have maximum power outputs of several μW to a few mW, and they, therefore, have had limited conventional uses. However, in recent years, the range of applications for energy-harvesting devices has expanded due to the development of low-power technology. In particular, maintenance-free autonomous power supplies are very important for the Internet of Things and the Trillion Sensors[5] initiative. Energy-harvesting technology has, therefore, attracted a significant amount of attention in relation to these technologies.

Among the many energy-harvesting technologies, vibration-powered generation is expected to provide a stable supply of electricity because its output does not depend on specific energy sources in the natural environment such as sunlight. Accordingly, vibration-powered generators can be widely used as stand-alone power sources for sensors in environments with vibration, such as transportation machinery, roads, and wearable devices.[6] Recently, a vibration-powered microelectromechanical generator with a potassium-ion electret has attracted increasing attention.[7–12]

The factor that contributes to the power output in vibration-powered generation is described by the change in capacitance. It is possible to create narrow gaps by using a potassium-ion electret and to produce large changes in the electrical capacitance, thus increasing the power output. This is referred to as vibrational acceleration. In addition, the lifetime of a potassium-ion electret has been estimated to be about 400 years by accelerated tests.[13] Therefore, a potassium-ion electret is superior to other electret materials.

A potassium-ion electret can be fabricated by adding potassium atoms to amorphous silica (a-SiO_2) and then subsequently removing them. A potassium-ion electret can permanently store a negative charge, and this enables the creation of maintenance-free power-generation devices. However, the mechanism by which this negative charge is stored in potassium-ion electrets is still unclear. In general,

scientific reports

Check for updates

OPEN

MEMS enabled miniaturized light-sheet microscopy with all optical control

Spyridon Bakas[1]✉, Deepak Uttamchandani[1], Hiroshi Toshiyoshi[2] & Ralf Bauer[1]

We have designed and implemented a compact, cost-efficient miniaturised light-sheet microscopy system based on optical microelectromechanical systems scanners and tunable lenses. The system occupies a footprint of 20 × 28 × 13 cm^3 and combines off-the-shelf optics and optomechanics with 3D-printed structural and optical elements, and an economically costed objective lens, excitation laser and camera. All-optical volume scanning enables imaging of 435 × 232 × 60 µm^3 volumes with 0.25 vps (volumes per second) and minimum lateral and axial resolution of 1.0 µm and 3.8 µm respectively. An open-top geometry allows imaging of samples on flat bottomed holders, allowing integration with microfluidic devices, multi-well plates and slide mounted samples, with applications envisaged in biomedical research and pre-clinical settings.

Over the last decade, light-sheet microscopy (LSM) has established itself in the fluorescence microscopy field as a fast 3D imaging technique with reduced background signal and lower photobleaching rates compared to the most commonly used approaches such as widefield fluorescence microscopy and confocal microscopy. These features originate from a spatial de-coupling of fluorescence excitation and imaging by using a sheet excitation of fluorescence in the focal plane of the imaging objective, allowing a full field read-out while exciting only a thin slice of a sample[1–3]. In general, LSM variants employ an excitation sheet generation through either cylindrical lenses or linear scanning of Gaussian or non-diffracting beams. Cylindrical lenses focus a Gaussian beam in only one axis, creating a reshaped thin slice of light in a design known as selective plane illumination microscopy (SPIM)[1,3,4]. Even though SPIM and its derivatives have shown good results for various imaging questions[4,5], they suffer from non-uniformity of the intensity profile of the light-sheet due to the Gaussian beam profile and allow less control over the excitation beam. Creating the light-sheet through scanned excitation is known as digital scanned light-sheet microscopy (DSLM) in its original representation and introduces a pivoting mirror in the illumination path[2,3,6]. The excitation beam gets reflected off a fast-rotating mirror, resulting in a scan line which is then focused down to the sample area. With this method the light-sheet can achieve a much more uniform intensity profile that can be tailored to the desired field of view (FOV) with the control of the mirror. These initial demonstrations have opened the door for a vast, growing field of system demonstrations for increasing imaging speed, resolution and adaptability, with notable examples being work on using non-diffracting beams for thinner light-sheets with wider FOV[7,8], super-resolution approaches to improve specifically axial resolution limits from light-sheets[9,10], single objective light-sheet approaches such as oblique plane microscopy[11], SCAPE[12] or SOPi[13] and multi-photon approaches[14]. In most variations, z-stacks are acquired by stage scanning approaches to create 3D data volumes, allowing for a pre-determined fixed alignment position between the two orthogonal excitation and detection light paths. This however limits imaging speeds to avoid movement artefacts, specifically in non-fixed samples. This limitation has been circumvented to an extent with mirror based volume scanning in SCAPE and adaptive optics elements for accessing different 3D image planes[15,16]. A further limitation requiring, in most LSM systems, special sample holders due to the spatial constraints of orthogonal objectives has in recent years been addressed by moving to open-top configurations with solid or water based immersion lens geometries[17–19] or the mentioned single objective variants[11–13] to allow investigations using samples in standard microscope slides and cover slips, cell dishes or well-plates.

Even though LSM has established itself as one of the main tools in fluorescence imaging for larger biomedical samples, its use can be limited due to the high cost for designing or purchasing an LSM imaging system. Additional limitations occur due to most LSM approaches targeting specific applications. As a result, the designs are not easily transferable between different studies, where a complete reconsideration of sample holders and optical path adjustment needs to be made. A few attempts have managed to make LSM more accessible by providing

[1]Department of Electronic and Electrical Engineering, University of Strathclyde, Glasgow, UK. [2]Institute of Industrial Science, University of Tokyo, Tokyo, Japan. ✉email: Spyridon.Bakas@strath.ac.uk

IOP Publishing Journal of Micromechanics and Microengineering

J. Micromech. Microeng. **31** (2021) 125008 (11pp) https://doi.org/10.1088/1361-6439/ac2e46

Power enhancement of MEMS vibrational electrostatic energy harvester by stray capacitance reduction

Hiroaki Honma[1,*], Yukiya Tohyama[1], Hiroyuki Mitsuya[2], Gen Hashiguchi[3], Hiroyuki Fujita[4] and Hiroshi Toshiyoshi[1]

[1] Institute of Industrial Science, The University of Tokyo, Meguro-ku, Tokyo 153-8505, Japan
[2] Saginomiya Seisakusho, Inc, Shinjuku-ku, Tokyo 169-0072, Japan
[3] Department of Mechanical and Engineering, Shizuoka University, Hamamatsu, Shizuoka 432-8011, Japan
[4] Advanced Research Laboratories, Tokyo City University, Setagaya-ku, Tokyo 158-0082, Japan

E-mail: honma-hh@iis.u-tokyo.ac.jp

Received 31 March 2021, revised 5 October 2021
Accepted for publication 8 October 2021
Published 27 October 2021

Abstract

We report a design method to enhance the output power of vibrational microelectromechanical system (MEMS) electrostatic energy harvesters by reducing the reactive power that does not contribute to the net output. The mechanism of enhancing the active current while reducing the reactive current is analytically studied using an equivalent circuit model of electret-based velocity-damped resonant-generator. Reduction of the internal parasitic capacitance associated to the contact pads and electrical interconnections significantly improves the power factor and increases the deliverable power. The design strategy is applied to an actual device that produces 1.3 mW from the vibrations of 0.65 G (1 G = 9.8 m s^{-2}) at 158 Hz, suggesting a 2.9-fold enhancement of output power by increasing the buried oxide layer thickness from 1 μm to 3 μm.

Keywords: MEMS, IoT, vibrational energy harvester, electret, reactive power

(Some figures may appear in colour only in the online journal)

1. Introduction

Energy harvester is a vital component as an autonomous power source for wireless sensor nodes in the coming internet-of-things (IoT) era [1]. Owing to the escalating demands for real-time monitoring capabilities, such wireless systems are expected to operate around the clock for a long time beyond the capacity of batteries [2–4]. This is where energy harvesters are used to supply extra power from the ubiquitous environmental energy sources such as light [5], heat [6], and vibrations [7].

Environmental vibrations are usually seen in the frequency range lower than 200 Hz and the acceleration range smaller than 1 G (=9.8 m s^{-2}) [8, 9], and they can be converted into electricity through a mechano-electric transduction mechanism such as piezoelectric effect [10–15], electromagnetic induction [16–21], and electrostatic induction [22–33]. Amongst them all, energy harvesters of electrostatic induction using the permanent electrical charge or so-called electret [34] are suitable for microelectromechanical systems (MEMS)-type implementation because of the technological compatibility with silicon micromachining processes using deep reactive ion etching (DRIE) of a silicon-on-insulator (SOI) wafer [35].

Figure 1(a) schematically shows the representative electrodes structure of electrostatic-type vibrational energy harvester [36]. The movable electrode with multiple protrusions is suspended in the gap between the fixed electrodes so that the sliding motion changes the overlapping area of the electrodes' side walls. Provided that the electret film is negatively

[*] Author to whom any correspondence should be addressed.

KAWAKATSU Laboratory

Current Research Activities 2020-2021

Kawakatsu Laboratory

1. Research Topics

1.1 Colour Atomic Force Microscopy with Chemical Contrast

In this project, the AFM cantilever is oscillated at 2 MHz, and the tip-sample distance is modulated at 1kHz. By employing such modulation techniques, the potential landscape is detected as the frequency shift of the cantilever. Three effective Morse parameters are calculated per pixel to best curve fit the measured values. The work was published in 2017 on APL and was selected as the editor's pick. In 2019, discussions on the control scheme as well as results on imaging of solder was published in JJAP.

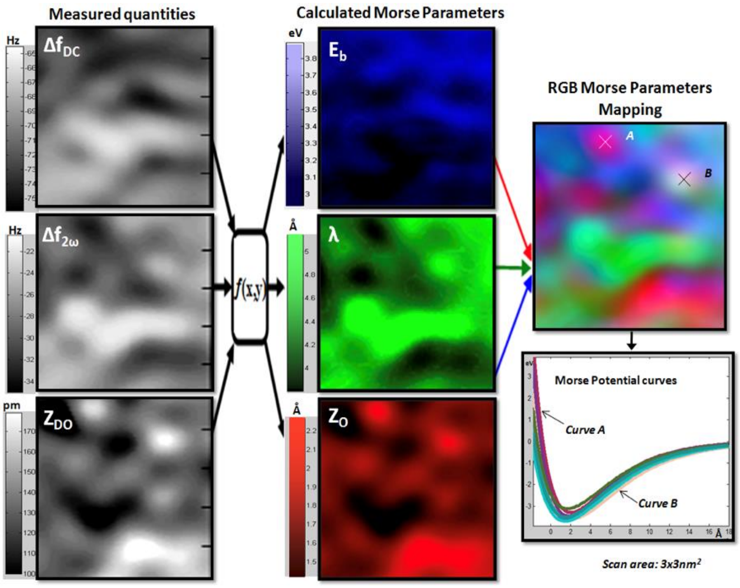

Figure 1. Effective Morse Parameters represented in RGB obtained from modulation of the tip sample distance. The sample was quenched Si(111). Cantilever Oscillation 2MHz.

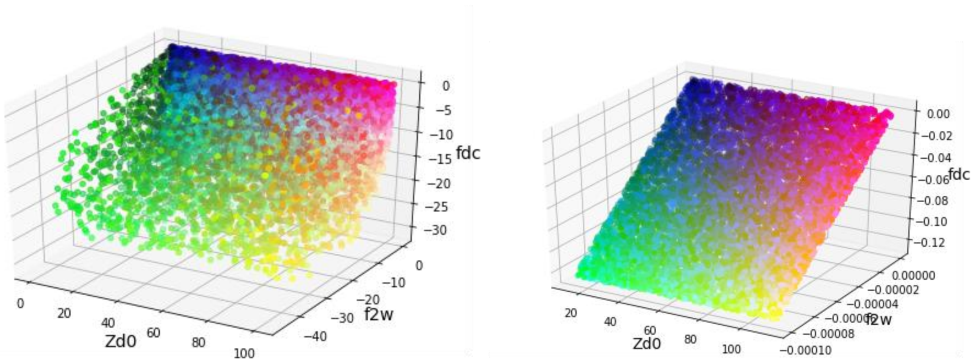

Figure 2. Study on uniqueness of conversion, conversion efficiency and expected resolution of the effective Morse parameters.

1.2 Theoretical Studies on Colour Atomic Force Microscopy

Following the successful implementation of Colour Atomic Force Microscopy, we have conducted theoretical studies on the physical meaning of the acquired data and issues governing quantitativity. Such issues as (i) the uniqueness of calculation of the effective Morse parameters, (ii) error factors, (iii) calculation efficiency, and (iv) resolution of the effective Morse parameters were studied. Figure 2 depicts examples of how raw data are converted to effective Morse parameters expressed as coloured dots, where the colours are generated from RGB values assigned to each Morse parameter.

1.3 Functionalisation of the AFM tip apex with thiol tripod structured molecules

Adamanitine-3-thiol (ATT) molecules are a new candidate for functionalizing AFM tip apexes due to their size, stability and their chemical bonding to the AFM tip. The molecules are synthesized by Professor T. Kitagawa of Mie University. Two projects are running under this topic. One is the macroscopic measurement of the range of stable operation with the ATT tips. Second is the simulation on tips functionalized with the ATTs when used for atomic force microscopy. Various functionalization schemes are studied. For the first experiment, quartz oscillators with gold electrodes are used for self-assembled monolayer growth of ATTs. The frequency of oscillation of the quartz oscillators, which lie in the range of 1MHz to 10MHz are monitored as a function of temperature in air and in vacuum to assess the detachment temperature of the molecules from the gold surface. Following the study on the optimal size of the molecule used for tip functionalization, we are accessing methods to functionalise the tip apex. Various tip functionalisation schemes are studied, together with simulations of force fields detected by such tips.

1.4 Atomic resolution AFM in ambient conditions

There is a growing demand for implementation of an atomic resolution AFM in ambient conditions. In collaboration with a major watch manufacturer, we are implementing an ultra-stable AFM. Photothermal excitation efficiency was mapped by scanning a focused laser beam on a tuning fork. Excitation laser was introduced to the tuning fork from different directions to induce various vibration modes.

1.5 Joint research with Tohoku University.

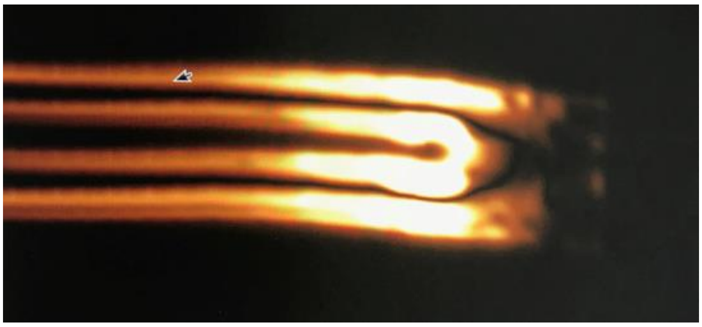

Figure 3. Visualisation of electrical output when the optical excitation laser spot at 405 nm wavelength was scanned over the tuning fork.

Conductive polymers have been known to show accumulation of humidity in air. This project is a collaboration with Professor Hikaru Kobayashi of Tohoku University. We focused on various design for removing humidity from air, as well as improving conductance of the functional polymers and its deterioration due to current, heat and exposure to light.

1.6 High slew rate circuit for ultra-high rigidity friction drives.

A new circuit was developed to allow the use of large surface area piezo-elements for unprecedented high rigidity and stability in SPM heads. UHV and ambient condition AFMs were implemented based on this driving principle.

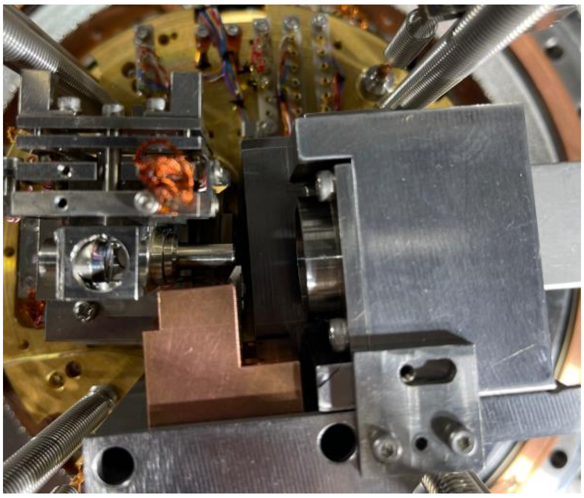

Figure 4. Improved Colour AFM head for higher rigidity and stability. From left to right, objective lens, cantilever holder, sample stage and coarse positionner.

1.7 Incubation chamber with Double spring suspended stage for gamete sound and vibration detection

High sensitivity detection schemes of AFM were applied to sound and vibration measurement of gametes. An incubation chamber equipped with O2, CO2 and temperature control was implemented to house a double spring suspended stage enabling ultra-quiet environment for detection of egg cleavage and force/sound measurement of sperms.

1.8 Schlieren Microscopy for visualization of flow for assisted reproduction technology studies.

Sperms are known to show motility affected by flow, temperature and chemicals. The terms given to these behaviours are rheotaxis, thermotaxis and chemotaxis. Schlieren microscopy adapted to observation of motility of sperms in a micro fluidic cell was implemented to allow observation of flow with different refractive index from its surroundings.

1.9 MakerSpace related activities

With a view to developing initiative and collaboration among students, emphasis was placed on founding a new MakerSpace at IIS. A joint workshop and invited talks were organised with Professor Woody De Yu Wang of iCenter , Tsinghua University.

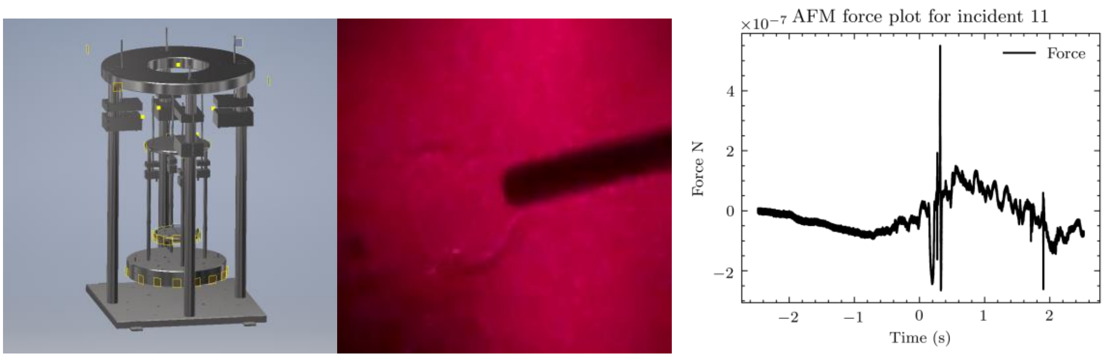

Figure 5. (a) Double suspension stage to house a gamete sound/vibration detection system, (b) Schlieren micrscopy of chemical attractant from a pipette, and (c) force and vibration caused by swim-by of a micro-organism near an AFM cantilever .

2. Research Achievements

2.1 Number of original journal papers: 2 (not accounted in last report)

2.2 International conference: 2 (including 2 invited presentations)

2.3 Domestic conference: 2

2.4 Number of patents: 0

3. List of awards

4. Research Grants

4.1 Total number of research grants: 3

4.2 Number of collaboration research with industry: 4 (not excluding non-Grant based collaborations)

5. Education

5.1 Number of Ph.D. students :0

5.2 Number of master students: 1

5.3 Number of other students: 1

6. Publication list

Journal Papers (selected)

1) "Bottom tracking: The possibilities and physical meaning of keeping the bottom of the frequency shift in atomic force microscopy" , D. Damiron, P. Allain, N. Sasaki, D. Kobayashi and H. Kawakatsu, Japan. Journal of Appl. Phys. https://iopscience.iop.org/article/10.35848/1347-4065/ab9231 (published after last report).

2) “High slew rate circuit for high rigidity friction drive”, D. Kobayashi and H. Kawakatsu, Japan. Journal of Appl. Phys. https://doi.org/10.35848/1347-4065/ab887f (published after last report).

3) “Innovation of the Driving Method and thereby Improvement of Frictional Fine Positioning System”, Dai Kobayashi and Hideki Kawakatsu, Seisan-Kenkyu 73-5(2021).

Conference Presentations (selected)

1) “Makerspace related education trials at the Precision Engineering Department”, iCenter Design Workshop 2021 “Hit Innovation, Hit the Future” (Inivited, Innovative Education Forum).

2) “Application of Atomic Force Microscopy detection schemes to mechanical detection of bio-samples”, The Fifth International Symposium on “Elucidation of Property of Next Generation Functional Materials and Surface/Interface”, Oct. 7th – 9th, Osaka, Japan. (Invited, On-line participation).

Japanese Journal of Applied Physics **59**, SN1008 (2020) **REGULAR PAPER**
https://doi.org/10.35848/1347-4065/ab887f

High slew rate circuit for high rigidity friction-drive

D. Kobayashi* and H. Kawakatsu*

Centre for Interdisciplinary Research on Micro-Nano Methods (CIRMM), Institute of Industrial Science, The University of Tokyo, Komaba 4-6-1, Meguro 153-8505, Japan

*E-mail: dai@iis.u-tokyo.ac.jp; kawakatu@iis.u-tokyo.ac.jp

Received January 27, 2020; revised March 18, 2020; accepted April 10, 2020; published online May 5, 2020

In various fields of research and development in the nanometre regime, a rigid and robust positioning device with nanometic resolution is indispensable. Rapid movement of the piezo-element to induce high shear or propulsive impulse has become one of the widely used mechanisms. The piezo-elements used for this impulsive lateral movement often serve as mechanical support of the moving object, and since they tend to be the narrowest path in the mechanical loop, their rigidity is of great importance in implementing a device with high natural frequency and mechanical stability. The paper presents circuitry to drive such piezo-elements with comparatively larger surface area and higher capacitance with high transient current and slew rate. The circuit could drive a capacitive load of 100 nF, corresponding to 90 cm^2 of the piezo-element, from 0 to 200 V in 1 μs, with a peak current of up to 100 A.

1. Introduction

In implementing an extremely rigid and stable scanning probe microscope (SPM) head, the coarse positioning mechanism has the possibility to become one of the weakest component in the mechanical loop between the tip and the sample. This is because the elements, such as piezo-elements used in coarse positioning mechanisms are usually smaller than the metal objects used in the SPM head, and are liable to decrease the entire rigidity and natural frequency. The so-called friction-drive or impact-drive are one of the most commonly used coarse positioning mechanisms in SPM. The mechanism uses static friction to keep the positioning point, and an acute impulsive force or shear motion of the piezo-element to achieve incremental motion. The natural frequency between the tip and the sample needs to be kept high because the servo bandwidth used to maintain a constant tunnelling current in scanning tunnelling microscopy (STM)[1] or force in atomic force microscopy (AFM)[2] is limited by this natural frequency. Such requirement is equally true for all kinds of microscopy and nano fabrication where the relative position of two objects to be positioned, such as the tip and the sample, needs to be stable up to a few kHz or even up to the 100 kHz range. As a simple but effective design rule, we propose the use of non-stacked shear piezo-elements with large surface area to achieve the goal. Many merits, such as mechanical stability, longevity,[3] and high natural frequency are brought about by this design guideline. One possible drawback, however, is the increased capacitive load due to the larger area of the piezo-element, and the increased requirements on the circuit. This paper addresses the circuitry that enable high driving current and short transient time of below 1 μs to achieve the goal for a wide range of SPM head design with larger piezo size and capacitive load.

Many incremental positioning devices used for coarse positioning of the scanning tip or the sample were proposed in the 1980s following the invention of the STM. Figure 1 depicts some of the major configurations. Figures 1(a)–1(c) depicts the basic designs. The basic principle of these mechanisms is to apply a saw tooth or a cycloidal voltage signal to the piezo-element, where the rapid movement of the piezo-element induces the sliding surfaces to slide against one another, resulting in an incremental step motion of the slider. The design of Fig. 1(a) uses rapid shear motion of the piezo-element to induce lateral displacement between the two sliding surfaces.[4] This paper will mainly focus on this design. The design of Fig. 1(b) uses a piezo-element to rapidly displace a guide rail where the slider rests.[5–8] This design has been used in cryostats. The design of Fig. 1(c) supports mass m2 in a piggie-back configuration.[9] Rapid deformation of the piezo-element exerts an impulsive force on the main mass m1, causing m1 to slide against the stator. Figures 1(d)–1(f) are variants of the former designs, though some were developed independently. The design of Fig. 1(d) uses a wedge to convert horizontal motion to vertical displacement.[10] Its merits are high payload and vertical rigidity. Application of the design of Fig. 1(c) with a wedge can also be found in the literature. The design of Fig. 1(e) has multiple legs. The design can be operated in both the inch-worm mode and the friction mode.[11] The design of Fig. 1(f) uses wedged surfaces to generate vertical motion of mass m1. Most common is the Beetle type STM,[12,13] where the wedges are positioned at 120° intervals in a spiral fashion. Generally speaking, basic requirements of the coarse positioning mechanism are; (i) stable incremental motion of about 10–100 nm resolution, (ii) no creep and low drift after positioning, (iii) low or no heat emission after positioning, (iv) high rigidity or high natural frequency, (v) possibility to move against gravity, (vi) operation in UHV and low temperature, and (vii) low or no electro-magnetic noise emission after positioning.

Many designs sought to fulfil the above requirements, with some excelling in certain aspects. The sliding surface is composed of a group of multi-asperities in contact with each other. Each asperity supports a part of the normal load N, and shows elastic deformation that rupture when put under lateral displacement in the nm order. What is often overlooked is the glue used to attach the piezo-elements to the slider or the stator. Ideally, the glue should be negligibly thin, with extremely high rigidity. However, in reality, the glue, such as epoxy, is more compliant than other mechanical components such as the piezo-element or the massive metal parts. Since the displacement employed is in the 10 nm regime, the lateral compliance of the glue and the multi asperity contact can not be overlooked. The layers of glue are not drawn in Fig. 1, but their presence is known to affect performance, namely, malfunction and asymmetry of performance depending on direction of movement.

There are designs using other types of force or displacment generating mechanisms. For example, a piezo-disk with

Japanese Journal of Applied Physics **59**, SN1012 (2020) **REGULAR PAPER**
https://doi.org/10.35848/1347-4065/ab9231

Bottom-tracking: the possibilities and physical meaning of keeping the bottom of the frequency shift in atomic force microscopy

Denis Damiron[1,2], Pierre E. Allain[1,2,3], Dai Kobayashi[1], Naruo Sasaki[4], and Hideki Kawakatsu[1,2*]

[1]Centre for Interdisciplinary Research on Micro-Nano Methods, Institute of Industrial Science, The University of Tokyo, Komaba, Tokyo 153-8505, Japan
[2]LIMMS CNRS-IIS/UTOKYO UMI 2820, Tokyo, 153-8505, Japan
[3]Matériaux et Phénomènes Quantiques, Université de Paris and CNRS, 75013 Paris, France
[4]The University of Electro-Communications, Chofu, Tokyo 182-8585, Japan

*E-mail: kawakatu@iis.u-tokyo.ac.jp

Received January 31, 2020; revised April 19, 2020; accepted May 11, 2020; published online May 29, 2020

In ultrahigh vacuum atomic force microscopy, the frequency of an oscillator holding the scanning tip takes a typical Lennard–Jones like curve with a local minima just before contact. We demonstrate here the application of a control scheme to keep this local minima, or the bottom of the frequency shift curve (FC) as the working point for imaging in UHV, and discuss its physical meaning and possible applications. Tip-sample distance modulation and Lock-in detection were used to obtain the gradient of the FC, where null control of the gradient signal resulted in implementing the designated control. Atomic resolution was confirmed for Si(111) and solder. The histogram of minimum frequency shift on the apex of atomic features on solder showed two to four peaks, implying the ability of the method to map characteristic differences of the depth of the FC per site. The method is an alternative to the existing constant-frequency-shift mode and constant-height mode, with the possibility to access chemical information on-the-fly.

1. Introduction

In dynamic mode atomic force microscopy (AFM),[1] the probing tip is held by an oscillator such as a cantilever[2] or a tuning fork.[3] The frequency modulation (FM) mode[4] implements self-excitation of the oscillator where the frequency is determined by the oscillator and the field where the tip is placed. As the tip is approached towards the surface of the sample, in the FM mode, the frequency of oscillation takes a negative frequency shift from its original value, and then changes to positive frequency shift just before contact. The constant-frequency-shift mode[5] sets the working point at a designated value of frequency shift, and this frequency is maintained by active control of the tip-sample distance. In this mode, the working point has to be chosen on a fixed slope of the frequency shift curve (FC). This is to ensure that the change in the mean tip-sample distance can be determined from the increase or decrease of the oscillation frequency. During operation, the mean tip-sample distance should not cross the local minima or the "bottom" of the FC, since that may lead to irreversible damage to the tip due to tip-sample distance regulation functioning in the wrong direction. Due to the well-defined apex, and due to the reduced volume of the tip, molecular terminated tips[6] are becoming increasingly important for ultrahigh resolution imaging and quantitative force spectroscopy.[7] The very low background force of such tips is in itself a merit, but the resulting FC has a very shallow FC well, of only a few Hz. This resulted in the common use of the constant-height mode,[8] where active tip-sample distance control is deactivated, and the frequency of oscillation mapped for imaging and force spectroscopy. Two issues related to the constant-height mode are; (i) any drift, such as thermal drift or creep of the piezo elements may result in tip crash or the tip becoming too far away from the sample, and (ii) imaging is possible within the amplitude of drive of the oscillator. Due to this reason, it is not well adapted for high corrugation samples. Working in a cryostat where drift is minimal ensures an ideal environment. The constant-frequency-shift mode, which is widely used for conventional tips is more difficult to use on very sharp molecular terminated tips exhibiting a small FC well, since setting the working point close to the bottom of the FC is liable to cause malfunction of the control direction.

To overcome the limitations listed above, and to introduce a few merits, we propose setting the working point at the local minima or "the bottom" of the FC. The mode will be called "Bottom-tracking" mode for simplicity. In this mode, a small position modulation amplitude or dither amplitude is applied to the tip-sample distance, and lock-in detection is used to measure the gradient of the FC. Since the bottom of the FC corresponds to the zero-crossing of the gradient signal, this null point can be chosen as the working point, and accidentally crossing the bottom of the FC will no longer cause problems.[9] Application of such method can be found for liquid AFM.[10] Though atomic resolution has not been confirmed, it is worth mentioning that a local minima of frequency shift was observed to allow use of the technique in liquid. Position modulation techniques in the vertical or lateral directions can be found in the literature.[11–17]

Although it is not hard to imagine that force at the atomic level may be the fingerprint of the atomic species and the characteristics of interatomic interactions,[18] it was not until 2001 that such expectations were experimentally confirmed with the AFM.[19,20] Force measurement evolved into 3D mapping of the force and potential landscape.[21,22] In 2007, it was shown that the ratio of the minimum force can be used to distinguish three known elements on the surface.[17,23] When we look into other techniques, identification is often based on spectroscopy of basic physical properties such as energy loss and mass. This ensures higher quantitativity. To name a few, (i) transmission microscopy with EELS,[24–27] (ii) atom probe,[28–30] (iii) X-ray diffraction,[31,32] (iii) scanning electron microscopy with XPS,[33] (iv) non-contact AFM with IR or NMR spectroscopy,[34,35] (v) TOF-SIMS,[36] and (vi) TOF-AFM.[37] If AFM is to enjoy widespread use as microscopy with chemical contrast, and coexist with other existing techniques, one would need to exploit such merits of AFM as the ease of sample preparation and the ability to

研 究 速 報

摩擦式微動機構の新しい駆動方式とそれによる性能向上

Innovation of the Driving Method and thereby Improvement of Frictional Fine Positioning System

小 林　大*・川 勝 英 樹*
Dai KOBAYASHI and Hideki KAWAKATSU

1. は じ め に

圧電素子はナノメートルオーダーの精密位置決めに不可欠であるが個々の素子のストロークは高々数マイクロメートルに過ぎないため，可動距離が長い別のアクチュエータを併用する場合も多い．図1に示す摩擦式微動機構は，静摩擦と動摩擦の係数の差と圧電素子の急速変形を利用してステップ状の移動を繰り返すアクチュエータであり，原理的に移動距離の制約を持たない．インパクト・ドライブ・アクチュエータ（図1(a)）はカウンターマスが付いた圧電素子をゆっくり縮めてから急速に伸ばすことで，ハンマーでタップして物体を少しずつ移動させるのに似た動作をする．図1(b) はせん断変形型の圧電素子を負荷の下面に接着したタイプで，負荷をゆっくり右に移動させた後圧電素子の変形を急速に元に戻す．この時反力が圧電素子と床の間の静止摩擦を超えると負荷が元の位置に戻らず少し右に進む．摩擦を利用した歩進動作は，直動のみならず回転位置決めに応用したものも含め複数の例が見られる[1)-17)]．本稿では (b) のタイプを念頭に駆動回路について論じるが，種々のバリエーションに対しても適用可能である．

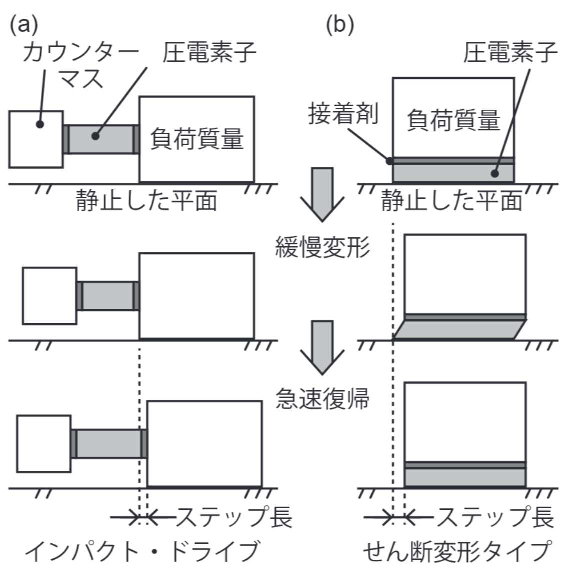

図1　摩擦式微動機構の例[1)-6)]

*東京大学生産技術研究所　機械・生体系部門

2. 駆動回路に求められる特性と課題

図2(a) と (b) に摩擦式微動機構の典型的な駆動電圧と電流の波形を示す．本稿ではサイクル中の4つのフェイズを仮にP1からP4と名付けることにする．微動機構を逆方向に移動させる場合も含めて電流と電圧の軌跡を図示すると図2(c) のようになる．電圧振幅は経験上少なくとも100 Vは必要であり，摺動面の状態が悪く摩擦係数が増加している場合も考慮すると250 Vまで掛けられると望ましい．圧電素子は電気的にはほぼ静電容量なので，P2期間とP4期間はそれぞれ充電と放電に相当し，P4期間にいかに速く放電できるかは駆動回路の電流容量に制約される．

筆者らは経験上，P4期間の放電時間は数μs程度，摺動面の状態が悪い場合も考慮すると1 μs以内が望ましいと考えている．しばしば5 mm × 5 mm程度の圧電素子を3個使用して3本脚で負荷を支える設計が見受けられるが，圧電素子の静電容量の合計を1 nF程度と見積もると，1 μs以内に放電するための電流値は200 mA以上になる．

筆者らが以前製作した20 mm × 15 mmの圧電素子1枚を使った摩擦式微動機構の場合静電容量は4 nF程度であり，放電電流は800 mA程度必要である．この微動機構の摺動面は鋼材とベアリング用のニードルローラーの組み合わせで，約20年間空気に晒されているが固着せずに動作する[18)]．これは圧電素子の面積が広いことが有利に作用するためと考えられる．図1(b) のタイプの摩擦式微動機構は負荷全体が接着層の上に乗っており，P4期間に圧電素子の変形速度がいかに速くても摺動面に発生できる最大のせん断力は接着剤のばね定数と圧電素子の変形量の積を超えられない．したがって圧電素子の面積は広いほうが接着面積が増大し摺動面の状態に対しロバストになると考えられる．現在計画中の装置では100 nFに達する大面積の圧電素子を使用する予定であり，放電電流は20 Aに達する．

図3(a) に示すように低電圧のランプ波形発生回路と市販の高電圧パワーアンプを組み合わせて駆動回路を実現す

KIM Laboratory

Current Research Activities 2020-2021

B.J. KIM Laboratory

1. Research Topics

Our research goals are to build smart nanosystems and integrate nanoscale components in micro sensors, in particular for environment, bio-sensing, through both bottom-up and top-down approaches. We focus on interdisciplinary research about local "bottom-up" surface modification using functional self-assembled monolayers and "top-down" approaches for micro/nano patterning technologies. Based on these studies on nano/micro components systems for the fabrication of novel nano devices, we investigate to develop various micro sensors for biological applications, health care as well as environmental monitoring.

In the transdermal drug delivery methods, **the microneedle-mediated drug delivery system (DDS)** has been developed to replace the hypodermic injection-mediated DDS, to provide painless self-administration of biological drug with patient friendly manner. Dissoluble microneedles are attracting much attentions as it has several advantages such as no needle-related risks. We have developed new fabrication method for biodegradable microneedles patches, which is different with the conventional fabrication ones, such as stepwise casting method. We anticipate that shadow mask assisted drawing lithography as well as 3D printing based novel mass fabrication methods, will be suitable to improve the fabrication throughput of dissoluble microneedle for new generation of drug delivery system.

On the other hands, we observed the permeability of several commercially-available microneedle patches for cosmetic purposes to human skin and investigated methods of evaluating permeability to the stratum corneum, and its' degree of pain.

1.1 Dissoluble Microneedle patch for transdermal drug delivery systems

The transdermal drug delivery has experienced several-generation revolutions: From the transdermal delivery of small, lipophilic, low-dose drug to the delivery system using chemical enhancer, non-cavitational ultrasound and iontophoresis. With the development of the micro-scale engineering, microneedles show the potential to be the next generation delivery system. The microneedle mediated drug delivery system has been developed to provide painless self-administration of biological drug with patient friendly manner. Especially, dissolving microneedles, which deliver the target drugs as the drug-loaded microneedle dissolves into the skin, have been spotlighted recently. We investigate a novel fabrication method to achieve the user-friendliest, low-cost, and safest way for dissoluble microneedle patches with vaccine delivery and several medical treatments.

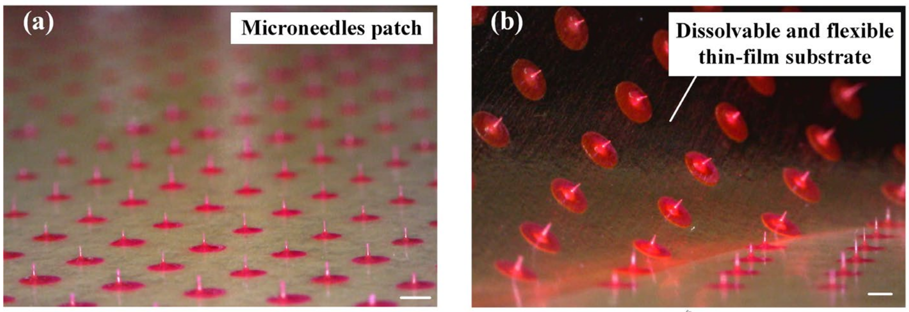

Fig. 1: *Dissoluble microneedles of Hyaluronic acid with red dye for transdermal drug delivery.*

1.2 Porous Microneedle for Self-testing diagnostic Bio-sensing

The porous microneedles are expected to have great potential for diagnostic application due to their ability to penetrate human skin painlessly and extract interstitial fluid (ISF) by capillary action. However, the prior approach about porous microneedles had not directly integrated sensor system as an application due to the small amount of sample porous microneedle can absorb. Here, we fabricated porous microneedle on a paper substrate to develop a novel platform for direct integration of sensors.

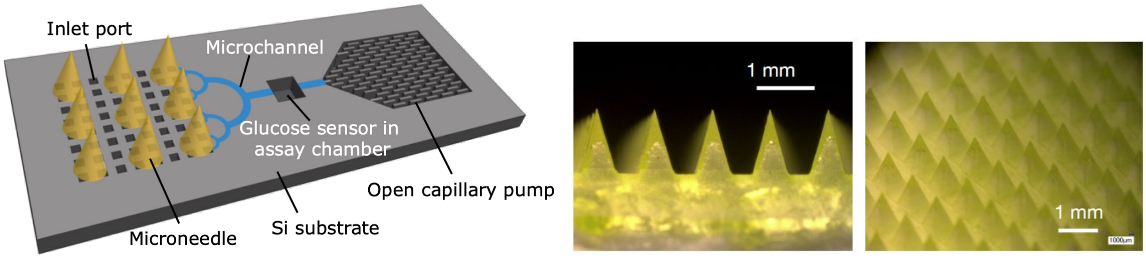

Fig.2: *Schematic of minimally invasive glucose monitoring system (left) integrated with an array of PDMS porous microneedles (right) in a microfluidic chip.*

ISF is a promising bio-sample since it contains a wide range of common biomarkers to blood such as glucose. In order to utilize ISF for continuous healthcare monitoring, ISF sampling is a key technology. However, the conventional ISF sampling technologies such as microdialysis have several drawbacks including highly invasive operation and limited measurement methodologies. Among the MNs, porous MNs have advantages such as applicability to fluidic systems and to biocompatible materials. Although the porous MNs were applied to ISF sampling, continuous ISF sampling has not been realized. For this, a new type of porous MN should be developed to address the challenges of mechanical and fluidic requirements for successful insertion into the skin and ISF extraction continuously. Furthermore, the microfluidic chip should also be realized to interface the porous MNs and realize a continuous flow of ISF, which is ideally at a flow rate of 0.08 μL/min.

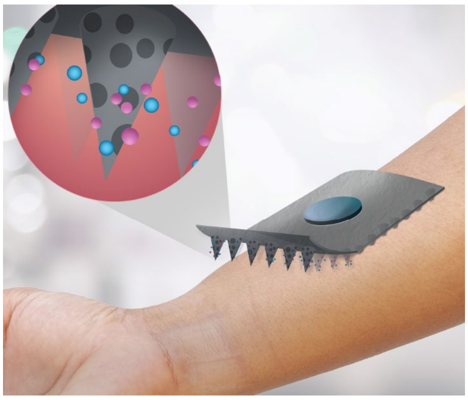

Fig.3*: Porous microneedle-on-paper device with a simple colorimetric sensor can painlessly measure glucose levels from interstitial fluid in the skin.*

One of the core targets is employing the micro-electro-mechanical systems (MEMS) fabrication technologies to the bio-degradable materials, then realizing specific structures, such as free-standing membrane, ultra-thin transparent film, etc. Therefore, our aim is to employ micro-nano technology to accurately control and deeply investigate the bio-degradable materials at micro/nano level, and develop novel materials for multiple application fields, such as biomedical field and energy harvesting.

As the power sources of wireless sensors, batteries are mainly utilized until now. These days, devices of energy harvesting become more focused. **Energy harvesting** is a methodology of scavenging power from ambient energy sources such as solar, thermal and vibration without the need for batteries.

In 2012, a novel energy harvesting approach was proposed and named TENG (**Triboelectric Nano Generator**), which is based on the combination of electrification effect and electrostatic induction. Due to remarkable properties, such as high-performance and the use of environmentally friendly materials, TENG has raised increasing interest. Several techniques have been developed to enhance the power density, including structural optimization, operation mechanism, surface texturing and hybrid TENG.

Herein, we propose a very simple and cost-efficient approach to fabricate high-performance TENG based on paper and graphite pencil. Moreover, we propose a novel device, which can utilize ambient vibration with wideband and low frequencies. Due to high stiffness of piezo electric energy harvesters, resonant frequency of the piezo electric energy harvesters tends to be much higher than ambient vibrational frequency. To solve these problems, the proposed energy-harvesting device is to utilize a stochastic resonance.

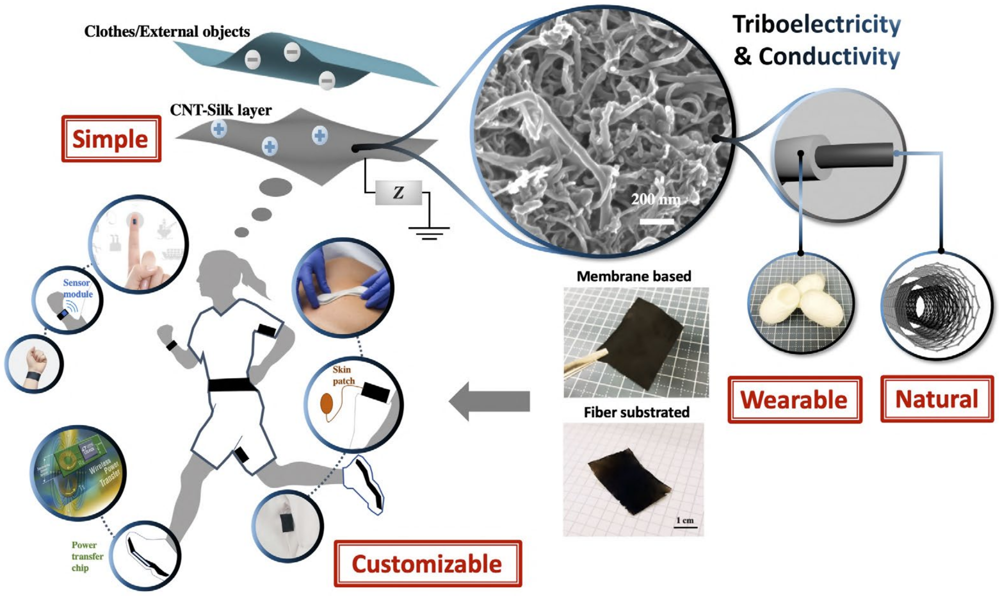

Fig. 4: *Wearable TENG device of the electro-sprayed silk fibroin fiber mixed with carbon nanotubes.*

This high-output energy harvester shows the attractive potential in the integrated flexible electronics and wearable device.

2. Research Achievements

2.1 Number of original journal papers: 11 (110 total, 6 in review)

2.2 International conference: 17 (including 1 best paper awarded),

2.3 Domestic conference: 15

2.4 Number of patents: 4 (15 total)

3. Research Grants

3.1 Total number of research grants: 7 (2020-2022)

3.2 Number of collaboration research with industries: 5

3.3 List of major research grants (serving as Principal Investigator)

- JSPS Core-to-Core A, JETMeE project, AMED 橋渡し研究戦略プログラム.

4. Education

4.1 Number of Ph.D. students (including current students): 13(4)

4.2 Number of master students (including current students): 47 (5)

4.3 Number of other students: 37 (including current students 2)

5. Publication list

Journal Paper (2020-2021) *attached

1. Leilei Bao, Jongho Park, Gwenael Bonfante, and Beomjoon Kim: Recent advances in porous microneedles: materials, fabrication, and transdermal applications, ***Drug Delivery and Translational Research***, 12, pp. 395-414, 2021

*2. Libo Wu, Jongho Park, Yuto Kamaki, and Beomjoon Kim: Optimisation of fused deposition modelling based fabrication process for polylactic acid microneedles, Springer Nature, ***Microsystems & Nanoengineering***, 7 (58), 2021

3. Dan-Liang Wen, De-Heng Sun, Peng Huang, Wen Huang, Meng Su, Ya Wang, Meng-Di Han, Beomjoon Kim, Jürgen

Brugger, Hai-Xia Zhang, and Xiaosheng Zhang: Recent Progress on Silk Fibroin-Based Flexible Electronics, ***Microsystems & Nanoengineering***, 7, 35, 2021

*4. Hai-Tao Deng, Xin-Ran Zhang, Zhi-Yong Wang, Dan-Liang Wen, Yan-Yuan Ba, Beomjoon Kim, Meng-Di Han, Hai-Xia Zhang, Xiao-Sheng Zhang: Super-stretchable multi-sensing triboelectric nanogenerator based on liquid conductive composite, ***Nano Energy***, Vol.83, 105823, 2021

*5. D. Decanini, A. Harouri, Y. Mita, B.J. Kim, and G. Hwang: 3D micro fractal pipettes for capillary based robotic liquid handling, ***Review of Scientific Instruments***, 91, 086104, 2020

6. Meng Su, Beomjoon Kim: Silk Fibrion-Carbon Nanotube Composites based Fiber Substrated Wearable Triboelectric Nanogenerator, ***ACS Applied Nano Materials***, 3, 10, pp. 9759-9770, 2020

*7. Kai Takeuchi, Nobuyuki Takama, Rie Kinoshita, Teru Okitsu, Beomjoon Kim: Flexible and porous microneedles of PDMS for continuous glucose monitoring, ***Biomedical Microdevices***, **22**, 79, 2020

*8. Hakjae Lee, Gwenael Bonfante, Yui Sasaki, Nobuyuki Takama, Tsuyoshi Minami and Beomjoon Kim: Porous microneedles on a paper for screening test of prediabetes, ***Medical Devices and Sensors***, Vol.3, Issue 4, e10109, 2020

9. Gwenaël Bonfante, Hakjae Lee, Leilei Bao, Jongho Park, Nobuyuki Takama, Beomjoon Kim: Comparison of Polymers to enhance mechanical properties of microneedles for bio-medical applications, ***Micro and Nano Systems Letters***, Vol. 8, 13, 2020

10. Libo Wu, Pranav Shrestha, Martina Iapichino, Yicheng Cai, BeomJoon Kim, Boris Stoeber: Characterization Method for Calculating Diffusion Coefficient of Drug from Polylactic Acid (PLA) Microneedles into The Skin, ***Journal of Drug Delivery Science and Technology***, 61, pp. 102192, February 2021

International Conference (selected)

1. Leilei Bao, Jongho Park, Soojin Shim, Misako Yoneda, Chieko Kai, Beomjoon Kim: A rapid COVID-19 diagnostic device integrating porous microneedles and the paper-based immunoassay biosensor, ***10th. IEEE CPMT Symposium Japan 2021*** (ICSJ 2021), Kyoto Univ. Clock Tower Centennial Hall, Japan, Proceeding of ICSJ 2021, pp.164-167, November 10-12, 2021 (oral) (Best paper Awarded)

2. Kotaro Shobayashi, Xiaobin Wu, Jongho Park, Beomjoon Kim: Gold coated optical microneedles lens array for photothermal therapy, ***10th. IEEE CPMT Symposium Japan 2021*** (ICSJ 2021), Kyoto Univ. Clock Tower Centennial Hall, Japan, Proceeding of ICSJ 2021, pp.160-163, November 10-12, 2021 (oral)

3. Beomjoon Kim: Biomolecular Needling System for Medicals, ***The 34th. International Microprocesses and Nanotechnology Conference MNC 2021***, Symposium C (biological Phenomena and functions within Micro- and Nanospace), October 26-29, Online and On-Demand conference, 2021 (Oct.28 invited talk)

4. Gilgueng Hwang, Atsushi Toyokura, Akio Higo, Beomjoon Kim, and Yoshio Mita: Miniaturized soft transformable swimmer for environmentally friendly and sustainable fluidic carrier, **DTIP 2021(the 23rd. edition of the Symposium on Design, Test, Integration & Packaging of MEMS and MOEMS)**, Virtual event, August 25th-27th., page 1-4, 2021

5. Beomjoon Kim: Biomolecular Needling System for Medicals, ***The 16th IEEE International Conference on Nano/Micro Engineered & Molecular Systems (IEEE-NEMS 2021 / ieee-nems.org/2021)***, Online Conference, Xiamen, China, April 25-29, 2021 (Keynote speaker)

6. Kai Takeuchi, Fengwen Mu, Yoshiie Matsumoto, Beomjoon Kim, Tadamoto Suga: Surface activated bonding of glass using Aluminum Oxide intermediate layer for microchannel fabrication, ***ECS PRiME 2020 (ECS Meeting Abstract)***, The Electrochemical Society the joint international meeting of PRiME 2020, MA2020-02, pp. 1631, October 4-9, 2020

Received: 2 May 2020 | Accepted: 30 June 2020
DOI: 10.1002/mds3.10109

RESEARCH ARTICLE

MEDICAL DEVICES & SENSORS WILEY

Porous microneedles on a paper for screening test of prediabetes

Hakjae Lee | **Gwenaël Bonfante** | **Yui Sasaki** | **Nobuyuki Takama** | **Tsuyoshi Minami** | **Beomjoon Kim**

Institute of Industrial Science, The University of Tokyo, Tokyo, Japan

Correspondence
Beomjoon Kim, Institute of Industrial Science, The University of Tokyo, 4 -6-1 Komaba, Meguro-ku, Tokyo 153-8505, Japan.
Email: bjoonkim@iis.u-tokyo.ac.jp

Funding information
JSPS Core-to-Core Program A (JETMeE), Japan

Abstract

Porous microneedles are expected to have a variety of potential for applications in diagnostics owing to their ability to penetrate human skin painlessly and extract bio-fluid by capillary action. In this paper, a 'Porous Microneedle on a Paper substrate' (PMP) is proposed as a novel platform for direct integration of sensors. A microneedle array with height of approximately 840 μm was prepared on a paper. The fabrication process consists of salt leaching and heat press moulding. In this method, the salt particles are utilized as porogen materials. Mixture of the biodegradable polymer and the salt was shaped into microneedles by moulding. Furthermore, the polymer penetrated the paper matrix owing to heating during the pressing process. Subsequently, the salt particles are removed to develop the porous structure. Various ratios of salt to polymer were investigated to adjust the porosity of microneedles as well as their sample absorption property. A paper-based glucose sensor was integrated into the platform to demonstrate the absorption property of the microneedles, and showed successful sample extraction and glucose concentration analysis from agarose gel-based skin mimic. The developed platform has the potential to integrate various paper-based bio-sensors to painless, disposal and fast screening and diagnostic test for patient, as well as those with prediabetes.

KEYWORDS
capillary action, glucose, paper-based sensor, porous microneedles

1 | INTRODUCTION

Microneedles (MNs) have been studied as a painless tool for drug delivery (Aditya et al., 2019; Chen, Chen, Wang, Jin, & Guo, 2017; Dardano et al., 2016; Leone, Mönkäre, Bouwstra, & Kersten, 2017; Niu, Chu, Burton, Hansen, & Panyam, 2019) and minimally invasive bio-sensor (Cahill et al., 2018; Nicholas et al., 2018; Ranamukhaarachchi, Padeste, Hafeli, Stoeber, & Cadarso, 2018; Takeuchi et al., 2019) to overcome the drawback of hypodermic needles (*i.e.*, pain or fear caused by needle phobia). Owing to its micro-scale size, which generally has a length <1 mm, it can puncture the human skin barrier and penetrate the epidermis to allow transdermal transportation without hurting nerves. Moreover, unlike conventional hypodermic injection, MNs do not require users with medical training (Donnelly et al., 2012; Lee, Park, & Prausnitz, 2008; Mcallister, Allen, & Prausnitz, 2000). In the field of bio-sensors, MNs have been applied to collect interstitial fluid (ISF) from the epidermis to analyse biomolecules for health monitoring (Kolluru, Williams, Chae, & Prausnitz, 2019; Miller et al., 2018). ISF is a bio-fluid that surrounds cells and shuttles various biomaterials such as glucose between cells and blood vessels. ISF is regarded as a satisfactory source for bio-sampling as well as blood due to its abundant types of bio-markers. According to previous reports, approximately 80% of proteins in serums are also contained in ISF,

Biomedical Microdevices (2020) 22: 79
https://doi.org/10.1007/s10544-020-00532-1

Flexible and porous microneedles of PDMS for continuous glucose monitoring

Kai Takeuchi[1] · Nobuyuki Takama[1] · Rie Kinoshita[1] · Teru Okitsu[1] · Beomjoon Kim[1]

Accepted: 13 October 2020 / Published online: 3 November 2020

Abstract

Microneedle (MN) is a key technology of the biomedical engineering field due to its capability of accessing the biological information in a minimally invasive manner. One of the huge demands for next-generation healthcare monitoring is continuous monitoring, especially of blood glucose concentration. For this, MN should be kept inserted into the human skin for a certain period of time, enduring stresses induced by daily human motion and at the same time measuring biomarkers in ISF. However, conventional MNs for biosensing are not suitable for a long term insertion due to the rigid structure and biological risks of MN breakage. In this study, a novel MN structure is proposed and investigated by combining flexible "sponge-like" porous PDMS matrix and coating by biodissolving hyaluronic acid (HA). The fabricated porous MNs coated with HA show ideal mechanical characteristics, by which the MNs are rigid enough to penetrate the skin and become flexible after insertion into the skin. It is also shown that the MN array successfully extracts ISF *in vitro* and *in vivo* not by capillary action but by repeated compressions. The results show the applicability of the flexible MNs to continuous blood glucose monitoring.

Keywords Microneedle · Interstitial fluids · Glucose monitoring

1 Introduction

The blood glucose level measurement takes an important role for healthcare monitoring with a huge demand from society. These days, type 1 and 2 diabetes have a significant impact on society owing to its long-term effects on the health of patients, a large number of patients involved, and the large amount of social and economic costs. In order to treat, predict, and diagnose diabetes, the blood glucose measurement is indispensable.

For this, the current main targeted biosample of glucose monitoring is blood. Currently, self-monitoring of blood glucose (SMBG) is the most widely used method to measure and control diabetes patients' blood glucose levels. The patients prick their finger to extract a drop of blood 2-5 times a day before colorimetric or electrochemical measurements of the blood glucose. The SMBG kits are widely distributed and commercially available all over the world although this method causes inevitable pain and mental strain on the patients (Le Floch et al. 2008).

In the meantime, interstitial fluids (ISF) is also the targeted biosample of glucose monitoring as ISF reflects the glucose concentration in the blood with a 4-10 min delay (Boyne et al. 2003). Since ISF contains common biomarkers to blood such as proteins and ions, therefore, ISF is now highly expected to be applied for not only glucose but also for various biomarkers measurement.

Furthermore, it should be noted that the continuous measurement of biomarkers is getting more and more important to monitor the human body. Especially, for diabetes patients, the concept of the continuous glucose monitoring system (CGMS) is spreading as a more effective approach to monitor and control blood glucose levels. CGMS enables patients to monitor their blood glucose levels seamlessly, even when they are not able to use SMBG kits by themselves. This allows precise and continuous measurements including swift change of blood glucose, resulting in an accurate treatment (Fokkert et al. 2017; Petrie et al. 2017).

In addition to CGMS, other biomarkers such as cortisol (Venugopal et al. 2011) and alcohol (Venugopal et al. 2008; Mohan et al. 2017) were reported valuable for continuous health monitoring. Therefore, continuous ISF

✉ Kai Takeuchi
takekai@iis.u-tokyo.ac.jp

[1] Institute of Industrial Science, The University of Tokyo, Komaba, Tokyo 1538505, Japan

3D micro fractal pipettes for capillary based robotic liquid handling

Cite as: Rev. Sci. Instrum. 91, 086104 (2020); doi: 10.1063/5.0018456
Submitted: 15 June 2020 • Accepted: 26 July 2020 •
Published Online: 11 August 2020

View Online Export Citation CrossMark

D. Decanini,[1] A. Harouri,[1] Y. Mita,[2,3] B. J. Kim,[3] and G. Hwang[1,2,3,a)]

AFFILIATIONS

[1] C2N-CNRS, University Paris-Saclay, 10 Boulevard Thomas Gobert, Palaiseau 91120, France
[2] Department of Electrical Engineering and Information Systems, The University of Tokyo, 7-3-1, Hongo, Bunkyo-ku, Tokyo 113-8656, Japan
[3] LIMMS-CNRS, Institute of Industrial Science, The University of Tokyo, 4-6-1 Komaba, Meguro-ku, Tokyo 153-8505, Japan

[a)] **Author to whom correspondence should be addressed:** gilgueng.hwang@c2n.upsaclay.fr and hwang@if.t.u-tokyo.ac.jp

ABSTRACT

Miniaturized and mobile liquid handling devices are essential elements to biological or clinical applications. This will innovate the conventional liquid handling methods such as manual or automated pipetting systems. Here, we propose the micro fractal pipette as the candidate device for this objective. It is made of epoxy polymer and printed by innovative 3D nanoprinting technology based on two-photon absorption polymerization with sub-micrometer resolution. We demonstrated the efficient liquid handling performance by using the micro fractal pipette between the source droplet and the target hydrogel substrate. This is due to the high porosity (78%) and the 8.5 times larger cavity surface area compared to the full pyramid. The biomimetic inner cavity microchannel networks contribute to the low pressure drop. The proposed micro fractal pipette could also innovate the versatile and miniaturized liquid handling system, promising to various biological or clinical applications.

Miniaturization of intelligent systems such as lab-on-a-chip, which integrates several microelectromechanical components, allows highly resolved, rapid, safe, and low-cost diagnostics with a small volume of specimens.[1] However, the diagnostics of clinical specimens require additional steps of liquid handling such as collection, preparations, and injection of specimens to biosensors. In biological laboratories, robotic pipetting systems are widely used by automating tedious liquid handling steps, but they are limited to be used inside laboratory. To extend the applications out of the laboratory, a portable microfluidic sample handling system is inevitable. A conventional syringe and a needle require to be tethered by an external syringe pump and tubing for precise liquid volume handling. This makes the entire system become bulky with several disadvantages such as high priming/dead/residual volumes, which are limiting factors toward remote and microfluidic sample handling. Another alternative technology could be the porous microneedles.[2] Although this shows some advanced features such as low dead volume and high portability, the liquid handling performance strongly depends on the geometrical parameters such as the wettable surface area, the porosity, and the inlet/outlet aperture size. Moreover, it is essential to control the cavity geometries for the repeatable liquid handling. Most of the porous microneedles have limited porosity, and their cavity dimensions are less controlled.[2] Our aim is to propose a microfluidic specimen handling system with enhanced porosity toward biomedical applications requiring specimen/drug collection and delivery. We propose the liquid handling system consisting of highly porous and bioinspired design with a fractal pyramid microstructure. The fabrication is realized by two-photon absorption 3D nanolithography having sub-micrometer fabrication resolution. The proposed micro fractal pipette (MFP) allows enhanced porosity, light weight, and less invasive liquid handling. Moreover, the fractal structures allow facile development of a photoresist for inner cavity channels after photopolymerization because the developer medium has better access through large inlet/outlet openings and also a biomimetic microchannel architecture. The MFP does not require an external syringe pump, and the dead volume of the proposed MFP is close to zero in theory. The liquid filling in and releasing out of the MFP are done by the capillary force of

Nano Energy 83 (2021) 105823

Contents lists available at ScienceDirect

Nano Energy

journal homepage: http://www.elsevier.com/locate/nanoen

Communication

Super-stretchable multi-sensing triboelectric nanogenerator based on liquid conductive composite

Hai-Tao Deng [a], Xin-Ran Zhang [a], Zhi-Yong Wang [a], Dan-Liang Wen [a], Yan-Yuan Ba [a], Beomjoon Kim [b], Meng-Di Han [c], Hai-Xia Zhang [d], Xiao-Sheng Zhang [a,*]

[a] School of Electronic Science and Engineering, University of Electronic Science and Technology of China, Chengdu 611731, China
[b] CIRMM, Institute of Industrial Science, The University of Tokyo, Tokyo 153-8505, Japan
[c] Department of Biomedical Engineering, College of Future Technology, Peking University, Beijing 100871, China
[d] Institute of Microelectronics, Peking University, Beijing 100871, China

ARTICLE INFO

Keywords:
Triboelectric nanogenerator
Self-powered
Liquid conductive composite
Energy harvesting
Functional sensing

ABSTRACT

Stretchable triboelectric nanogenerators (TENGs) attract much attentions in the field of wearable electronics owing to their unique capabilities of ambient energy harvesting, especially from human activities, serving as sustainable power source as well as functional sensing device. The essential challenge of super-stretchable triboelectric nanogenerator (SS-TENG) is to overcome the non-stretchable drawback of conventional electrodes and endow them with remarkable extension capability. In this work, we developed a carbon nanotubes (CNT)-silicone rubber liquid composite with outstanding conductivity and fluidity, which provides an essential opportunity to realize a SS-TENG with the remarkable capability of 900% stretchable deformation. This newly developed SS-TENG successfully achieved the integration of bio-mechanical energy harvesting and multi-functional sensing. The electric output performance was comprehensively investigated and a maximum power density of 21.7 W/m^2 was obtained, which is large enough to power common low-power-consumption electronic devices. As for passive sensing, the proposed SS-TENG can be utilized as a strain gauge with good sensitivity (gauge factor (*GF*) of 11.4) and low hysteresis (degree of hysteresis (*DH*) of 0.71%). Moreover, as for active sensing, the detection of dynamic motions of human body joints was realized due to the correlation between gesture and corresponding electrical signal. Eventually, a self-powered wearable keyboard based on SS-TENG arrays with outstanding conformability on curved surfaces was demonstrated, which reveals a promising potential of the proposed liquid conductive composite and the developed SS-TENG for self-powered wearable electronic applications, especially in the healthcare field.

1. Introduction

Wearable electronics have become an important part of the Internet of Things (IoT) [1], and have widely penetrated into various sectors of human life, such as medical, wellness, communication and so on [2–5]. Although wearable electronics play an important role in modern society, challenges still exist due to their unsustainable power source, limited stretchability and poor conformability on curved surfaces, which restrict them to further wider applications. Massive wearable electronics still adopt battery as the power source, however, it exists the native drawbacks of cyclically recharge and regularly replacement resulting in unsustainable energy supplying for devices. One promising method to address this issue is to scavenge energy from the natural living environments. Light energy [6,7], heat energy [8,9], mechanical energy [10–16], etc. [17–19] are widely distributed in environments and all of them can be converted into electricity based on several technologies, e.g., photovoltaic effect, thermoelectric effect, electromagnetic effect, piezoelectric effect, triboelectric effect, etc. Among them, mechanical energy is the most widely distributed. Therefore, massive efforts have been devoted to harvesting ubiquitous mechanical energy from ambient environments, especially from the human body, where hundreds of watts of electricity is generated from physical motions [20–22].

In 2012, a novel mechanical energy harvesting mechanism of triboelectric generator (TENG) was firstly developed, which can convert ubiquitous mechanical energy into electricity based on a coupled effect of triboelectrification and electrostatic induction [23]. In recent years,

* Corresponding author.
E-mail address: zhangxs@uestc.edu.cn (X.-S. Zhang).

https://doi.org/10.1016/j.nanoen.2021.105823
Received 5 November 2020; Received in revised form 21 January 2021; Accepted 22 January 2021
Available online 26 January 2021

Wu et al. *Microsystems & Nanoengineering* (2021)7:58
https://doi.org/10.1038/s41378-021-00284-9

Microsystems & Nanoengineering
www.nature.com/micronano

ARTICLE Open Access

Optimization of the fused deposition modeling-based fabrication process for polylactic acid microneedles

Libo Wu[1], Jongho Park[1], Yuto Kamaki[1] and Beomjoon Kim[1]✉

Abstract

A microneedle (MN) array is a novel biomedical device adopted in medical applications to pierce through the stratum corneum while targeting the viable epidermis and dermis layers of the skin. Owing to their micron-scale dimensions, MNs can minimize stimulations of the sensory nerve fibers in the dermis layer. For medical applications, such as wound healing, biosensing, and drug delivery, the structure of MNs significantly influences their mechanical properties. Among the various microfabrication methods for MNs, fused deposition modeling (FDM), a commercial 3D printing method, shows potential in terms of the biocompatibility of the printed material (polylactic acid (PLA)) and preprogrammable arbitrary shapes. Owing to the current limitations of FDM printer resolution, conventional micron-scale MN structures cannot be fabricated without a post-fabrication process. Hydrolysis in an alkaline solution is a feasible approach for reducing the size of PLA needles printed via FDM. Moreover, weak bonding between PLA layers during additive manufacturing triggers the detachment of PLA needles before etching to the expected sizes. Furthermore, various parameters for the fabrication of PLA MNs with FDM have yet to be sufficiently optimized. In this study, the thermal parameters of the FDM printing process, including the nozzle and printing stage temperatures, were investigated to bolster the interfacial bonding between PLA layers. Reinforced bonding was demonstrated to address the detachment challenges faced by PLA MNs during the chemical etching process. Furthermore, chemical etching parameters, including the etchant concentration, environmental temperature, and stirring speed of the etchant, were studied to determine the optimal etching ratio. To develop a universal methodology for the batch fabrication of biodegradable MNs, this study is expected to optimize the conditions of the FDM-based fabrication process. Additive manufacturing was employed to produce MNs with preprogrammed structures. Inclined MNs were successfully fabricated by FDM printing with chemical etching. This geometrical structure can be adopted to enhance adhesion to the skin layer. Our study provides a useful method for fabricating MN structures for various biomedical applications.

Introduction

A commercially available microneedle (MN) patch is primarily a cosmetic product that contains micron-sized polymer needles. The concept of MNs was first introduced in 1976 for transdermal drug delivery[1]. Biomedical applications of MNs have been further developed for wound healing and biosensing[2–4]. MNs can bypass the stratum corneum, which is the outermost barrier layer of the skin. Active pharmaceutical ingredients (APIs) are subsequently administered to the viable epidermis and dermis layers of the skin. MN-mediated applications enable delivered APIs to block abnormal cell cycles in the skin, which can treat lesions[5]. Compared with the systemic drug delivery method, drug delivery by MNs targeting affected dermal cells can improve the efficiency of

Correspondence: Beomjoon Kim (bjoonkim@iis.u-tokyo.ac.jp)
[1]Institute of Industrial Science, The University of Tokyo, 4-6-1 Komaba, Meguro-ku, Tokyo 153-8505, Japan
These authors contributed equally: Libo Wu, Jongho Park, Yuto Kamaki, Beomjoon Kim

TAKAMIYA Laboratory

Current Research Activities 2021-2022

Takamiya Laboratory

1. Research Topics

1.1 <u>48 V-to-5 V Fibonacci Hybrid DC-DC Converter IC for Automotive Applications</u>

For 48 V mild hybrid vehicles, a sub-0.5 W, 48 V-to-5 V DC-DC converter, fulfilling (1) high efficiency with small volume, (2) constant switching frequency of less than 500 kHz to avoid the frequency band of AM radio, and (3) constant output voltage (V_{OUT}) against the sudden drop of input battery voltage (V_{IN}) under the cold cranking, is required. To meet the requirements, a 0.55 W, 88%, 78 kHz, 48 V-to-5 V Fibonacci hybrid (FH) DC-DC converter IC using 66 mm^3 of passive components is proposed. In the FH DC-DC converter, by adding an inductor and an output capacitor to a 1/5 Fibonacci switched-capacitor (SC) DC-DC converter, the SC DC-DC converter also works as a buck converter without adding power transistors. When V_{IN} drops from 48 V to 20 V in 1 ms in the automotive cold cranking, the FH DC-DC converter cannot keep 5-V V_{OUT}, because the output voltage of the internal 1/5 SC DC-DC converter drops from 9.6 V to 4 V and the internal buck converter cannot generate 5-V V_{OUT} from the 4 V. To solve the problem, a new control method named automatic change of converter topology and duty ratio (ACCD) is proposed. In ACCD, when V_{IN} drops less than 31 V, the converter topology automatically changes from 1/5 SC DC-DC converter to 1/3 SC DC-DC converter and the duty ratio of the PWM signal automatically decreases 3/5 times, thereby achieving the constant 5-V V_{OUT} under the cold cranking. To reduce the volume of the FH DC-DC converter, all transistors and diodes, including ten power transistors, gate drivers, bootstrap circuits, and the controller, are fully integrated on 4.6 mm x 2.3 mm IC fabricated with 180 nm BCD process. In the measurements, the proposed 0.55 W, 48 V-to-5 V FH DC-DC converter IC achieved the highest efficiency (88%) with the smallest volume of passive components (66 mm^3) at the lowest switching frequency (78 kHz) compared with previous publications.

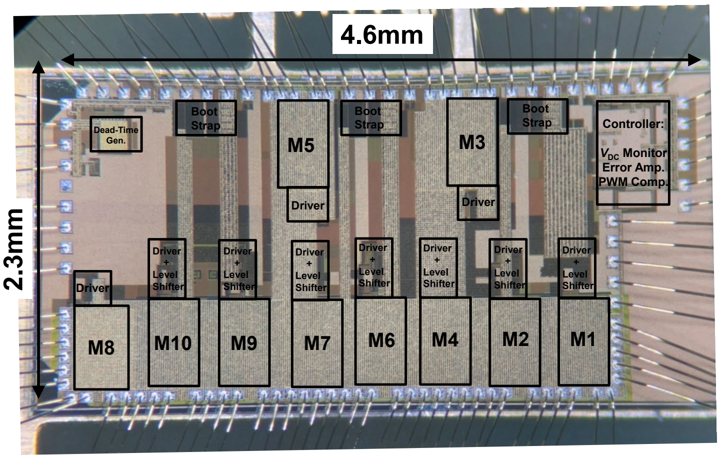

1.2 <u>Dual-Path Hybrid Synchronous Rectifier in Active Clamp Forward Converter</u>

A dual-path hybrid synchronous rectifier (DPH-SR) in active clamp forward (ACF) converters is proposed for inductor current reduction to solve inductor cooling problems under heavy load. In the proposed DPH-SR, the flying capacitor also supplies current to the output, thereby reducing the inductor current. In the measurement, the peak efficiency of the ACF converters with the proposed DPH-SR and conventional SR was 90.9 % and 89.0 % at 10 A_{OUT}, respectively, resulting in the improvement in efficiency by 1.9 %. In addition, the inductor conduction loss of the proposed DPH-SR is reduced by 43.0 % by reducing the inductor current by 24.8 % at 20 A_{OUT}.

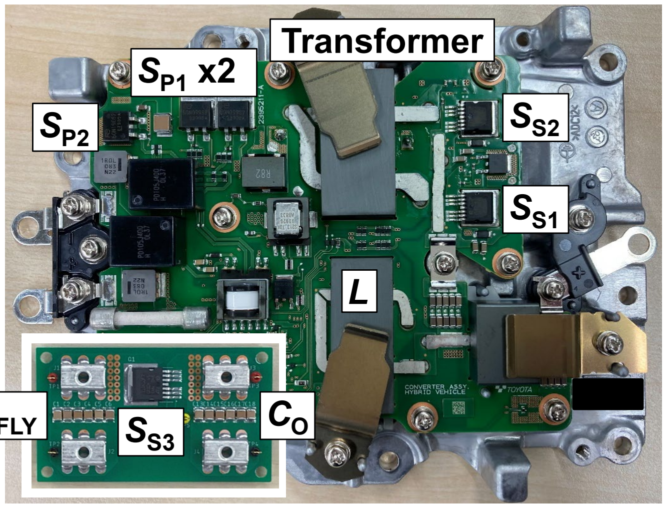

1.3 <u>Equalization of DC and Surge Components of Drain Current of Two Parallel-Connected SiC MOSFETs Using Single-Input Dual-Output Digital Gate Driver IC</u>

A single-input, dual-output (SIDO) digital gate driver (DGD) IC, integrating two 6-bit DGDs, two current sensors, and a controller, is proposed to equalize the drain current (I_D) variation of two parallel-connected SiC MOSFETs. The DC and surge components of I_D of each MOSFET are equalized by digitally controlling the gate voltage amplitude and the gate current at turn-on, respectively. In the double pulse test at 300 V and 40 A using two parallel SiC MOSFETs with different threshold voltages of 0.5 V, the proposed SIDO DGD IC reduces the differences in the DC and surge components of I_D of the two MOSFETs from 2.6 A to 0.13 A by 95 % and from 1.9 A to 0.32 A by 83 %, respectively. The automatic equalization of the DC components of I_D of the two MOSFETs using SIDO DGD IC is also successfully demonstrated.

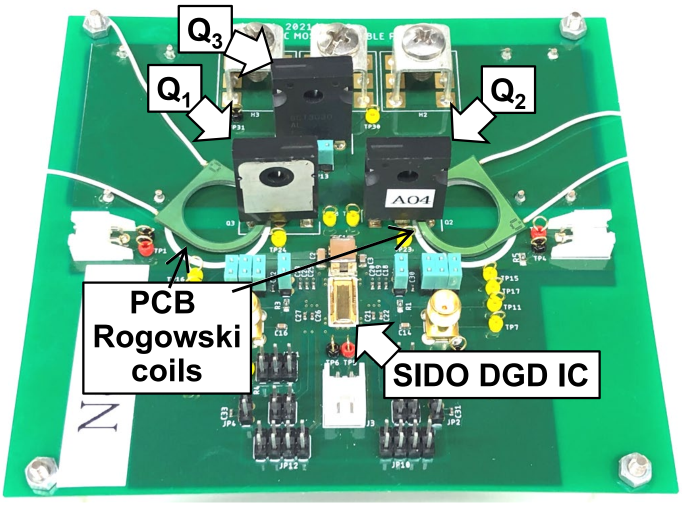

2. Research Achievements

2.1 Number of original journal papers: 6

2.2 International conference: 10 (including 3 invited presentations)

2.3 Domestic conference: 11(including 2 invited presentations)

2.4 Number of patents: 0

3. List of awards

- Young Investigator Award, 2021/5/26, International Electric Vehicle Technology Conference 2021 (EVTeC2021) (K.Hata)

4. Research Grants

4.1 Total number of research grants: 6

4.2 Number of collaboration research with industries: 3

4.3 List of major research grants (serving as Principal Investigator)

- Research Grant for “ Grant-in-Aid for Exploratory Research” from KAKENHI

5. Education

5.1 Number of Ph.D. students (including current students): 1

5.2 Number of master students (including current students):5

5.3 Number of other students: 1

6. Publication list

Journal Papers

1. D. Yamaguchi, Y. S. Cheng, T. Mannen, H. Obara, K. Wada, T. Sai, M. Takamiya, and T. Sakurai, "An Optimization Method of a Digital Active Gate Driver Under Continuous Switching Operation Being Capable of Suppressing Surge Voltage and Power Loss in PWM Inverters," IEEE Transactions on Industry Applications, Vol.58, No.1, pp. 481 - 493, Jan./Feb. 2022.
2. H. Qiu, Y. Jiang, Y. Shi, T. Sakurai, and M. Takamiya, "Analysis and Mitigation of Coupling-Dependent Data Flipping in Wireless Power and Data Transfer System," IEEE Transactions on Circuits and Systems—I: Regular Papers, Vol. 68, No. 12, pp. 5182 - 5193, Dec. 2021.
3. Q. Ma, X. Zhang, Y. Jiang, K. Hata, M. Takamiya, M.-K. Law, P.-I. Mak, and R. P. Martins, "A Multi-Path Switched-Capacitor-Inductor Hybrid DC-DC Converter with Reduced Inductor Loss and Extended Voltage Conversion Range," IEICE Electronics Express, Vol.18, Issue 22, Pages 20210405, Nov. 2021.
4. Y. Yamauchi, T. Sai, K. Hata, and M. Takamiya, "0.55 W, 88%, 78 kHz, 48 V-to-5 V Fibonacci Hybrid DC–DC Converter IC Using 66 mm3 of Passive Components With Automatic Change of Converter Topology and Duty Ratio for Cold-Crank Transient," IEEE Transactions on Power Electronics, Vol.36, No.8, pp. 9273 - 9284, Aug. 2021.
5. F. -B. Yang, J. Fuh, Y. -H. Li, M. Takamiya, and P. -H. Chen, "Structure-Reconfigurable Power Amplifier (SR-PA) and 0X/1X Regulating Rectifier for Adaptive Power Control in Wireless Power Transfer System," IEEE Journal of Solid-State Circuits, Vol.56, No.7, pp. 2054 - 2064, July 2021.

Conference Presentations

C1. K. Horii, R. Morikawa, R. Katada, K. Hata, T. Sakurai, S. Hayashi, K. Wada, I. Omura, and M. Takamiya, "Equalization of DC and Surge Components of Drain Current of Two Parallel-Connected SiC MOSFETs Using Single-Input Dual-Output Digital Gate Driver IC," IEEE Applied Power Electronics Conference and Exposition (APEC), Houston, USA, pp. 1406-1412, March 2022.

C2. K. Hata, S. Suzuki, and M. Takamiya, "Dual-Path Hybrid Synchronous Rectifier in Active Clamp Forward Converter for Inductor Current Reduction," IEEE Applied Power Electronics Conference and Exposition (APEC), Houston, USA, pp. 1011-1015, March 2022.

C3. M. Takamiya, "Digital Gate Driver ICs to Automatically Reduce both Switching Loss and Switching Noise in Power Devices," State Key Laboratory of Analog and Mixed-Signal VLSI, Institute of Microelectronics, University of Macau, Distinguished Lecture, Virtual, Feb. 2022.

C4. M. Takamiya, "Programmable Digital Gate Driver IC to Automatically Reduce both Switching Loss and Switching Noise," European Center for Power Electronics (ECPE) Workshop: Advanced Drivers for Si, SiC and GaN Power Semiconductor Devices, Virtual, Feb. 2022.

C5. R. Katada, K. Hata, Y. Yamauchi, T. -W. Wang, R. Morikawa, C. -H. Wu, T. Sai, P. -H. Chen, and M. Takamiya, "Digital Gate Driving (DGD) is Double-Edged Sword: How to Avoid Huge Voltage Overshoots Caused by DGD for GaN FETs," IEEE Energy Conversion Congress & Exposition (ECCE), Virtual, pp. 5412-5416, Oct. 2021.

C6. M. Takamiya, "Digitalized Power Electronics for Incorporating IoT and AI," International Conference on Solid State Devices and Materials (SSDM), Virtual, pp. 712-713, Sep. 2021. (Invited)

C7. H. Qiu and M. Takamiya, "A 6.78 MHz Wireless Power Transfer System for Simultaneous Charging of Multiple Receivers with Maximum Efficiency using Adaptive Magnetic Field Distributor IC," IEEE Symposium on VLSI Circuits, Virtual, pp. 1-2, June 2021.

C8. K. Hata, Y. Jiang, M. -K. Law, and M. Takamiya, "Always-Dual-Path Hybrid DC-DC Converter Achieving High Efficiency at Around 2:1 Step-Down Ratio," IEEE Applied Power Electronics Conference and Exposition (APEC), Virtual, pp. 1302-1307, June 2021.

C9. R. Katada, K. Hata, Y. Yamauchi, T. -W. Wang, R. Morikawa, C. -H. Wu, T. Sai, P. -H. Chen, and M. Takamiya, "5 V, 300 MSa/s, 6-bit Digital Gate Driver IC for GaN Achieving 69 % Reduction of Switching Loss and 60 % Reduction of Current Overshoot," The Institute of Electrical Engineers of Japan, 33rd International Symposium on Power Semiconductor Devices and ICs (ISPSD), Virtual, pp. 55 – 58, May 2021.

C10. H. Yamasaki, R. Katada, K. Hata, and M. Takamiya, "Momentary High-Z Gate Driving (MHZGD) at Miller Plateau for IGBT Load Current Estimation from Gate Driver," IEEE Energy Conversion Congress & Exposition - Asia (ECCE Asia), Virtual, pp. 1698-1704, May 2021.

2021 IEEE Energy Conversion Congress and Exposition (ECCE) | 978-1-7281-5135-9/21/$31.00 ©2021 IEEE | DOI: 10.1109/ECCE47101.2021.9595264

Digital Gate Driving (DGD) is Double-Edged Sword: How to Avoid Huge Voltage Overshoots Caused by DGD for GaN FETs

Ryunosuke Katada[1], Katsuhiro Hata[1], Yoshitaka Yamauchi[1], Ting-Wei Wang[1,2], Ryuzo Morikawa[1], Cheng-Hsuan Wu[1], Toru Sai[1], Po-Hung Chen[2], and Makoto Takamiya[1]
[1]The University of Tokyo, Tokyo, Japan
[2]National Chiao Tung University, Hsinchu, Taiwan
Email: khata@iis.u-tokyo.ac.jp

***Abstract*— In this paper, a problem of huge voltage overshoots ($V_{OVERSHOOT}$) of V_{DS} in GaN FETs, which rarely happens during an automatic search of optimum gate driving parameters in a digital gate driving (DGD), is clarified for the first time, and a solution to avoid the problem is proposed. The highest $V_{OVERSHOOT}$ in 165k measurements, where parameters of 6-bit DGD IC in 6 time slots in 3.3-ns time intervals are randomly changed in the turn-off of GaN FET at 20 V and 10 A, is 27.6 V, which is 115 % larger than the conventional single-step gate driving (CSG) and is almost equal to the maximum rated voltage of the GaN FET. To solve the problem, a safe and fast search method of optimum parameters for DGD is proposed, which achieved 61 % reduction of the switching loss and 59 % reduction of $V_{OVERSHOOT}$ compared with CSG.**

Keywords*— *digital gate drive, GaN FET, switching loss, overshoot

I. INTRODUCTION

Fast switching of GaN FETs reduces the switching loss (E_{LOSS}), while current overshoot ($I_{OVERSHOOT}$) and voltage overshoot ($V_{OVERSHOOT}$) increase, which is a critical problem in GaN FETs, because a huge overshoot that exceeds the maximum rating of GaN FETs causes serious device damage. Active gate driving [1] and digital gate driving (DGD) [2-3] are important technologies to reduce both $V_{OVERSHOOT}$ and E_{LOSS} in GaN FETs. The advantage of DGD is its programmability in supporting a wide variety of power devices [4] and its ease of use, because the parameters of DGD can be automatically optimized using software [4-5].

In this paper, however, it is shown for the first time that DGD is a double-edged sword. As far as the authors know, no previous papers show the risk of DGD. Specifically, DGD with good parameters achieves lower $V_{OVERSHOOT}$ and E_{LOSS} than the conventional single-step gate driving (CSG), while DGD with bad parameters causes higher $V_{OVERSHOOT}$ and E_{LOSS} than CSG, which suggests a risk of overvoltage breakdown of GaN FETs during the random parameter search process for DGD. In order to understand the cause of the problem and to avoid it, in this paper, the principle of huge $V_{OVERSHOOT}$ generation is analyzed and a safe and fast search method for the parameters, that achieves low E_{LOSS} and $V_{OVERSHOOT}$ without generating huge $V_{OVERSHOOT}$, is proposed.

II. DIGITAL GATE DRIVER IC FOR GAN FETS [6]

Figs. 1 and 2 show a circuit schematic and a timing chart of the developed 5 V, 300 MSa/s, 6-bit DGD IC for GaN FETs, respectively. The IC is designed using only 5 V transistors and requires a single power supply of 5 V. The gate current (I_G) can be varied in 64 levels for each of the 16 3.3-ns time intervals during turn-on/off of the GaN FETs depending on scan-in data. 64-level I_G control from 0 A to 5 A in 80 mA increments is achieved by selectively turning on or off six nMOSFETs or pMOSFETs with binary weighted gate widths ($1W_N$, $2W_N$, $4W_N$, $8W_N$, $16W_N$, and $32W_N$ in case of nMOSFETs) in the output stage with 6-bit digital signals. I_G control in 3.3-ns intervals is required, because the turn-on/off

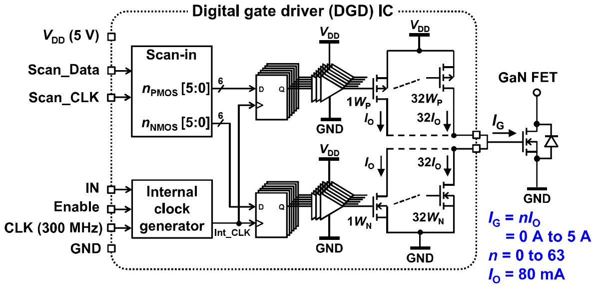

Fig. 1. Circuit schematic of 5 V, 300 MSa/s, 6-bit DGD IC for GaN FETs.

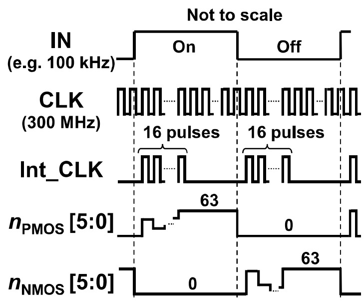

Fig. 2. Timing chart of 5 V, 300 MSa/s, 6-bit DGD IC for GaN FETs.

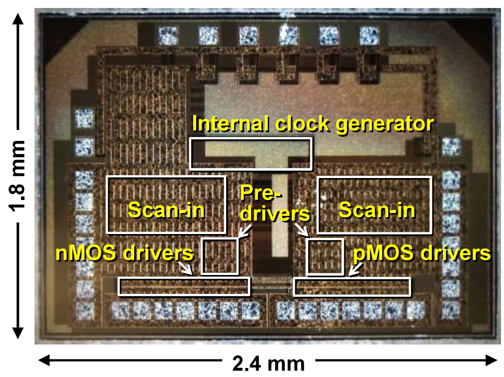

Fig. 3. Die photo of DGD IC fabricated with 180-nm BCD process.

Analysis and Mitigation of Coupling-Dependent Data Flipping in Wireless Power and Data Transfer System

Hao Qiu, *Member, IEEE*, Yuntao Jiang, Yi Shi, *Member, IEEE*, Takayasu Sakurai, *Life Fellow, IEEE*, and Makoto Takamiya, *Senior Member, IEEE*

***Abstract*— Load shift keying (LSK) has been widely used in a wireless power and data transfer (WPDT) system, owing to its low cost and power consumption. It was discovered that the demodulated data can flip when the coupling coefficient (k) between the transmitter (TX) and receiver (RX) coils becomes less than a critical value (k_{DF}) in a system with four basic compensation topologies (series–series, series–parallel, parallel–series, and parallel–parallel). This problem is called coupling-dependent data flipping (CDDF). Even more seriously, the transferred data cannot be recovered when k equals k_{DF}. On the basis of a comprehensive circuit analysis of CDDF, a universal method applicable to all four compensation topologies was proposed. By monitoring the current through the TX coil rather than its voltage for data demodulation, CDDF can be avoided. Furthermore, a WPDT system was implemented in which the voltage information of the load resistance (R_{Load}) was transferred to the TX side to control the source voltage for load power (P_{Load}) regulation. Using the conventional method, CDDF along with its corresponding k_{DF} (0.35) was verified. On the other hand, using the proposed method, the data was successfully transferred even when k is less than or equal to k_{DF}. By a correct data transfer, P_{Load} has been successfully regulated at around 1.1 W with a high system efficiency of up to 60% under the variation in k from 0.09 to 0.45.**

***Index Terms*— Coupling-dependent data flipping (CDDF), critical coupling coefficient, inductive coupling, load shift keying (LSK), uplink, wireless power and data transfer (WPDT).**

I. Introduction

WIRELESS power transfer (WPT) based on inductive coupling has been applied in a wide range of applications [1] such as electric vehicles (EVs) [2], [3], mobile devices [4] and biomedical implanted devices [5], [6]. During wireless charging, the coupling coefficient (k) between the transmitter (TX) and receiver (RX) coils can change drastically and thus affects the load power (P_{Load}) [7]. To monitor and regulate P_{Load}, it is necessary to establish a communication link from the RX side to the TX side that is an uplink [8]–[10]. It is preferrable that the uplink design has a low implementation cost, consumes low power, and is robust against the variation in k. Recently, many works have focused on the communication link design in wireless power and data transfer (WPDT) systems.

For the uplink design of WPDT systems, one intuitive idea is to use an additional pair of coils for data transfer [11], [12]. However, it will result in a high implementation cost as well as suffer from crosstalk with the pair of coils used for power transfer. On the other hand, the simplest way is to use a single pair of coils to transfer both power and data. To enable the data transfer simultaneously with power transfer, a modulation mechanism is necessary. In [13], a data transfer method based on splitting frequencies was proposed. However, the data transfer range is limited to strong-coupled regions. In [14], cyclic ON-OFF keying (COOK) was proposed to support a simultaneous WPDT. However, an accurate time control is required and increases the cost of the system. Compared with these methods, load shift keying (LSK) has been extensively used owing to its simple architecture and low power consumption [15]–[17]. As shown in Fig. 1, the data is first modulated utilizing a shorting switch (SW) across the load resistance (R_{Load}) on the RX side and then demodulated by monitoring the voltage (V_L) across the inductance (L_{TX}) on the TX side. The connection of compensation capacitances on the TX side (C_{TX}) and RX side (C_{RX}) depends on the compensation topology.

Thus, a WPDT system with LSK as its data modulation mechanism is a good option. However, few works have examined its performance against the variation in k. Our major contributions in this paper are summarized as follows: 1) A problem called coupling-dependent data flipping (CDDF) was discovered, in which the uplink data can be incorrectly demodulated when k is less than or equal to a critical value (k_{DF}). 2) We performed a comprehensive circuit analysis of CDDF in a WPTD system with four commonly-used compensation topologies [series–series (SS), series–parallel (SP), parallel–series (PS), and parallel–parallel (PP)] [18], [19]. 3) For all these four compensation topologies, a universal method to avoid CDDF was proposed. 4) In an implemented WPDT system, we demonstrated that the uplink data can

Manuscript received June 4, 2021; revised August 7, 2021; accepted August 30, 2021. Date of publication September 15, 2021; date of current version November 29, 2021. This work was supported in part by the Japan Science and Technology Agency (JST) Exploratory Research for Advanced Technology (ERATO). This article was recommended by Associate Editor G. Di Capua. *(Corresponding author: Hao Qiu.)*

Hao Qiu, Yuntao Jiang, and Yi Shi are with the School of Electronic Science and Engineering, Nanjing University, Nanjing 210023, China (e-mail: haoqiu@nju.edu.cn; yshi@nju.edu.cn).

Takayasu Sakurai and Makoto Takamiya are with the Institute of Industrial Science, The University of Tokyo, Tokyo 153-8505, Japan (e-mail: mtaka@iis.u-tokyo.ac.jp).

Color versions of one or more figures in this article are available at https://doi.org/10.1109/TCSI.2021.3111100.

Digital Object Identifier 10.1109/TCSI.2021.3111100

0.55 W, 88%, 78 kHz, 48 V-to-5 V Fibonacci Hybrid DC–DC Converter IC Using 66 mm^3 of Passive Components With Automatic Change of Converter Topology and Duty Ratio for Cold-Crank Transient

Yoshitaka Yamauchi, *Member, IEEE*, Toru Sai, *Member, IEEE*, Katsuhiro Hata, and Makoto Takamiya, *Senior Member, IEEE*

***Abstract*—For 48 V mild hybrid vehicles, a sub-0.5 W, 48 V-to-5 V dc–dc converter fulfilling: 1) high efficiency with small volume; 2) constant switching frequency of less than 500 kHz to avoid the frequency band of AM radio; and 3) constant output voltage (V_{OUT}) against the sudden drop of input battery voltage (V_{IN}) under cold cranking is required. To meet the requirements, a 0.55 W, 88%, 78 kHz, 48 V-to-5 V Fibonacci hybrid (FH) dc–dc converter IC using 66 mm^3 of passive components is proposed. In the FH dc–dc converter, by adding an inductor and an output capacitor to a 1/5 Fibonacci switched-capacitor (SC) dc–dc converter, the SC dc–dc converter also works as a buck converter without adding power transistors. When V_{IN} drops from 48 V to 20 V in 1 ms in the automotive cold cranking, the FH dc–dc converter cannot keep 5-V V_{OUT}, because the output voltage of the internal 1/5 SC dc–dc converter drops from 9.6 to 4 V and the internal buck converter cannot generate 5-V V_{OUT} from 4 V. To solve the problem, a new control method named automatic change of converter topology and duty ratio (ACCD) is proposed. In ACCD, when V_{IN} drops less than 31 V, the converter topology automatically changes from 1/5 SC dc–dc converter to 1/3 SC dc–dc converter and the duty ratio of the pulsewidth modulation signal automatically decreases 3/5 times, thereby achieving the constant 5-V V_{OUT} under cold cranking. To reduce the volume of the FH dc–dc converter, all transistors and diodes, including ten power transistors, gate drivers, bootstrap circuits, and the controller, are fully integrated on 4.6 mm × 2.3 mm IC fabricated with 180 nm BCD process. In the measurements, the proposed 0.55 W, 48 V-to-5 V FH dc–dc converter IC achieved the highest efficiency (88%) with the smallest volume of passive components (66 mm^3) at the lowest switching frequency (78 kHz) compared with previous publications.**

***Index Terms*—Automotive, BCD technology, cold cranking, Fibonacci, hybrid dc–dc converter.**

Manuscript received June 13, 2020; revised October 5, 2020 and December 23, 2020; accepted January 27, 2021. Date of publication February 10, 2021; date of current version May 5, 2021. Recommended for publication by Associate Editor T. Qian. (*Corresponding author: Yoshitaka Yamauchi.*)

Yoshitaka Yamauchi is with the Institute of Industrial Science, The University of Tokyo, Tokyo, Japan. He is now with Taiwan Semiconductor Manufacturing Company (TSMC), Hsinchu, Taiwan (e-mail: yyama@iis.u-tokyo.ac.jp).

Toru Sai is with the Institute of Industrial Science, The University of Tokyo, Japan. He is now with Tokyo Polytechnic University, Tokyo, Japan (e-mail: sai@iis.u-tokyo.ac.jp).

Katsuhiro Hata and Makoto Takamiya are with the Institute of Industrial Science, The University of Tokyo, Tokyo, Japan (e-mail: khata@iis.u-tokyo.ac.jp; mtaka@iis.u-tokyo.ac.jp).

Color versions of one or more figures in this article are available at https://doi.org/10.1109/TPEL.2021.3058207.

Digital Object Identifier 10.1109/TPEL.2021.3058207

I. Introduction

The target of this article is to develop a sub-0.5 W, 48 V-to-5 V step-down dc–dc converter IC for 48 V mild hybrid electric vehicles. In the mild-hybrid system, the battery voltage changes from conventional 12 to 48 V, while ECUs (electronic control units), including processors, memories, and sensors for the automobile, still require 5 V with less than 100 mA load current. Therefore, the conventional 12 V-to-5 V dc–dc converter should be replaced with the 48 V-to-5 V dc–dc converter. The required step-down ratio increases from 2.4:1 to 9.6:1.

Fig. 1 shows the requirements for the sub-0.5 W, 48 V-to-5 V dc–dc converter IC for the 48 V mild hybrid vehicles. The high efficiency is required because the heat generation due to the loss of the dc–dc converter will increase the cost and the volume for the heat sink. The small volume of the dc–dc converter is also required because the number of ECUs is increasing with the evolution of cars, though the total space for ECUs is constant. For sub-0.5 W output power, highly integrated dc–dc converter IC including power transistors is an effective choice to achieve the small volume. For the automotive applications, dc–dc converters with the switching frequency (f_{SW}) of less than 500 kHz [1]–[3] or f_{SW} of more than 2 MHz [4]–[6] are required to avoid the electromagnetic interference (EMI) with an in-car radio receiver using the AM frequency band of 500 kHz–1.6 MHz [7], [8]. Constant f_{SW} is also required because fluctuating f_{SW} in the pulse frequency modulation (PFM) control for the dc–dc converter makes EMI countermeasures difficult [9]. The most challenging problem for the automotive dc–dc converters is the undervoltage transients of the input battery voltage (V_{IN}). The most severe of the undervoltage transients is known as a cold crank, which occurs when the engine is initially started. As defined in the test standard of the cold cranking for the automotive dc–dc converters [10], V_{IN} drops from 48 to 20 V in 1 ms, when the starter motor begins turning over the engine from a dead stop. Once the engine starts, V_{IN} recovers to its nominal voltage of 48 V. During the cold-crank transients, the automotive dc–dc converters must keep the constant 5-V output voltage (V_{OUT}).

Table I summarizes possible options to realize a sub-0.5 W, 48 V-to-5 V dc–dc converter IC fulfilling the above-mentioned

Dual-Path Hybrid Synchronous Rectifier in Active Clamp Forward Converter for Inductor Current Reduction

Katsuhiro Hata[1], Sadanori Suzuki[2], and Makoto Takamiya[1]
[1]The University of Tokyo, Tokyo, Japan
[2]Toyota Industries Corporation, Aichi, Japan
E-mail: khata@iis.u-tokyo.ac.jp

***Abstract*— A dual-path hybrid synchronous rectifier (DPH-SR) in active clamp forward (ACF) converters is proposed for inductor current reduction to solve inductor cooling problems under heavy load. In the proposed DPH-SR, the flying capacitor also supplies current to the output, thereby reducing the inductor current. In the measurement, the peak efficiency of the ACF converters with the proposed DPH-SR and conventional SR was 90.9 % and 89.0 % at 10 AOUT, respectively, resulting in the improvement in efficiency by 1.9 %. In addition, the inductor conduction loss of the proposed DPH-SR is reduced by 43.0 % by reducing the inductor current by 24.8 % at 20 AOUT.**

Keywords*— *Active clamp forward converter, Synchronous rectifier, Hybrid DC-DC converter, Dual-path

I. Introduction

Active clamp forward (ACF) converters [1–2] are suitable for a high step-down conversion in applications such as EV/HEV, servers, and data centers [3–5]. Due to the conduction loss in the output inductor, however, the heat generated by the coil increases the cost of cooling. To solve the problem, rectification circuits to reduce the inductor current are beneficial for the ACF converter in high current applications.

Previous studies have proposed indirect hybrid step-down DC-DC converters [6–10], where the inductor is indirectly connected to the output, which can achieve the smaller inductor current than the output current because the output current is supplied from a dual path (inductor and capacitor path) unlike the conventional buck converter and direct hybrid converters [11–16]. Based on the circuit topologies of indirect hybrid DC-DC converters, in this paper, a dual-path hybrid synchronous rectifier (DPH-SR) for the ACF converter is proposed to reduce the inductor conduction loss by reducing the inductor current.

This paper describes the operation principle and basic characteristics of the proposed DPH-SR. In addition, the feasibility of the ACF converter with the proposed DPH-SR is demonstrated by experiments.

II. Proposed Dual-Path Hybrid Synvronous Rectifier

A. Circuit operation and voltage conversion ratio

Fig. 1 shows the ACF converter with the conventional synchronous rectifier (SR). In this topology, the output current I_O is supplied through the output inductor L, which can cause inductor cooling problems under heavy load. To reduce the inductor losses, the dual-path hybrid synchronous rectifier (DPH-SR) is proposed as shown in Fig. 2. Compared to the conventional SR, the switch $S_{S3,\Phi2}$ and the flying capacitor C_{FLY} are added in the proposed DPH-SR.

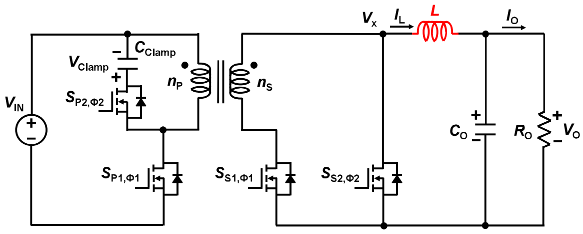

Fig. 1. Active clamp forward converter with conventional synchronous rectifier.

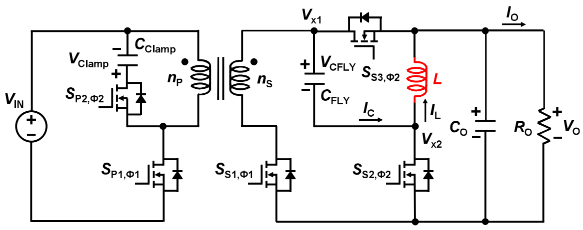

Fig. 2. Active clamp forward converter with proposed dual-path hybrid synchronous rectifier (DPH-SR).

Fig. 3 shows the two circuit states in the proposed DPH-SR. Although the two switches on the primary side of the ACF converter operate in opposition to apply the AC voltage to the secondary side, the transformer supplies current to the load only during State 1. Then, the flying capacitor C_{FLY} is connected to the inductor L in series. On the other hand, during State 2, C_{FLY} is in parallel with L and I_O is supplied from the dual path, which helps to reduce the inductor DC current I_L.

Fig. 4 shows the key operation waveforms in the proposed DPH-SR. By considering the voltage-second balance in L and the charge balance in C_{FLY} and C_O at the periodic steady state, the voltage conversion ratio M of the ACF converter with the proposed DPH-SR is expressed as follows:

$$\begin{aligned} 0 &= \langle V_L \rangle \\ &= \left(\frac{n_S}{n_P}V_{IN} - V_{CFLY} - V_O\right)DT_S + (0 - V_O)(1-D)T_S \\ &= \left(\frac{n_S}{n_P}V_{IN} - 2V_O\right)DT_S - V_O(1-D)T_S \\ \Leftrightarrow\ & \frac{V_O}{V_{IN}} = \frac{n_S}{n_P}\frac{D}{1+D} \end{aligned} \tag{1}$$

Equalization of DC and Surge Components of Drain Current of Two Parallel-Connected SiC MOSFETs Using Single-Input Dual-Output Digital Gate Driver IC

Kohei Horii[1], Ryuzo Morikawa[1], Ryunosuke Katada[1], Katsuhiro Hata[1], Takayasu Sakurai[1], Shin-Ichiro Hayashi[2], Keiji Wada[2], Ichiro Omura[3], and Makoto Takamiya[1]
[1]The University of Tokyo, Tokyo, Japan
[2]Tokyo Metropolitan University, Tokyo, Japan
[3]Kyushu Institute of Technology, Fukuoka, Japan

***Abstract*— A single-input, dual-output (SIDO) digital gate driver (DGD) IC, integrating two 6-bit DGDs, two current sensors, and a controller, is proposed to equalize the drain current (I_D) variation of two parallel-connected SiC MOSFETs. The DC and surge components of I_D of each MOSFET are equalized by digitally controlling the gate voltage amplitude and the gate current at turn-on, respectively. In the double pulse test at 300 V and 40 A using two parallel SiC MOSFETs with different threshold voltages of 0.5 V, the proposed SIDO DGD IC reduces the differences in the DC and surge components of I_D of the two MOSFETs from 2.6 A to 0.13 A by 95 % and from 1.9 A to 0.32 A by 83 %, respectively. The automatic equalization of the DC components of I_D of the two MOSFETs using SIDO DGD IC is also successfully demonstrated.**

Keywords*— Parallel connected, SiC, DC current, Surge current, Gate driver

I. Introduction

In power electronics systems, when large current exceeding the rated current of a power device is applied, it is common to connect multiple power devices in parallel. Due to variations in the characteristics of the power devices, however, the current concentrates in part of the devices and the heat generation due to losses is localized, which degrades the reliability of the power devices. In the conventional method of parallel connection of power devices, the characteristics of the power devices are measured in advance, and power devices with matching characteristics are selected for parallel connection, which will increase the cost. Therefore, a technology to automatically equalize the current of power devices connected in parallel is required. The problem with the previous papers of current equalization is that they require a lot of ICs including such as current sensors [1–2], timing control circuits [1–4], and regulators for gate voltage amplitude control [5–6], which will also increase the cost.

In this paper, a single-input, dual-output (SIDO) digital gate driver (DGD) IC, integrating all necessary circuits including two 6-bit DGDs, two current sensors, and a controller, is proposed to automatically equalize the drain current (I_D) of two parallel-connected SiC MOSFETs. DGD that can digitally control the gate waveform is gaining attention as a technology to reduce both loss and noise during switching of power devices [7]. The proposed SIDO DGD IC will enable a high-performance power electronics systems using SiC MOSFETs at low cost, because SiC MOSFETs with large variations can be connected in parallel without prior testing and selection.

II. Proposed Drain Current Equalization Using SIDO DGD IC

Fig. 1 shows a circuit schematic of the fabricated half-bridge circuit and SIDO DGD IC. The half-bridge consists of three SiC MOSFETs (Q_1 – Q_3 : SCT3030AL, 650V, 70A) including the low-side two-parallel Q_1 and Q_2. In order to equalize DC ($I_{D1,DC}$, $I_{D2,DC}$) and surge ($I_{D1,SURGE}$, $I_{D2,SURGE}$) components of I_D of Q_1 and Q_2 (I_{D1}, I_{D2}) with variations in device characteristics by controlling the gate waveforms, SIDO DGD IC is newly developed. Except for two PCB Rogowski coils [8], all the necessary circuits including two 6-bit DGDs, two current sensors, and a controller are fully integrated into a single chip.

Fig. 2 shows the circuit schematic of the current sensor to measure $I_{D1,DC}$ and $I_{D2,DC}$. The current sensor cannot measure the high-frequency $I_{D1,SURGE}$ and $I_{D2,SURGE}$ waveforms. Two current sensors are integrated on SIDO DGD IC. In order to obtain the current waveform, the output of the PCB Rogowski coil is integrated.

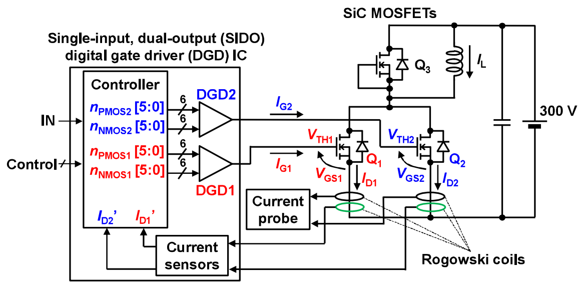

Fig. 1. Circuit schematic of fabricated half-bridge circuit and proposed SIDO DGD IC.

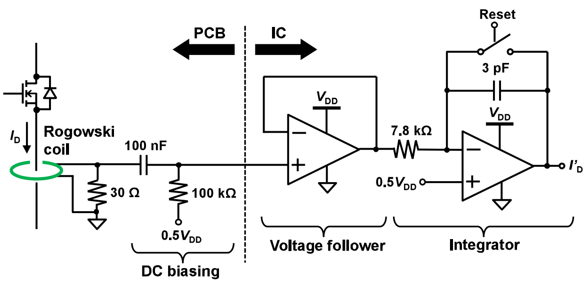

Fig. 2. Circuit schematic of current sensor to measure $I_{D1,DC}$ and $I_{D2,DC}$.

MIZOGUCHI Laboratory

Current Research Activities 2021-2022

Mizoguchi Laboratory

1. Research Topics

1.1 Nanoscale Investigation of Local Thermal Expansion at $SrTiO_3$ Grain Boundaries by Electron Energy Loss Spectroscopy

Grain boundaries (GBs), interfaces between crystallites in polycrystals, possess unique atomic arrangement. The distinct structure of GBs may have great impacts on various physical properties such as ion diffusivity, thermal conductivity and elastic response. These local properties near GBs have attracted great interests especially in nanocrystalline materials, which contain large volume fraction of GBs. The coefficient of thermal expansion (CTE) is of the essence for materials selection. Many physical failures in real world arise from it. For instance, the thermal expansion mismatch between silicon nitride and GBs may lead to the crack formation, further reducing the fracture toughness of materials. However, it is still not clear how the presence of GBs modifies the CTE of polycrystals.

In this work, electron energy loss spectroscopy (EELS) in a scanning transmission electron microscope (STEM) was utilized to investigate the local CTE of two $SrTiO_3$ (STO) GBs, with misorientation angles of 36.8° and 45°, respectively. The former corresponds to a coincidence site lattice (CSL) number Σ5, while the latter is a non-CSL GB. Local structure of two GBs was confirmed by an atomic-resolution high angle annular dark field (HAADF) image as well as a density functional theories (DFT) calculation. To determine the CTE near GBs, we measured the local volume expansion at two GBs by recording valence EELS in a nm-scale spatial resolution. In low energy region of EELS, namely low loss, the bulk plasmon peaks represent as the main feature of EEL spectrum and their energy (E_p) is known to be sensitive to volume change. The amount of thermal expansion can be deduced by probing temperature-induced plasmon peak shift.

Our findings indicate that GB do possess larger CTE in direction normal to GB plane, which could largely enhance the CTE of polycrystals, especially in nanocrystalline materials, while the degree of enhancement might be related to GB excess volume, which could differ according to local structure. In this respect, precise control of local CTE in polycrystals could be possibly achieved through GB engineering, which might be of particularly interest for development of nanoscale devices.

Right Figure shows the schematic illustration of this study.

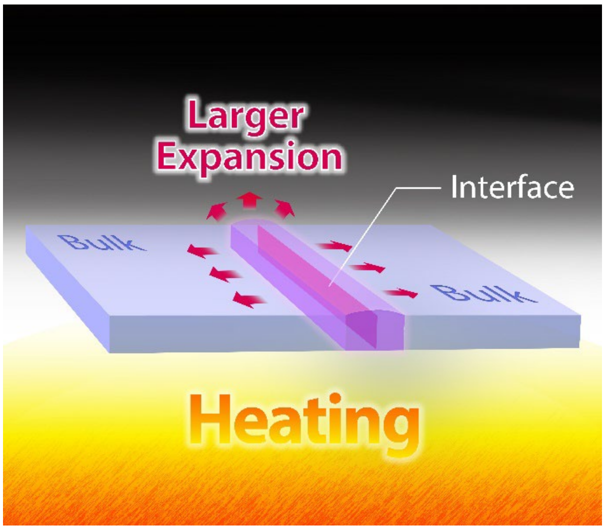

1.2 Quantification of the properties of organic molecules using core-loss spectra as neural network descriptors

The characterization of materials is key to their development as the knowledge obtained by various characterization techniques, such as atomic coordination and chemical bonding, is often correlated with material properties. In other words, material characterization is conducted to determine the relationships among the structure, properties, processing, and performance of materials.

Among the many available characterization techniques, core-loss spectroscopy using electrons and X-rays, specifically electron energy loss near-edge structure (ELNES) and X-ray near-edge structure (XANES), correspond to the core electron adsorption spectrum reflecting the partial densities of state (PDOS) of unoccupied orbitals. These spectroscopic techniques offer experimental characterization with atomic-scale spatial resolution, high temporal resolution, and high sensitivity. Thus, ELNES/XANES techniques have been used to characterize a wide variety of materials systems including electronic devices, biological samples, and drug delivery systems

Although ELNES/XANES measurements can provide useful information for the development of materials, the relationships between their spectral features and material properties are ambiguous. Furthermore, the relationship between ELNES/XANES and extensive properties such as molecular weight and internal energy has not yet been explored.

If direct connections between the spectral features and those properties are established with machine learning, measurements of properties, such as optical properties, electron conductivity, density, and stability, with high sensitivity, high spatial resolution, and high temporal resolution, can be achieved by utilizing the merit of ELNES/XANES. Furthermore, the prediction and design of material properties using the calculated ELNES/XANES spectra can be achieved through direct connection.

In recent years, machine learning (ML) approaches have been widely adopted in materials science to predict material properties with suitable descriptors for screening in a huge materials space and to overcome the limitations of the manual analysis of big data. In the field of spectroscopy, ML approaches have been utilized from the viewpoint of characterization to analyze spectral data obtained from Raman spectroscopy, nuclear magnetic resonance (NMR) spectroscopy, and infrared spectroscopy (IR).

In this study, we developed a new ML approach to directly and quantitatively unveil hidden information on material properties from ELNES/XANES spectral data. Using the molecular structures of organic molecules in computational databases, we performed simulations on the carbon K-edge ELNES/XANES spectra of 22,155 organic molecules and used them as the input to the neural network model to predict the molecular properties. In other words, ELNES/XANES spectra were used as descriptors to quantify the properties of the organic molecules.

We demonstrated that the property predictions of unknown (hypothetical) molecules and predictions using experimental spectra are also available. In addition to single-output predictions, we also achieved the simultaneous prediction of all 12 properties investigated using the C K-edge spectra as descriptors. We expect that our ML approach using the core-loss spectrum as a descriptor paves the way for direct measurement of material properties with high sensitivity, high spatial resolution, and high temporal resolution and for high-throughput screening of materials through prediction of various properties, which will accelerate materials development.

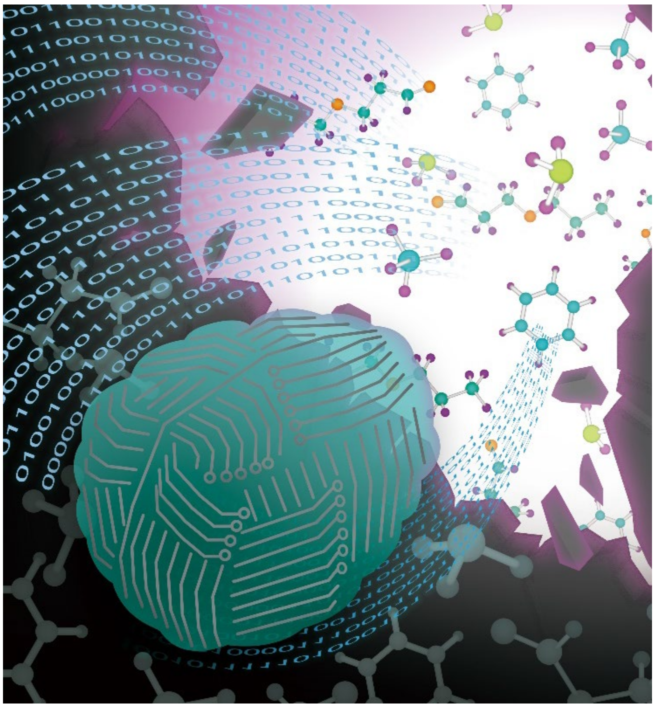

The right figure is the illustration that represents the artificial brain breaking down the insurmountable wall and exposes the various properties of organic molecules.

2. Research Achievements

2.1 Number of original journal papers: 20

2.2 International conference: 15 (including 6 invited presentations)

2.3 Domestic conference: 41 (including 26 invited presentation)

2.4 Number of patents: 0

3. List of awards

- 5 awards in domestic conferences, society, and university.

4. Research Grants

4.1 Total number of research grants: 3

4.2 Number of collaboration research with industries: 3

4.3 List of major research grants (serving as Principal Investigator)

- Grant-in-Aid for Scientific Research A “Materials design via atomic resolution vibrational analysis” from MEXT
- Grant-in-Aid for Scientific Research on Innovative Areas (Research in a proposed research area) “Computational design of functional core using informatics approaches” from MEXT

5. Education

5.1 Number of Ph.D. students (including current students): 3

5.2 Number of master students (including current students): 7

5.3 Number of other students: 0

6. Publication list

Journal Papers (selected)

1. "Determination of the Spectrum–structure Relationship by Tree Structure-based Unsupervised and Supervised Learning" *S. Kiyohara, *K. Kikumasa, K. Shibata, and T. Mizoguchi, Ultramicroscopy, 233 (2022) 113438-1-8.
2. "A brute-force code searching for cell of non-identical displacement for CSL grain boundaries and interfaces", YS. Xie, K. Shibata, and T. Mizoguchi, Comp. Phys. Comm. 273 (2022) 108260-1-8.
3. "Quantification of the Properties of Organic Molecules Using Core-Loss Spectra as Neural Network Descriptors", K. Kikumasa, S. Kiyohara, K. Shibata, and T. Mizoguchi, Advanced Intelligent Systems, 4 (2022) 2100103-1-10. doi:10.1002/aisy.202100103.
4. "Nanoscale Investigation of Local Thermal Expansion at SrTiO3 Grain Boundaries by Electron Energy Loss Spectroscopy", K. Liao, K. Shibata,and T. Mizoguchi, Nano Letters, 21 (2021) 10416-10422.
5. "Quantum Deep Descriptor: Physically Informed Transfer Learning from Small Molecules to Polymers", M. Tsubaki and T. Mizoguchi, J. Chem. Theory Comput., 17 (2021) 7814-7821.
6. "Robotic fabrication of high-quality lamellae for aberration-corrected transmission electron microscopy", H. Tsurusawa, N. Nakanishi,K. Kawano, Y. Chen,B. V. Leer, T. Mizoguchi, Scientifc Reports, 11 (2021) 21599-1-12.
7. "First principles study on formation and migration energies of sodium and lithium in graphite", I.

Takahara and T. Mizoguchi, Phys. Rev. Mater. 5 (2021) 085401-1-7. doi:10.1103/PhysRevMaterials.5.085401.
8. "Accurate prediction of bonding properties by a machine learning–based model using isolated states before bonding", E. Suzuki, K. Shibata, and T. Mizoguchi, Appl. Phys. Exp. 14 (2021) 085503-1-6 doi: 10.35848/1882-0786/ac083b
9. "Revealing Spatial Distribution of Al-Coordinated Species in a Phase-Separated Aluminosilicate Glass by STEM-EELS", K. Liao, A. Masuno, A. Taguchi, H. Moriwake, H. Inoue, and T. Mizoguchi, J. Phys. Chem. Lett., 11 (2020) 9637–9642.
10. "Quantum Deep Field: Data-Driven Wave Function, Electron Density Generation, and Atomization Energy Prediction and Extrapolation with Machine Learning", M. Tsubaki and T. Mizoguchi¸Phys. Rev. Lett., 125 (2020) 206401-1-6.
11. "In situ observation of the dynamics in the middle stage of spinodal decomposition of a silicate glass via scanning transmission electron microscopy", K. Nakazawa, S. Amma, and T. Mizoguchi,Acta Mater. 200 (2020) 720-726.
12. "Learning excited states from ground states by using an artificial neural network", S. Kiyohara, M. Tsubaki, and T. Mizoguchi, npj Comp. Mater., 6 (2020) 68-1-6 DOI:10.1038/s41524-020-0336-3
13. "Real-Space Mapping of Oxygen Coordination in Phase-Separated Aluminosilicate Glass: Implication for Glass Stability", K. Liao, M. Haruta, A. Masuno, H. Inoue, H. Kurata, and T. Mizoguchi, ACS Applied Nano Materials, 3 (2020) 5053-5060 DOI:10.1021/acsanm.0c00196
14. "Prediction of interface and vacancy segregation energies at silver interfaces without determining interface structures", R. Otani, S. Kiyohara, K. Shibata and T. Mizoguchi, Applied Physics Express, 13 (2020) 065504-1-6.
15. "Machine learning applications for ELNES/XANES" (Invited review), T. Mizoguchi and S. Kiyohara, Microscopy, 69 (2020) 92-109. doi.org/10.1093/jmicro/dfz109

Conference Presentations (selected)

Teruyasu Mizoguchi, "Prediction of materials properties from core-loss spectrum using neural network", Americal Physical Society (APS) Spring Meeting 2022, 3/18, Online. (Invited)

Teruyasu Mizoguchi, "Data-driven approaches for EELS", Thailand-Japan international sympo. In Japanese Microscopy Society 2022, 5/13. (Invited)

Teruyasu Mizoguchi, "Vibrational and coordinational structures in glass investigated by STEM-EELS", Symposium of Glass Science and Technology， Zhejiang University, Online， (Invited)

Teruyasu Mizoguchi, "In-situ STEM observation of heterogeneous structure in glass and ionic liquid", PacificChem 2021， Hawaii, Online， Dec. 20, 2021 (Invited)

Teruyasu Mizoguchi, "Data-driven analysis of XAFS and EELS", International symposium in Japanese Chemical Society， 3/22， 2021, Online, (Invited)

OPEN ACCESS

Applied Physics Express **14**, 085503 (2021)

LETTER

https://doi.org/10.35848/1882-0786/ac083b

Accurate prediction of bonding properties by a machine learning–based model using isolated states before bonding

Eiki Suzuki, Kiyou Shibata, and Teruyasu Mizoguchi*

Institute of Industrial Science, The University of Tokyo, 153-8505 Tokyo, Japan

*E-mail: teru@iis.u-tokyo.ac.jp

Received April 27, 2021; revised June 1, 2021; accepted June 3, 2021; published online July 19, 2021

Bonding characters, such as length and strength, are of key importance for material structure and properties. Here, a machine learning (ML) model is used to predict the bonding properties from information pertaining to isolated systems before bonding. This model employs the density of states (DOS) before bond formation as the ML descriptor and accurately predicts the binding energy, bond distance, covalent electron amount, and Fermi energy even when only 20% of the whole dataset is used for training. The results show that the DOS of isolated systems before bonding is a powerful descriptor for the prediction of bonding and adsorption properties. © 2021 The Japan Society of Applied Physics

Supplementary material for this article is available online

The crystal structures and electronic structure of materials are largely influenced by characters of bonding between their constituent atoms. Bond length and strength and their formations are involved in the vacancy formations and surface reactions, and thus plays a crucial role for the materials functions.[1–6] Although numerous first-principles electronic structure simulations and spectroscopic experiments have been conducted to probe bonding character, there is still much to be learned in this regard.[1,7–9]

To obtain a working understanding of bonding character, Linus Pauling and others introduced electronegativity, a parameter that describes the strength and nature of bonds between atoms,[10–13] but, when used on its own, is poorly suited for the accurate quantitative description of bonding between two chemical species.

If the parameters of bonded systems can be predicted from those of the corresponding isolated systems before bonding, some combinations may enable generalization and thus allow one to make predictions for a vast array of other bonded systems comprising combinations of isolated systems. This advantage cannot be obtained using the parameters of bonded systems as explanatory variables. Using isolated systems are also effective from the perspective of efficiency since obtaining the parameters of bonded systems requires much higher computational cost than isolated system due to structural optimization. Furthermore, such accurate predictions should facilitate the selection of materials and the design of their functions related to adsorption and chemical reactions.

In this study, inspired by the recent use of machine learning (ML) to extract useful information from a large amount of atomic and electronic structure data,[14–18] we developed a new ML-based method of bonding property prediction. The constructed model quantitatively predicted bonding properties, such as bond length and strength, from the electronic densities of states (DOSs) of isolated systems before bonding. Since the DOS is an isolated system parameter that can be uniquely calculated not only for single atoms but also for various molecules and surfaces, the use of combination of the DOS of isolated systems as a descriptor has the potential to be used universally for the effective prediction of general systems after bonding, which cannot be achieved by descriptors defined only for isolated atoms or bonded systems.

The DOS is an energy distribution of the states that can be occupied by electrons and is usually used to describe the electronic structure of materials. Previously, the DOS has been used as a ML descriptor to predict the DOS at the Fermi level and other DOS features.[19,20] Furthermore, the DOS was recently used for predicting the binding energy of molecules on metal surfaces.[21,22] However, no attempt has been made to predict several bonding properties, including binding energy, bond length, and chemical bonding, from the DOSs of isolated systems before bonding.

Figure 1 schematically shows the concept of this study. The DOSs of isolated systems before bonding were used as inputs to predict four bonding properties, viz. binding energy, bond length, covalent electron amount, and Fermi energy after bonding. To understand the bonding between atoms in different bonding pairs, we created databases for three types of systems, demonstrating that the DOSs of isolated systems before bonding are powerful descriptors for predicting the properties of the above bonding systems.

First-principles calculations were performed based on the density functional theory (DFT) using the projector-augmented wave (PAW) method with a plane-wave basis set, as implemented in the Vienna ab initio Simulation Package (VASP).[23] Semi-core orbitals were included in the valence. Spin-polarized calculations were performed, but the spin–orbit interaction was not considered. The PAW potentials incorporating scaler relativistic (mass velocity and Darwin terms) were used.

Effects of exchange correlation and van der Waals (vdW) force functionals on the simulation of the surface adsorption have been extensively investigated.[7,8,24,25] In this study, as isolated atoms, molecule, bulk, and adsorption systems are needed to be simulated, the density functional was selected by following criteria: (1) the calculation of some isolated systems are stably converged and the calculated total energies are negative (stable). (2) The accuracy of the functionals was estimated using a simulated interlayer distance of bulk graphite. We have examined six functionals, including

ADVANCED INTELLIGENT SYSTEMS
Open Access
www.advintellsyst.com

Quantification of the Properties of Organic Molecules Using Core-Loss Spectra as Neural Network Descriptors

*Kakeru Kikumasa, Shin Kiyohara, Kiyou Shibata, and Teruyasu Mizoguchi**

Artificial neural networks are applied to quantify the properties of organic molecules by introducing a new descriptor, a core-loss spectrum, which is typically observed experimentally using electron or X-ray spectroscopy. Using the calculated C K-edge core-loss spectra of organic molecules as the descriptor, the neural network models quantitatively predict both intensive and extensive properties, such as the gap between highest occupied molecular orbital (HOMO) and lowest unoccupied molecular orbital (LUMO) (HOMO–LUMO gap) and internal energy. The prediction accuracy estimated by the mean absolute errors for the HOMO–LUMO gap and internal energy is 0.205 and 97.3 eV, respectively, which are comparable with those of previously reported chemical descriptors. This study indicates that the neural network approach using the core-loss spectra as the descriptor has the potential to deconvolute the abundant information available in core-loss spectra for both prediction and experimental characterization of many physical properties. The study shows the practical potential of machine-learning-based material property measurements taking advantage of experimental core-loss spectra, which can be measured with high sensitivity, high spatial resolution, and high temporal resolution.

1. Introduction

The characterization of materials is key to their development as the knowledge obtained by various characterization techniques, such as atomic coordination and chemical bonding, is often correlated with material properties. In other words, material characterization is conducted to determine the relationships among the structure, properties, processing, and performance of materials.

K. Kikumasa, S. Kiyohara, K. Shibata, T. Mizoguchi
Institute of Industrial Science
The University of Tokyo
Tokyo 153-8505, Japan
E-mail: teru@iis.u-tokyo.ac.jp

S. Kiyohara
Laboratory for Materials and Structures
Institute of Innovative Research
Tokyo Institute of Technology
Yokohama 226-8503, Japan

The ORCID identification number(s) for the author(s) of this article can be found under https://doi.org/10.1002/aisy.202100103.

DOI: 10.1002/aisy.202100103

Among the many available characterization techniques, core-loss spectroscopy using electrons and X-rays, specifically electron energy loss near-edge structure (ELNES) and X-ray near-edge structure (XANES), corresponds to the core electron adsorption spectrum reflecting the partial densities of state (PDOS) of unoccupied orbitals. These spectroscopic techniques offer experimental characterization with atomic-scale spatial resolution,[1–3] high temporal resolution,[4,5] and high sensitivity.[6] Thus, ELNES/XANES techniques have been used to characterize a wide variety of materials systems, including electronic devices, biological samples, and drug delivery systems.[7–9]

Although ELNES/XANES measurements can provide useful information for the development of materials, the relationships between their spectral features and material properties are ambiguous. Furthermore, the relationship between ELNES/XANES and extensive properties such as molecular weight and internal energy has not yet been explored.

If direct connections between the spectral features and those properties are established with machine learning (ML), measurements of properties, such as optical properties, electron conductivity, density, and stability, with high sensitivity, high spatial resolution, and high temporal resolution, can be achieved by utilizing the merit of ELNES/XANES. Furthermore, the prediction and design of material properties using the calculated ELNES/XANES spectra can be achieved through direct connection.

In recent years, ML approaches have been widely adopted in materials science to predict material properties with suitable descriptors for screening in a huge materials space and to overcome the limitations of the manual analysis of big data.[10–14] In the field of spectroscopy, ML approaches have been utilized from the viewpoint of characterization to analyze spectral data obtained from Raman spectroscopy, nuclear magnetic resonance (NMR) spectroscopy, and infrared spectroscopy (IR).[15–17] From ELNES/XANES spectral data, ML can extract structural information, such as the bond length and angle,[18] oxidation state,[19] radial distribution function (RDF),[20] and 3D metallic structure.[21] In addition to extract structural information, interpretations and classifications of ELNES/XANES spectra have also been performed by combining supervised and unsupervised ML approaches.[22,23]

In a recent study by our group, we developed an ML approach to directly quantify the local structure and chemical bonding

Ultramicroscopy 233 (2022) 113438

Contents lists available at ScienceDirect

Ultramicroscopy

journal homepage: www.elsevier.com/locate/ultramic

Automatic determination of the spectrum–structure relationship by tree structure-based unsupervised and supervised learning

Shin Kiyohara [a,b,*,1], Kakeru Kikumasa [a,1], Kiyou Shibata [a], Teruyasu Mizoguchi [a,*]

[a] *Institute of Industrial Science, the University of Tokyo, Tokyo 153-8505, Japan*
[b] *Laboratory for Materials and Structures, Institute of Innovative Research, Tokyo Institute of Technology, Yokohama 226-8503, Japan*

ARTICLE INFO

Keywords:
ELNES/XANES
Informatics
Machine learning

ABSTRACT

Spectroscopy is widely used for the analysis of chemical, vibrational, and bonding information. Interpretations of the spectral features have been performed by comparing the objective spectra with reference spectra from experiments or simulations. However, the interpretation process by humans is not always straightforward, especially for spectra obtained from unknown or new materials. In the present study, we developed a method using machine learning techniques to obtain human-like interpretation automatically. We combined unsupervised and supervised learning methods; then applied it to the spectrum database which includes more than 400 spectra of water and organic molecules containing various ligands and chemical bonds. The proposed method has successfully found the correlations between the spectral features and descriptors of the atoms, bonds, and ligands. We demonstrated that the proposed method enabled the automatic determination of reasonable spectrum–structure relationships such as between π^* resonance in C-K edges and multiple bonds. The proposed method enables the automatic determination of physically and chemically reasonable spectrum–structure relationships without arbitrariness in data-driven manner, which is considerably difficult only with simulation or conventional machine leaning techniques. Such relationships are useful for understanding what structural parameters cause changes in the spectrum, providing a way for the better interpretation of spatial distributed or time evolutionary data. Furthermore, although the present work focused on the ELNES/XANES spectrum from small organic molecules, the proposed method can be readily extended to other spectral data. It is expected to contribute to a better understanding of the spectrum–structure relationship in various spectroscopy applications.

1. Introduction

Characterization of atomic and electronic structures is indispensable in materials chemistry. The process is necessary for the development of new materials; thus a variety of analytical techniques are employed based on the relevant system, the desired information, and the required resolution. Since chemical reactions particularly occur in very local environments, an understanding of the atomic and electronic structures is very important. Moreover, during chemical reactions, the atomic and electronic structures of molecules undergo dynamic changes depending on the reaction environment; hence an understanding of the entire transition is also imperative.

In the context of the foregoing, ELNES/XANES spectroscopy is a promising technique for the analysis of both atomic and electronic structures with nano-order spatial resolution and time resolution. The technique utilizes X-ray or fast electrons as probes; the spectral data thus reflects the atomic and electronic structures at the nano- subnano-scale in real space. It specifically offers very local information such as the constituent elements, oxidation state, coordination environment, and chemical bonds [1–6]. Furthermore, ELNES/XANES experiments can be performed in operando, in the case of which the spectrum changes also reflect the atomic and electronic structure transitions that occur during a chemical reaction. This has informed the broad use of ELNES/XANES spectroscopic techniques in the investigation of chemical materials science processes such as catalytic reaction, oxygen reduction reaction (ORR), and electrochemical reaction [7–12].

However, the interpretation of the obtained ELNES/XANES spectra is not usually straightforward. Even if distinct feature changes in the time-

* Corresponding authors.
E-mail address: kiyohara@msl.titech.ac.jp (S. Kiyohara).

[1] S.K. and K.K. contributed equally to this work. S.K., K.K. and T.M. designed research; S.K. and K.K. performed research; S.K., K.K, K.S. and T.M. analyzed data; and S.K., K.K., K.S. and T.M. wrote the paper.

https://doi.org/10.1016/j.ultramic.2021.113438
Received 6 July 2021; Received in revised form 19 November 2021; Accepted 27 November 2021
Available online 4 December 2021
0304-3991/

NANO LETTERS

pubs.acs.org/NanoLett

Letter

Nanoscale Investigation of Local Thermal Expansion at $SrTiO_3$ Grain Boundaries by Electron Energy Loss Spectroscopy

Kunyen Liao, Kiyou Shibata, and Teruyasu Mizoguchi*

Cite This: *Nano Lett.* 2021, 21, 10416−10422

Read Online

ACCESS | Metrics & More | Article Recommendations | Supporting Information

ABSTRACT: The presence of grain boundaries (GBs) has a great impact on the coefficient of thermal expansion (CTE) of polycrystals. However, direct measurement of local expansion of GBs remains challenging for conventional methods due to the lack of spatial resolution. In this work, we utilized the valence electron energy loss spectroscopy (EELS) in a scanning transmission electron microscope (STEM) to directly measure the CTE of Σ5 and 45°GBs of $SrTiO_3$ at a temperature range between 373 and 973 K. A CTE that was about 3 times larger was observed in Σ5 GB along the direction normal to GB plane, while only a 1.4 time enhancement was found in the 45° GB. Our result provides direct evidence that GBs contribute to the enhancement of CTE in polycrystals. Also, this work has revealed how thermodynamic properties are varied in different GB structures and demonstrated the potential of EELS for probing local thermal properties with nanometer-scale resolution.

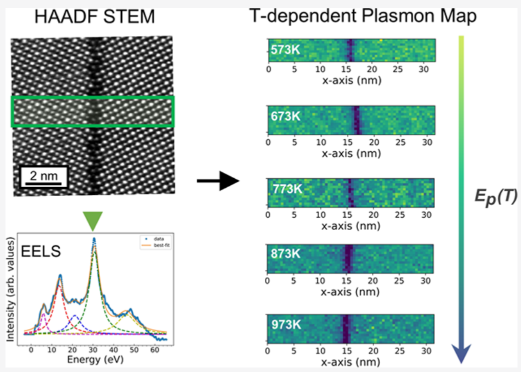

KEYWORDS: *scanning transmission electron microscopy, electron energy loss spectroscopy, grain boundaries, thermal expansion*

Grain boundaries (GBs), interfaces between crystallites in polycrystals, possess unique atomic arrangement. The distinct structure of GBs may have a large impact on various physical properties such as ion diffusivity, thermal conductivity, and elastic response.[1−6] These local properties near GBs have attracted great interest especially in nanocrystalline materials, which contain large volume fraction of GBs.[7−9] The coefficient of thermal expansion (CTE) is the essence for materials selection and design.[10−13] Many physical failures in the real world arise from it. For instance, the thermal expansion mismatch between silicon nitride and GBs may lead to the crack formation, further reducing the fracture toughness of materials.[14] However, it is still not clear how the presence of GBs modifies the CTE of polycrystals. Klam et al. reported a 2.5−5 times increase of CTE in Cu as crystallite size reduced from millimeter to micrometer scale.[15] Fitzsimmons et al. measured the lattice parameters and thermal displacement near Σ13 twist GB in Au,[16] where they obtained an about 3 times larger CTE in the direction normal to the GB plane. Sutton performed the molecular dynamic simulation on Au GBs and obtained the same result.[17] Although these experimental and theoretical studies generally conclude that increasing amounts of GBs to enhance the CTE of polycrystals, inconsistent results are also reported that CTEs of polycrystals could be independent or even smaller as volume fraction of GBs increases.[18−20]

The disparity of previous reports about thermal expansion near GBs is likely attributed to the following issues. First, the most previous studies were carried out in a polycrystalline sample with the fraction of GBs estimated by crystallite size. The misorientation angles of GBs and their local structure were neglected in the conventional measurement. However, it is well-known that GBs with varied misorientation angles may exhibit wide energy landscapes which ultimately lead to different physical properties.[21−23] In this respect, CTEs of GBs also differ greatly according to their local structure. Second, CTEs of bulk and GBs cannot be well separated by the conventional measurements such as dilatometry or X-ray diffraction (XRD). None of these methods has enough spatial resolution to directly measure the local expansion near the GB plane, which typically has a width of about 1 nm. Third, compositional changes, microstructural evolution, and growth of pores are common sources of error for CTE measurement, whereas they are hard to be evaluated by conventional methods.[20,24] Under these considerations, a technique for local CTE measurement with nanoscale resolution is required to unravel the relationship of GB local structure and its thermal expansion behavior.

In this work, electron energy loss spectroscopy (EELS) in a scanning transmission electron microscope (STEM) was utilized to investigate the local CTE of two $SrTiO_3$ (STO) GBs with misorientation angles of 36.8° and 45°, respectively. The former corresponds to a coincidence site lattice (CSL) number Σ5, while the latter is a non-CSL GB. Local structure of

Received: September 27, 2021
Revised: October 28, 2021
Published: December 2, 2021

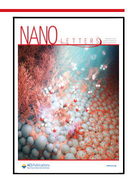

https://doi.org/10.1021/acs.nanolett.1c03735
Nano Lett. 2021, 21, 10416−10422

Quantum Deep Field: Data-Driven Wave Function, Electron Density Generation, and Atomization Energy Prediction and Extrapolation with Machine Learning

Masashi Tsubaki*
National Institute of Advanced Industrial Science and Technology, 2-3-26 Aomi, Koto-ku, Tokyo 135-0064, Japan

Teruyasu Mizoguchi†
Institute of Industrial Science, University of Tokyo, 4-6-1 Komaba, Meguro-ku, Tokyo 153-8505, Japan

(Received 16 March 2020; accepted 23 September 2020; published 10 November 2020)

Deep neural networks (DNNs) have been used to successfully predict molecular properties calculated based on the Kohn-Sham density functional theory (KS-DFT). Although this prediction is fast and accurate, we believe that a DNN model for KS-DFT must not only predict the properties but also provide the electron density of a molecule. This Letter presents the quantum deep field (QDF), which provides the electron density with an unsupervised but end-to-end physics-informed modeling by learning the atomization energy on a large-scale dataset. QDF performed well at atomization energy prediction, generated valid electron density, and demonstrated extrapolation.

DOI: 10.1103/PhysRevLett.125.206401

Quantum chemical simulations, such as Kohn-Sham density functional theory (KS-DFT) calculations have been recently approximated by machine learning (ML) techniques such as kernel methods [1–3]. Very recently, deep neural networks (DNNs) [4,5] have been used to successfully predict molecular properties, such as the atomization energy, HOMO, and LUMO, on large-scale datasets. Although this prediction is fast and accurate, there is a problem: a DNN model for KS-DFT must be consistently based on an understanding of the underlying physics and must not only predict the properties but also provide the fundamental quantum characteristics (i.e., the wave function or orbital and electron density) of a molecule. Most existing DNN models, however, cannot provide the electron density because they consider only the atomic coordinates and ignore the molecular field. Furthermore, they are mainly interested in predicting the final output, i.e., the interpolation accuracy of a molecular property within a benchmark dataset, and do not focus on capturing the fundamental characteristics of molecules. This does not lead to learning a physically meaningful model and extrapolation, i.e., prediction for totally unknown molecules in terms of its size and structure that do not appear in the dataset. Extrapolation is important in not only molecular science but also real applications for transferring to other molecules or crystals and predicting their properties [6,7] in materials informatics.

In this Letter, we present a simple framework called the quantum deep field (QDF) that provides the electron density of molecules by learning their atomization energies on a large-scale dataset. Crucially, our data-driven QDF framework requires only the molecule-energy pairs (e.g., the QM9 dataset [8]) and does not require the molecule-density pairs for training; in other words, QDF generates the electron density indirectly or in an unsupervised fashion with end-to-end physics-informed modeling. The QDF model involves three linear and nonlinear components: (i) a linear combination of atomic orbitals (LCAO): $\phi \to \psi$, where ϕ is the atomic basis function given by the Gaussian-type orbital (GTO) and ψ is the KS molecular orbital, (ii) a nonlinear energy functional: $\psi \to E$, where E is the atomization energy, and (iii) a nonlinear Hohenberg–Kohn (HK) map: $\rho \to V$, where ρ is the electron density and V is the external potential. We optimize all parameters of the LCAO, energy functional, and HK map, in which the latter two are implemented by simple DNNs, simultaneously using the backpropagation and stochastic gradient descent (SGD) [9].

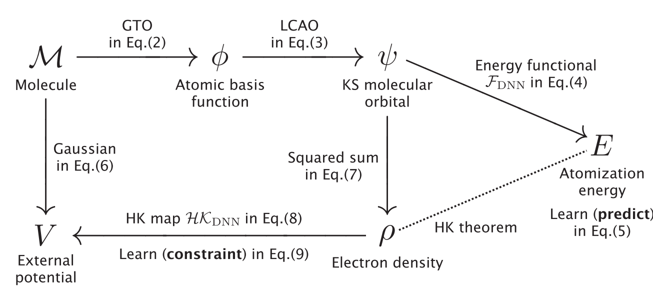

FIG. 1. An overview of the computational flow of our proposed QDF framework. The details of each arrow in this figure are described in the corresponding equation.

NOMURA Laboratory

Current Research Activities 2021-2022

Nomura Laboratory

1. Research Topics

1.1 Nanoscale heat transfer in nanostructured semiconductors

We investigate heat conduction control in a semiconductor membrane by nanostructuring from the viewpoint of photonics. What we can learn from photonics and phonon-photon hybrid systems is an interesting approach to study nanoscale heat transfer.

The light propagation in ray optics and phonon transport in the nanoscale are similar due to ballisticity. The characteristic propagation of light and mechanical vibration in band-engineered structures, i.e. photonic and phononic crystals [1], stems from the wave property of electromagnetic wave and elastic wave. Some recent works on heat conduction control by well-designed nanostructures are picked to discuss how we design nanostructures to control heat flow more effectively by considering the similarity and difference of photons and thermal phonons. The ballisticity of phonons in their mean free path MFP enables advanced heat flux control such as directional heat flux and heat focusing [2]. These phenomena seem against the law of entropy increase but are possible in a thermal nonequilibrium state. The interaction and hybridization of photons and phonons are also interesting and will give new functionality. Phonons can control the emission of a single photon from a quantum dot embedded in a high-Q optical microcavity [3]. Phonons can travel faster by four orders of magnitude by shaking hands with photons; forming surface phonon polaritons (SPhPs). Also, "phonon" scattering is strongly suppressed by dressing electromagnetic wave, which results in the enhancement of thermal conduction in thin dielectric membranes [4]. The collective behavior, which exists in electronic and phononic systems, but not in photonic system, of phonons provide interesting thermal transport known as phonon hydrodynamics will also interesting [5].

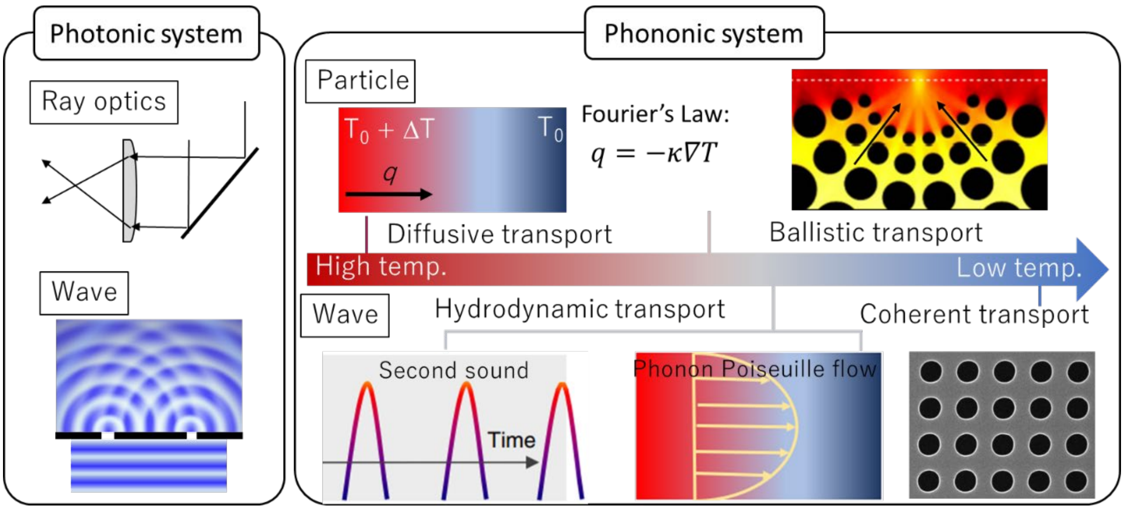

Figure 1. Similarity of photonics and phononics. Ballisticity and wave property of photons and phonons enable the same description in transport but more complexity in thermal phonon transport.

References [1] J. Maire, *et al.*, Sci. Adv. **3**, e1700027 (2017). [2] R. Anufriev, *et al.*, ACS Nano **12**, 11928 (2018). [3] M. Nomura, *et al.*, Nat. Phys. **6**, 279 (2010). [4] Y. Wu, *et al.*, Sci. Adv. 6, eabb4461 (2020). [5] X. Huan, *et al.*, under review.

1.2 Thermoelectric energy harvesting ~device and monitoring~

Thermoelectric generators (TEGs) are one of the promising devices to supply electricity to components of sensor networks by harvesting energy from the environmental heat source. The performance of thermoelectric materials is given by the figure of merit ZT defined as $ZT = S^2 sT/k$ where S, s, k, and T are Seebeck coefficient, electrical conductivity, thermal conductivity, and temperature, respectively. Silicon is an inherently inferior thermoelectric material due to the relatively high k (~130 $Wm^{-1}K^{-1}$ for bulk). However, since the hundredth reduction of k by nanostructuring the material is demonstrated in various nanostructures.

We develop planar-type Si TEGs with phononic crystal (PnC) nanostructures fabricated in n-type poly-Si films under collaboration with University of Freiburg. The planar-type TEG is fabricated by all lithography-based processes, considering future mass and low-cost production. We perform a finite element method (FEM) simulation on the device to optimize the structural parameters and enhance the performance.

Figure 2 shows the schematic pictures of a planar-type TEG with four unit structures and a whole device chip. We define the temperature difference between the bottom of the substrate and the top of the cap wafer as ΔT_{DEV} and the temperature gradient along the nanostructured thermoelectric membrane as ΔT_{TE}. TEG is composed of uni-leg devices using only n-type thermoelectric material, and unit devices are connected between the hot side and the cold side in the poly-Si layer. The cap Si wafer is placed on top of the device layer with the supporting spacer material. Thermal design of the device is important to increase the ratio of $\Delta T_{TE}/\Delta T_{DEV}$ for larger power generation. We estimate that an order of micro Watt per square centimeter at 1 K temperature difference with this structure, which enables to send a sensing data to a network in a day.

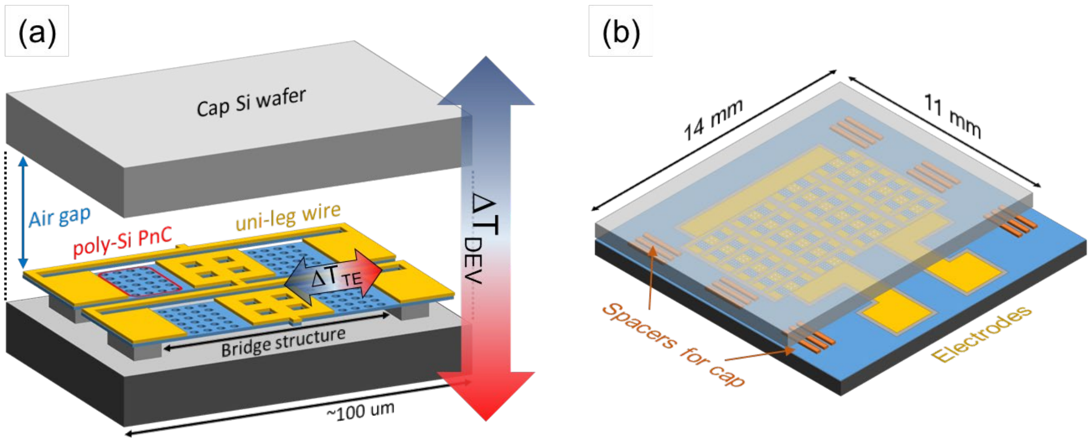

Figure 2. Schematic pictures of the planar-type Si TEG with PnC nanostructures for (a) unit devices with the top cavity structure and (b) a whole chip device.

Reference:

[1] M. Nomura, Y. Kage, D. Müller, D. Moser and O. Paul, Appl. Phys. Lett. 106, 223106 (2015).

[2] R. Yanagisawa, N. Tsujii, T. Mori, P. Ruther, O. Paul, and M. Nomura, "Nanostructured planar-type uni-leg Si thermoelectric generators," Appl. Phys. Express 13, 095001 (2020).

2. Research Achievements

2.1 Number of original journal papers: 20

2.2 International conference: 27 (including 9 invited presentations),

2.3 Domestic conference: 24 (including 9 invited presentation)

2.4 Number of patents: 0

3. List of awards

None

4. Research Grants

4.1 Total number of research grants: 12

4.2 Number of collaboration research with industries: 6

4.3 List of major research grants (serving as Principal Investigator)

- CREST, JST
- Research Grants by Japan Society for the Promotion of Science (KAKENHI)

5. Education

5.1 Number of Ph.D. students (including current students): 4

5.2 Number of master students (including current students): 3

5.3 Number of other students: 0

6. Publication list

Journal Paper

1. Y. Ishii, R. Yanagisawa, N. Watanabe, M. Nomura, N. Sasaki, and K. Miura, “Large lateral contact stiffness on Si nanopillar surfaces,” AIP Adv. 12, 025225 (2022).
2. M. Nomura, R. Anufriev, Z. Zhang, J. Maire, Y. Guo, R. Yanagisawa, and S. Volz, “Review of thermal transport in phononic crystals,” Mater. Today Phys. 22, 100613 (2022). (Invited review)
3. Z. Zhang, Y. Guo, M. Bescond, J. Chen, M. Nomura, and S. Volz, “Heat conduction theory including phonon coherence,” Phys. Rev. Lett. 128, 015901 (2022).
4. K. Li, Y. Cheng, H. Wang, Y. Guo, Z. Zhang, M. Bescond, M. Nomura, S. Volz, X. Zhang, and S. Xiong, "Phonon resonant effect in silicon membranes with different crystallographic orientations," Int. J. Heat Mass Transf. 183, 122144 (2022).

5. S. Jin, Z. Zhang, Y. Guo, J. Chen, M. Nomura, and S. Volz, “Optimization of interfacial thermal transport in Si/Ge heterostructure driven by machine learning,” Int. J. Heat Mass Transf. 182, 122014 (2022).
6. Y. Guo, S. Tachikawa, S. Volz, M. Nomura, and J. Ordonez-Miranda, “Quantum of thermal conductance of nanofilms due to surface-phonon polaritons,” Phys. Rev. B. 104. L201407 (2021).
7. J. Ordonez-Miranda, Y. Guo, J. J. Alvarado-Gil, S. Volz, and M. Nomura, “Thermal-Wave Diode,” Phys. Rev. Appl. 16, L041002 (2021).
8. Y. Guo, M. Bescond, Z. Zhang, S. Xiong, K. Hirakawa, M. Nomura, and S. Volz, “Thermal conductivity minimum of graded superlattices due to phonon localization,” APL Mater. 9, 091104 (2021).
9. Y. Guo, Z. Zhang, M. Bescond, S. Xiong, M. Wang, M. Nomura, and S. Volz, “Size effect on phonon hydrodynamics in graphite microstructures and nanostructures,” Phys. Rev. B 104, 075450 (2021).
10. Z. Zhang, Y. Guo, M. Bescond, J. Chen, M. Nomura, and S. Volz, “Thermal self-synchronization of nano-objects,” J. Appl. Phys. 130, 084301 (2021).
11. Y. Guo, M. Nomura, S. Volz, and J. Ordonez-Miranda, “Heat Transport Driven by the Coupling of Polaritons and Phonons in a Polar Nanowire,” Energies, 14(16), 5110 (2021).
12. R. Anufriev, Y. Wu, and M. Nomura, “Ballistic heat conduction in semiconductor nanowires,” J. Appl. Phys. 130, 070903 (2021). (Invited Review)
13. Z. Zhang, Y. Guo, M. Bescond, J. Chen, M. Nomura, and S. Volz, “Coherent thermal transport in nano-phononic crystals: An overview,” APL Mater. 9, 081102 (2021). (Invited Review)
14. Y. Cheng, M. Nomura, S. Volz, and S. Xiong, “Phonon-dislocation interaction and its impact on thermal conductivity,” J. Appl. Phys. 130, 040902 (2021).
15. R. Anufriev, J. Maire, and M. Nomura, “Review of coherent heat and phonon transport control in one-dimensional phononic crystals,” APL Mater. 9, 070701 (2021).(Invited Review)
16. H. Wang, Y. Cheng, Z. Fan, Y. Guo, Z. Zhang, M. Bescond, M. Nomura, T. Ala-Nissila, S. Volz, and S. Xiong, “Anomalous thermal conductivity enhancement in low dimensional resonant nanostructures due to imperfections,” Nanoscale, 13, 10010-10015 (2021).
17. J. Ordonez-Miranda, S. Volz, and M. Nomura, “Surface Phonon-Polariton Heat Capacity of Polar Nanolms,” Phys. Rev. Appl. 15, 054068 (2021).

18. T.-H. Xiao, Z. Cheng, Z. Luo, A. Isozaki, K. Hiramatsu, T. Itoh, M. Nomura, S. Iwamoto, and K. Goda, “All-dielectric chiral-field-enhanced Raman optical activity,” Nat. Commun. 12, 3062 (2021).
19. Y. Guo, Z. Zhang, M. Bescond, S. Xiong, M. Nomura and S. Volz, “Anharmonic phonon-phonon scattering at the interface between two solids by non-equilibrium Green's function,” Phys. Rev. B 103, 174306 (2021).
20. Z. Zhang, Y. Guo, M. Bescond, J. Chen, M. Nomura, and S. Volz, “Generalized decay law for particlelike and wavelike thermal phonons,” Phys. Rev. B 103, 184307 (2021).

International Conference

1. M. Nomura (Invited), “Planar-type nano phononic Si energy harvesters,” TMS2022, online (2022).
2. T.-H. Xiao, Z. Cheng, Z. Luo, A. Isozaki, K. Hiramatsu, T. Itoh, M. Nomura, S. Iwamoto, and K. Goda, “Chiral-field-enhanced Raman optical activity by a silicon nanodisk array,” SPIE Photonics West 2022, 11957-35 (2022).
3. M. Nomura (Invited), “Planar-type nano phononic Si energy harvesters,” TMS2022, online (2022).
4. T.-H. Xiao, Z. Cheng, Z. Luo, A. Isozaki, K. Hiramatsu, T. Itoh, M. Nomura, S. Iwamoto, and K. Goda, “Chiral-field-enhanced Raman optical activity by a silicon nanodisk array,” SPIE Photonics West 2022, 11957-35 (2022).
5. R. Yanagisawa, P. Ruther, O. Paul and M. Nomura, “Development of planar-type thermoelectric generator with double cavity and silicon nanostructure,” NAMIS Marathon Workshop, B-6, online (2021).
6. T. Nawae, R. Yanagisawa and M. Nomura, “Investigation of high aspect ratio phononic crystal” NAMIS Marathon Workshop, C-10, online (2021).
7. S. Tachikawa, J. Ordonez-Miranda, Y. Wu, L. Jalabert, R. Anufriev, S. Volz, and M. Nomura, “Propagation of surface phonon-polaritons in the multilayer system,” NAMIS Marathon Workshop, C-11, online (2021).
8. Y. Wu, J. Ordonez-Miranda, L. Jalabert, S. Tachikawa, R. Anufriev, H. Fujita S. Volz, and M. Nomura, “Quasi-ballistic propagation of surface phonon-polaritons in dielectric thin films,” NAMIS Marathon Workshop, C-14, online (2021).
9. M. Nomura (Invited), “Advanced thermal transport control in semiconductors by nanostructuring,” POSTEC Korea, online (2021).
10. M. Nomura (Invited), “Planar-type nanophononic Si thermoelectric energy harvesters,” International Conference on Materials and Systems for Sustainability 2021, Area4, online (2021).

11. S. Koike, R. Yanagisawa, M. Kurosawa, and M. Nomura, “Design of a planar-type uni-leg SiGe thermoelectric generator,” International Conference on Materials and Systems for Sustainability 2021, 1142, online (2021).
12. M. Nomura and R. Anufriev (Invited), “Ray phononics: heat flux engineering by nanostructuring,” The 3rd IIS-MESA+ Workshop, 26-6, online (2021).
13. M. Nomura (Invited), “Phonon-engineered Si thermoelectric energy harvesting,” AMU/CNRS-IIS/UTokyo Energy Workshop, 2-1, onlline (2021).
14. R. Yanagisawa, P. Ruther, O. Paul, and M. Nomura, “Planar-type Si phononic crystal thermoelectric generator with a top cavity structure,” 1st Japan France Virtual Workshop on Thermoelectrics, 1B.04, online (2021).
15. E. Sido, R. Yanagisawa , S. Koike, and M. Nomura, “Design and Fabrication of world's smallest uni-leg thermoelectric cooler,” VCT 2021, AS-O.2-09, online (2021).
16. Z. Zhang (Invited), Y. Guo, M. Bescond, J. Chen, S. Volz, M. Nomura, “Self-synchronization of Thermal phonons in a Charged Silicon Resonator System,” META 2021, the 11th International Conference on Metamaterials, Photonic Crystals and Plasmonics, Session 1A8, online (2021).
17. J. Ordonez-Miranda, Y. Guo, J. J. Alvarado-Gil, S. Volz, and M. Nomura, “Thermal Diode Based on the Spatiotemporal Modulation of Thermal Properties,” 27th International Workshop on Thermal Investigation of ICS and Systems, (2021).
18. M. Nomura (invited), Y. Wu, J. Ordonez-Miranda, R. Anufriev, and S. Volz, “Surface phonon polariton: the 4th heat carrier in SiN nanofilms,” CLEO®/Europe-EQEC 2021, JSI-4.1, online (2021)
19. Z. Zhang, Y. Guo, M. Nomura, J. Chen, and S. Volz, “Generalized law of heat conduction including the intrinsic coherence of thermal phonons,” CLEO®/Europe-EQEC 2021, JSI-P.1, online (2021)
20. Y. Guo, Z. Zhang, M. Bescond, M. Nomura, and S. Volz, “Thermal boundary conductance of Si/Ge interface by anharmonic phonon non-equilibrium Green function formalism,” CLEO®/Europe-EQEC 2021, JSI-1.2, online (2021)
21. Y. Guo, Z. Zhang, M. Bescond, S. Xiong, M. Nomura, S. Volz, “Heat Transport at Si/Ge Interface by Anharmonic Phonon Non-Equilibrium Green Function Formalism,” 2021 Virtual MRS Spring Meeting & Exhibit, NM08.15.08: Late News, online (2021).
22. R. Anufriev, J. Ordonez-Miranda, M. Nomura, “Phonon Mean Free Path Spectroscopy in Semiconductor Membranes,” 2021 Virtual MRS Spring Meeting & Exhibit, NM08.11.02, online (2021).
23. R. Anufriev, M. Nomura, “Ray Phononics for Advanced Heat Flux Manipulations in Ballistic Regime,” 2021 Virtual MRS Spring Meeting & Exhibit, NM08.06.02, online

(2021).

24. Z. Zhang, Y. Guo, M. Bescond, J. Chen, M. Nomura, and S. Volz, “Generalized Law of Heat Conduction Including the Intrinsic Coherence of Thermal Phonons,” 2021 Virtual MRS Spring Meeting & Exhibit, NM08.05.09: Late News, online (2021).
25. S. Tachikawa, J. Ordonez-Miranda, Y. Wu, L. Jalabert, R. Anufriev, S. Volz, M. Nomura, “Thickness Dependence of Surface Phonon-Polariton Propagation Length in SiO2/Si/SiO2 Structures,” 2021 Virtual MRS Spring Meeting & Exhibit, NM08.01.02: Late News, online (2021).
26. Y. Wu, J. Ordonez-Miranda, L. Jalabert, S. Tachikawa, R. Anufriev, S. Volz, M. Nomura, “Experimental Observation of Quasi-Ballistic Thermal Transport of Surface Phonon-Polaritons Over Hundreds of Micrometers,” 2021 Virtual MRS Spring Meeting & Exhibit, NM08.01.01: Late News, online (2021).
27. Y. Wu, J. Ordonez-Miranda, R. Anufriev, S. Volz, and M. Nomura (Keynote), “Heat Transfer in SiN Nanomembranes with Surface Phonon Polariton,” ICMDA 2021, Speech III, Chiba (2021).

Materials Today Physics 22 (2022) 100613

Contents lists available at ScienceDirect

Materials Today Physics

journal homepage: https://www.journals.elsevier.com/materials-today-physics

Review of thermal transport in phononic crystals

Masahiro Nomura [a, b, *], Roman Anufriev [a], Zhongwei Zhang [a], Jeremie Maire [c], Yangyu Guo [a], Ryoto Yanagisawa [a], Sebastian Volz [a, d]

[a] *Institute of Industrial Science, The University of Tokyo, Tokyo, 153-8505, Japan*
[b] *Research Center for Advanced Science and Technology, The University of Tokyo, Tokyo, 153-8904, Japan*
[c] *I2M, UMR 5295, CNRS-UB-ENSAM, 33405, Talence, France*
[d] *LIMMS, CNRS-IIS IRL 2820, The University of Tokyo, Tokyo, 153-8505, Japan*

A R T I C L E I N F O

Article history:
Received 5 November 2021
Received in revised form
21 December 2021
Accepted 12 January 2022
Available online 18 January 2022

Keywords:
Phonon
Phononic crystal
Thermal conductivity
Thermal transport
Thermoelectrics

A B S T R A C T

Thermal transport at the nanoscale level is attracting attention not only because of its physically interesting features such as the peculiar behavior of phonons due to their pronounced ballistic and wave-like properties but also because of its potential applications in alleviating heat dissipation problems in electronic and optical devices and thermoelectric energy harvesting. In the last quarter-century, researchers have elucidated the thermal transport properties of various nanostructured materials, including phononic crystals (PnCs): artificial periodic structures for phonons. PnCs are excellent platforms for investigating thermal transport owing to their well-defined structural parameters. In addition, it is interesting to control thermal transport by interference, as demonstrated in the low-frequency regime with elastic waves and sounds. In this article, we focus on high-frequency phonons and review the thermal transport in semiconductor PnCs. This comprehensive review provides an understanding of recent studies and trends, organized as theoretical and experimental, in terms of the quasiparticle and wave aspects.

1. Introduction

A phonon is a collective excitation in condensed matter, which is a quantization of the vibration mode in elastic structures. Although phonons are not as popular as photons or electrons, they are ubiquitous in our daily lives. Phonons have a broad spectrum and are labeled in different frequency ranges as sound waves ($10–10^4$ Hz), ultrasound ($10^4–10^8$ Hz), hypersound ($10^8–10^{11}$ Hz), and heat (over 10^{11} Hz). Phonons in the lower frequency range are often excited electrically in the GHz range and are used in various applications, including musical instruments, measurements, sensing, imaging, and piezoelectric transducers. Micro- or nano-electromechanical systems, known as MEMS/NEMS, are exemplary applications of well-defined phonons generated in artificial mechanical structures [1,2]. In the very-high-frequency range, although the boundary is unclear, the thermal vibrations of atoms or molecules are the sources of phonons, called thermal phonons.

It is challenging and interesting to pursue the possibility of reducing or increasing the thermal conductivity by nanostructuring. The phonon propagation can be engineered by using phononic crystals (PnCs)—artificial materials with a periodic structure—for phonon interference owing to the induced periodicity. PnCs are often used to investigate or control sound waves, acoustic waves, and even heat transfer in solids. There are many insightful books and reviews on phonon transport in PnCs in various frequency ranges [3–8]; we focus on PnCs in the thermal spectral range in this review.

Fig. 1 shows an increasing number of articles on PnCs and thermal transport in PnCs, published since 2005. The percentage of articles on thermal transport in terms of the articles on PnCs also shows an increasing trend. The dimensions of PnCs used for heat conduction engineering are typically at the scale of the thermal phonon mean free path (MFP), the average distance between the scatterings, or the thermal phonon wavelength depending on the phenomenon of interest. Fig. 2 shows the different types of PnC structures for thermal transport studies in the incoherent and coherent regimes.

In the incoherent thermal transport regime, materials with high thermal conductivity and established process technologies, such as

* Corresponding author. Institute of Industrial Science, The University of Tokyo, Tokyo, 153-8505, Japan.
E-mail address: nomura@iis.u-tokyo.ac.jp (M. Nomura).

https://doi.org/10.1016/j.mtphys.2022.100613

Heat Conduction Theory Including Phonon Coherence

Zhongwei Zhang,[1,*] Yangyu Guo,[1] Marc Bescond,[2] Jie Chen,[3,†] Masahiro Nomura,[1] and Sebastian Volz[1,2,3,‡]
[1]Institute of Industrial Science, The University of Tokyo, Tokyo 153-8505, Japan
[2]Laboratory for Integrated Micro and Mechatronic Systems, CNRS-IIS UMI 2820, The University of Tokyo, Tokyo 153-8505, Japan
[3]Center for Phononics and Thermal Energy Science, School of Physics Science and Engineering and China-EU Joint Lab for Nanophononics, Tongji University, Shanghai 200092, People's Republic of China

(Received 20 June 2021; accepted 3 December 2021; published 3 January 2022)

Understanding and quantifying the fundamental physical property of coherence of thermal excitations is a long-standing and general problem in physics. The conventional theory, i.e., the phonon gas model, fails to describe coherence and its impact on thermal transport. In this Letter, we propose a general heat conduction formalism supported by theoretical arguments and direct atomic simulations, which takes into account both the conventional phonon gas model and the wave nature of thermal phonons. By naturally introducing wave packets in the heat flux from fundamental concepts, we derive an original thermal conductivity expression including coherence times and lifetimes. Our theory and simulations reveal two distinct types of coherence, i.e., intrinsic and mutual, appearing in two different temperature ranges. This contribution establishes a fundamental frame for understanding and quantifying the coherence of thermal phonons, which should have a general impact on the estimation of the thermal properties of solids.

DOI: 10.1103/PhysRevLett.128.015901

Phonons, i.e., quanta of vibrational waves, are commonly considered as one of the fundamental quasiparticles, simultaneously exhibiting wave- and particlelike characteristics in nanostructured crystals or bulk materials. The wavelike behavior of phonons impacts thermal properties via coherence mechanisms, as highlighted by several pioneering [1,2] and recent works [3,4]. The particlelike behavior has been treated by the Boltzmann transport equation (BTE) and the phonon-gas model in most solids [5–10]. Experiments [1,2,11–13] have revealed, however, that the wave nature of thermal phonons plays a substantial role in thermal transport, as, for example, in the observations of coherent thermal transport in nanophononic crystals [1,2,11,12]. Later, theoretical and simulation studies [14–18] were devoted to the understanding of phonon coherence, such as the one producing band folding [19–21], but missing the particle behavior. Recently, the theoretical study [22] revealed that the realistic phonon dynamics can only be manifested if both intrinsic coherence relevant to the extension of phonon wave packets and the particlelike behavior of thermal phonons are taken into account.

The conventional BTE also fails in complex crystals, as a pure particle picture cannot yield a complete description of thermal conductivity, such as in Tl_3VSe_4 [23,24]. Recently, Simoncelli *et al.* [3] developed a theory for thermal transport in glasses and complex crystals, in which the coherence between densely packed phonon branches contributes to thermal transport. A similar approach has been developed by Isaeva *et al.* [4] as well, at the same time. This mutual coherence among branches is identified as an additional phonon wave-relevant term [25–27]. The picture of this mutual coherence, which might be compared to a hopping process, however, remains physically unclear. Finally, quantifying the full coherence of thermal phonons and its effect on heat conduction remains a critical issue in transport physics.

In this Letter, a general heat conduction theory is proposed to establish an original expression for the thermal conductivity that includes the full coherent nature of phonon excitations. This expression involves both phonon lifetimes and coherence times. Those are obtained by tracking the real phonon dynamics and using a wavelet transform of the atomic trajectories during an equilibrium molecular dynamic (EMD) simulation. We show that the predictions of our theory yield significant differences from those of the conventional phonon-gas model, as demonstrated in the Tl_3VSe_4 case [see atomic structure in Fig. 1(a)]. We find that there are two types of coherence, i.e., intrinsic and mutual, which take a critical role over different temperature regions. These conclusions open unexpected insights on the reality of thermally activated phonon modes and the importance of the diverse coherence mechanisms when assessing thermal properties.

The thermal conductivity (κ) can be calculated based on the Green-Kubo approach with the autocorrelation of the heat flux $\mathbf{S}(t)$ as [28]

$$\kappa = \frac{V}{3k_B T^2} \int \langle \mathbf{S}(t) \cdot \mathbf{S}(0) \rangle dt, \quad (1)$$

where V corresponds to the system volume, k_B is the Boltzmann constant, and T is the temperature. We now

Size effect on phonon hydrodynamics in graphite microstructures and nanostructures

Yangyu Guo,[1,*] Zhongwei Zhang,[1] Marc Bescond,[2] Shiyun Xiong,[1] Moran Wang,[3]
Masahiro Nomura,[1,†] and Sebastian Volz[1,2,‡]
[1]*Institute of Industrial Science, The University of Tokyo, Tokyo 153-8505, Japan*
[2]*LIMMS, CNRS-IIS UMI 2820, The University of Tokyo, Tokyo 153-8505, Japan*
[3]*Department of Engineering Mechanics, Tsinghua University, Beijing 100084, China*

(Received 7 June 2021; revised 20 July 2021; accepted 17 August 2021; published 30 August 2021)

The understanding of hydrodynamic heat transport in finite-sized graphitic materials remains elusive due to the lack of an efficient methodology. In this paper, we develop a computational framework enabling an accurate description of heat transport in anisotropic graphite ribbons by a kinetic theory approach with full quantum mechanical first-principles input. A unified analysis of the size scaling of the thermal conductivity in the longitudinal and transverse directions of the system is made within the computational framework complemented with a macroscopic hydrodynamic approach. As a result, we demonstrate a strong end effect on the phonon Knudsen minimum, as a hallmark of the transition from ballistic to hydrodynamic heat transports, along a rectangular graphite ribbon with finite length and width. The phonon Knudsen minimum is found to take place only when the ribbon length is ∼5–10 times the upper limit of the width range in the hydrodynamic regime. This paper contributes to a unique methodology with high efficiency and a deeper understanding of the size effect on phonon hydrodynamics, which would open opportunities for its theoretical and experimental investigation in graphitic micro- and nanostructures.

DOI: 10.1103/PhysRevB.104.075450

I. INTRODUCTION

Hydrodynamic heat transport is a collective phenomenon in condensed matter in the presence of dominant momentum-conserving normal scattering of phonons [1–3]. The investigation of phonon hydrodynamics was motivated by the exploration of second sound (wavelike heat transport) in solids at low temperatures [4,5]. On the other hand, it has significantly promoted the development of macroscopic hydrodynamic equations for non-Fourier heat transport [5–9]. There is a renewed interest in hydrodynamic heat transport in graphitic materials in recent years due to its occurrence at relatively high temperatures [10–12], which shows great potential for thermal management applications [13–15].

The theoretical prediction of phonon hydrodynamics in graphitic materials is mainly based on the homogenous solution of the Boltzmann equation in the bulk limit [10,11,16]. To have a deeper understanding of hydrodynamic heat transport in micro- and nanostructures, a direct solution of the space- and time-dependent phonon Boltzmann equation becomes indispensable yet a challenging task. The widely used phonon Boltzmann equation under single mode relaxation time (SMRT) approximation does not work well in this situation due to the collective effect from strong normal scattering [10,16,17]. Crucial progress toward this challenge is the Monte Carlo solution of the phonon Boltzmann equation with a full scattering term on two-dimensional (2D) reciprocal space [18], which has been mostly applied to study phonon hydrodynamics in 2D graphene ribbons [3,19] due to the model applicability and a considerable computational cost. As the theoretical prediction has been confirmed by the recent experimental reports of second sound [12] and phonon Poiseuille flow [20] in graphite, an efficient methodology for modeling the hydrodynamic heat transport in micro- and nanoribbons of graphite with three-dimensional (3D) reciprocal space is highly desired, which is the main aim of this paper.

Callaway's dual relaxation model [21] represents a good approximation to the full scattering term in the phonon Boltzmann equation [10,22] and has been widely adopted in analyzing heat transport in the hydrodynamic regime by analytical or semi-analytical methods [5,23–29]. The direct solution of the phonon Boltzmann equation under Callaway's model has been advanced recently by a few numerical schemes including both deterministic methods [30,31] and stochastic ones [32,33]. However, the deterministic numerical method [30,31] was designed for heat transport in 2D graphene ribbons with empirical isotropic phonon properties. The gray Monte Carlo simulation [32,33] was conducted in hypothetical graphitic materials due to the lack of knowledge of normal and Umklapp scattering rates and the pending development of the methodology. Thus, none of the previous methods [30–33] are available to describe heat transport in realistic anisotropic graphite ribbons. In this paper, a pertinent computational framework is developed based on a deterministic numerical solution of Callaway's model. The normal and Umklapp phonon scattering rates in graphite are calculated

*yyguo@iis.u-tokyo.ac.jp
†nomura@iis.u-tokyo.ac.jp
‡volz@iis.u-tokyo.ac.jp

APL Materials RESEARCH UPDATE scitation.org/journal/apm

Review of coherent phonon and heat transport control in one-dimensional phononic crystals at nanoscale

Cite as: APL Mater. 9, 070701 (2021); doi: 10.1063/5.0052230
Submitted: 30 March 2021 • Accepted: 21 June 2021 •
Published Online: 7 July 2021

View Online Export Citation CrossMark

Roman Anufriev,[1,a)] Jeremie Maire,[2] and Masahiro Nomura[1]

AFFILIATIONS

[1] Institute of Industrial Science, The University of Tokyo, Tokyo 153-8505, Japan
[2] Institut de mécanique et d'ingénierie (I2M), CNRS UMR5295, Talence 33405, France

Note: This paper is part of the Special Topic on Phononic Crystals at Various Frequencies.
[a)]**Author to whom correspondence should be addressed:** anufriev@iis.u-tokyo.ac.jp

ABSTRACT

Phononic crystals are the acoustic analogs of photonic crystals and aim at manipulating phonon transport using phonon interference in periodic structures. While such periodic structures are typically two-dimensional, many applications require one-dimensional (1D) wire-like or bulk structures instead. In this Research Update, we summarize the past decade of theoretical and experimental studies of coherent control of phonon and heat transport in one-dimensional phononic crystals. At the hypersonic frequencies, phononic crystals successfully found applications in optomechanical devices at the microscale. However, at higher terahertz frequencies, experimentalists struggle to demonstrate that coherent thermal transport at room temperature is possible at length scales of hundreds of nanometers. Although many theoretical works predict a reduction in the thermal conductivity in 1D phononic crystals due to coherent effects, most observations conclude about the incoherent nature of heat conduction at least at room temperature. Nevertheless, experiments on superlattices and carbon nanotubes have demonstrated evidence of coherent heat conduction even at room temperature in structures with the periodicity of a few nanometers. Thus, further miniaturization and improving fabrication quality are currently the main challenges faced by 1D phononic nanostructures.

INTRODUCTION

Phonons are the primary carriers of sound, heat, and mechanical vibrations in semiconductors. Thus, controlling phonon transport has always been one of the primary goals for researchers working on thermoelectric, electromechanical, and optomechanical systems. Being inspired by light manipulations based on the wave interference of photons,[1,2] researchers applied a similar approach to manipulations of phonons, as phonons are essentially waves in the atomic lattice.

This wave-based approach led to the development of acoustic analogs of photonic crystals called phononic crystals[3–5]—the artificial structures with periodic boundaries that systematically reflect phonons and cause phonon interference. Ever since, phononic crystals have been gradually decreasing in size from the micro- to nanoscale, thus increasing the frequency of phonons they could affect and potentially control.[6–8]

Today, two-dimensional (2D) phononic crystals became an alternative component in various systems, including optomechanical cavities,[9,10] sensors,[11,12] and thermoelectric generators.[13,14] However, advances in nanowire fabrication, electron-beam lithography, and molecular beam epitaxy motivated the use of one-dimensional (1D) structures as a base for future phononic devices.[15–18] Subsequently, 1D phononic crystals emerged as an enhancement of 1D wires, beams, and bulk materials with applications at ultrasonic, hypersonic, and even terahertz frequencies.

This Research Update summarizes the past decade of studies on the coherent transport of phonons and heat in 1D phononic structures. First, we illustrate the basic principles of coherent control of phonon dispersion in 1D phononic structures. Next, we review

Letter

Thermal-Wave Diode

Jose Ordonez-Miranda,[1,2,*] Yangyu Guo,[2] Juan J. Alvarado-Gil,[3] Sebastian Volz,[1,2]
and Masahiro Nomura[1,2]

[1] *LIMMS, CNRS-IIS UMI 2820, The University of Tokyo, Tokyo 153-8505, Japan*
[2] *Institute of Industrial Science, The University of Tokyo, Tokyo 153-8505, Japan*
[3] *Applied Physics Department, CINVESTAV-IPN, Mérida, Yucatán 97310, Mexico*

(Received 22 February 2021; revised 24 September 2021; accepted 8 October 2021; published 28 October 2021)

Based on the spatiotemporal modulation of thermal conductivity and volumetric heat capacity, we propose a thermal-wave diode characterized by the rectification of the heat currents carried by thermal waves. By transforming Fourier's law for the heat flux and the diffusion equation for the temperature into equations with constant coefficients, it is shown that: (i) the rectification effect is generated by the simultaneous wavelike modulation of both thermal properties, such that it disappears in the absence of either of them, and (ii) the rectification factor can be optimized and tuned by means of the speed and phase difference of the variations of the heat capacity and thermal conductivity. High rectification factors, greater than 86%, are obtained for lower frequencies driving the propagation of thermal waves. The proposed thermal-wave diode is thus analogous to its electronic counterpart operating with modulated electrical currents and can open a vista for developing different types of thermal-wave logic components.

DOI: 10.1103/PhysRevApplied.16.L041002

Nonlinear heat transport based on the metal-insulator transition of materials [1] and the coupling of dissimilar lattices [2–5] has recently attracted great interest for the control of conductive and radiative heat currents [6–10]. This phenomenon is observed in materials with thermal and optical properties depending on temperature, which has been exploited to conceive and develop thermal diodes [6,11–17], thermal transistors [18–21], thermal memories [22,23], and thermal memristors [24,25] that make possible the processing of information via thermal electrons, phonons, and photons. The operation of these thermal devices is, however, usually limited temperatures in which the material properties exhibit significant changes with temperature. Heat control with nonlinear materials is thus typically restricted to narrow temperature ranges.

Materials with properties periodically modulated in space and time are able to overcome the major drawbacks of nonlinear ones, given that they are able to operate at required temperature, frequency, and scale [26,27]. This spatiotemporal modulation of material properties has been theoretically and experimentally studied in elastic [8,28,29], acoustic [30–33], photonic [34,35], and thermal [36–39] systems. As a result of the wavelike variation of their properties, these materials exhibit a nonreciprocal response for the propagation of waves, which provides an effective method to allow the flow of energy in a given direction and impede it in the opposite one. By considering the spatiotemporal modulation of thermal conductivity and heat capacity in the form of a traveling wave, Torrent *et al.* [39] showed that a material behaves like an effective medium with constant thermal properties and an internal convectionlike term in the diffusion equation describing its temperature profile. This convective term induces the nonreciprocal response of the material for heat flux, which takes different values depending on its direction parallel or antiparallel to the traveling waves of the thermal properties. Those authors thus demonstrated that materials with thermal conductivity and heat capacity periodically modulated in space and time can be used to develop thermal diodes operating with steady-state heat fluxes [39]. As this modulation of the thermal properties has a dynamic origin, its impact on the transient heat conduction regime is expected to be strong, but has not been studied yet. In particular, given that this dynamic regime is driven by the heat capacity, its spatiotemporal modulation may induce a nonreciprocal behavior on the heat flux carried by the thermal waves predicted by Fourier's law [40]. These diffusion waves are periodic temperature fluctuations widely applied in thermal detection via photothermal and photoacoustic techniques [40–42] that could be implemented to generate and detect the rectification of their heat currents.

The purpose of this Letter is to demonstrate the proof of principle of a thermal-wave diode based on the spatiotemporal modulation of thermal conductivity and volumetric heat capacity. This is done by determining and optimizing the rectification of the heat fluxes carried by the nonreciprocal thermal waves propagating in the forward and

*jose.ordonez@cnrs.fr

TIXIER-MITA Laboratory

Current Research Activities 2021-2022

Tixier-Mita Laboratory

1. Research Topics

1.1 <u>Electrophysiology of Pancreatic β cell using Thin-Film-Transistor based bio-sensing platform</u>

The purpose of thin research is to study and elucidate the pathophysiology of pancreatic islet of Langerhans related diseases. As the functional unit of the pancreas, islets of Langerhans play vital roles in regulating glycaemia by secreting insulin at the right moment and in appropriate amounts. Dysfunction of the insulin-secreting β cells perturbs glucose homeostasis, leading to life-threatening hypoglycemia due to excessive insulin secretion or to damaging hyperglycemia owing to insufficient insulin secretion. On technique to study these islet is by measuring the action potential released by the β cell during chemical stimulation with glucose, with a Multi-Electrode Array (MEAs). However, resolution with standard MEAs is quite low, and monitoring of the different β cells activity is not possible. This is why a Thin-Film-Transistor platform has been used for that investigation.

Thin Film Transistor (TFT) technology, originally used for panel display fabrication, is used in our group for a new kind of bio-sensing devices for various applications like cell manipulation, cell electrophysiology investigation and biomolecule sensing.

Compared to standard bio-sensors based on MEMS and CMOS technology, TFT devices combine at the same time large and high resolution array of microelectrode as well as transparency of the whole device. Actually, the large and high resolution array of microelectrodes are made of transparent Indium-Tin-Oxide (ITO) micro-electrodes fabricated on a glass substrate, which is compatible with optical

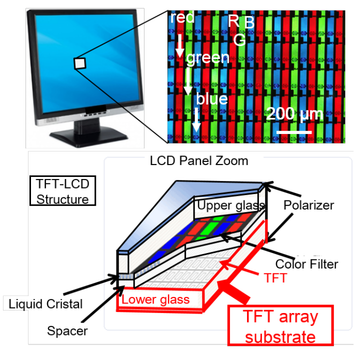

TFT array substrate description

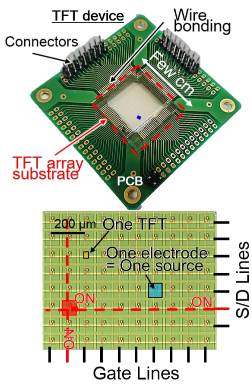

Mounted substrate and microscopic view

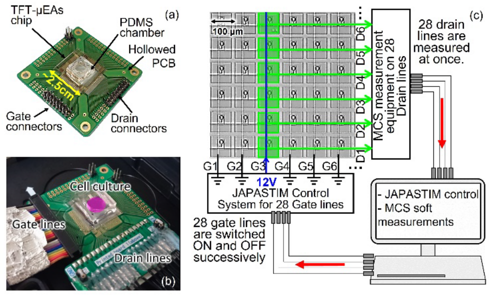

Set-up of for electrophysiology measurements

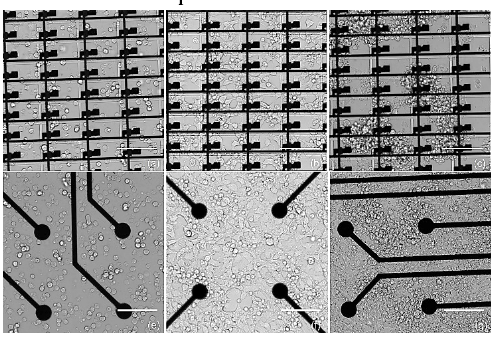

Top lane: iGL cells on the TFT-platform at (a) day 0; (b) day 3; (c) day 7

Bottom lane: iGL cells on MEAs at (e) day 0; (f) day 3; (g) day 7. Scale bar: 100 μm.

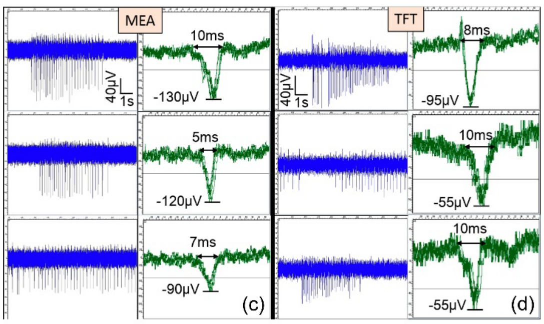

Extracellular voltage of iGL cells (day 4) on three microelectrodes of standard MEA and TFT platform in HBSS containing 15 mM glucose.

observation with an inverted microscope. In addition the microelectrodes are controlled individually by an array of switch TFTs and can be used either as sensors, or to apply a signal.

In this study, we demonstrated real-time electrophysiological monitoring on pancreatic β cell line (iGL cell) with TFT bio-sensing platform. At the surface of the platform, iGL cells were successfully cultured and attached via poly-l-lysine and laminin coating. Action potentials of iGL cells stimulated by 15 mM glucose were successfully observed with the TFT bio-sensing platform and compared to standard MEA devices, showing similar signals, in term of duration time, amplitude and signal-to-noise ratio. Finally, luminescent intensity of insulin secreted by iGL cells cultured on the TF platform and standard MEAs was measured and shows higher intensity in the case of TFT bio-sensing platform.

This work was performed in collaboration with Prof. Sakai from the Chemical System Engineering Dpt., The University of Tokyo, and Prof. Komori from Kindai University.

1.2 <u>Multi-modal sensing with Thin-Film-Transistor based bio-sensing platform</u>

In this research, the same TFT bio-sensing platform as the above paragraph was applied to electrophysiology and electrochemical measurements, giving a first demonstration of multi-modality measurements with that platform. In particular, 2-D mapping of the activity of cardiomyocyte cell cultured on the platform was realized and confirmed with simultaneous optical observation of cell contraction. In addition, tyramine was also measured by voltammetry and amperometry techniques using the transparent microelectrodes as working electrodes and an integrated Ag/AgCl reference electrode

The dynamical property of the heart bioelectrical system is closely associated with cardiac diseases. There is thus a growing interest in the development of system analysis for studying the cardiac signaling network. The signals are either electrical signals as chemical signals. So, to obtain overall information

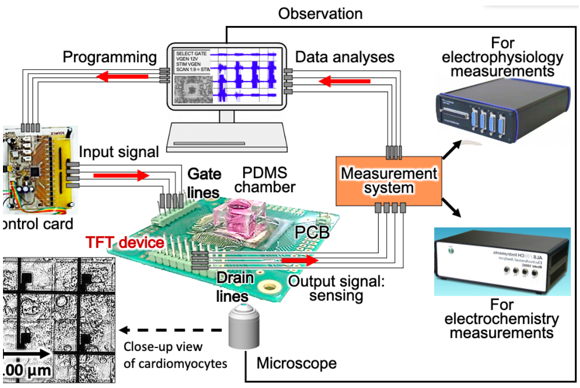

Experimental set-up.

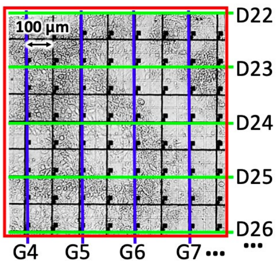

Heart cells cultured on the platform.

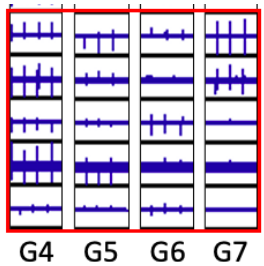

Corresponding cell activity

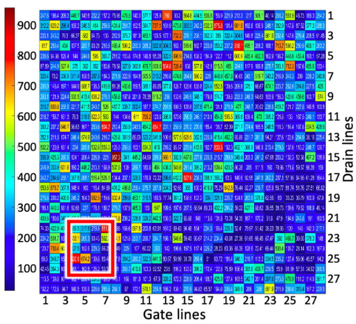

2-D cardiomyocyte cell culture activity on a 5.6 mm square area.

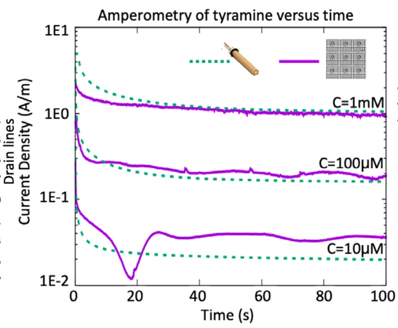

Amperommetry of tyramine vs. time with standard gold WE and TFT microelectrode WE.

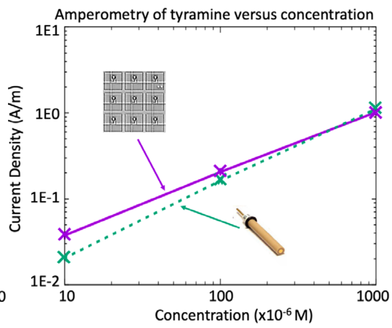

Amperommetry of tyramine vs. C° with standard gold WE and TFT microelectrode WE.

of cell activity, multi-modal sensors able to measure all these different signals are essential.

Here, we took advantage of the high resolution of the microelectrodes array to realize the action potential 2-D mapping of cardiomyocyte cell culture. For that purpose, an array of 28x28 microelectrodes was selected from the 22,500 (150x150) microelectrodes of the platform. This array corresponds to a surface of 5.6mm square, with microelectrodes dimensions of 100μm square, and spacing of 100μm. Then a Matlab spiking sorting algorithm was developed to reconstruct the 2-D cells potential activity mapping from the measurements obtained electrode by electrode.

This work was performed in collaboration with Prof. Fujiu from the Graduate School of Medicine, The University of Tokyo.

1.3 Matlab Spiking Sorting Algorithm for the processing of data from a TFT bio-sensing platform

A Matlab Spiking Sorting Algorithm was developed to process electrophysiology data of cardiomyocyte cells cultured on the TFT bio-sensing platform described here above. An array of 28x28 microelectrodes (784 microelectrodes in total) was selected from the 22,500 (150x150) microelectrodes of the platform for measurement. Such large data cannot be processed using available software of the data acquisition system used. This algorithm includes specific functions adapted to the TFT platform functioning and can be applied also to larger TFT electrode arrays.

The program algorithm consists in: 1) Opening the datafile; 2) Extract the data for each electrode; 3) Filter the data; 4) Detect the spikes; 5) Characterize the spikes; 6) Localize the microelectrode; 7) Display the results. This process is repeated for all measured electrodes. A map of the peak to peak amplitude, as well as the map of the average period can be obtained. Comparison with optical observation is performed by comparing cell contraction and measured electrical activity.

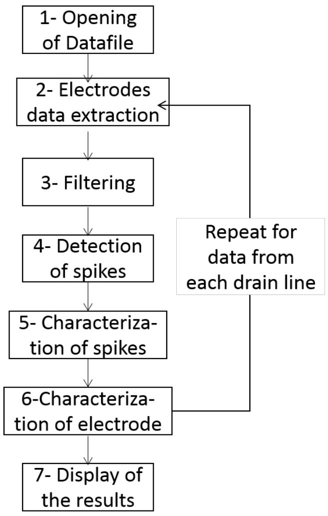

Matlab algorithm description

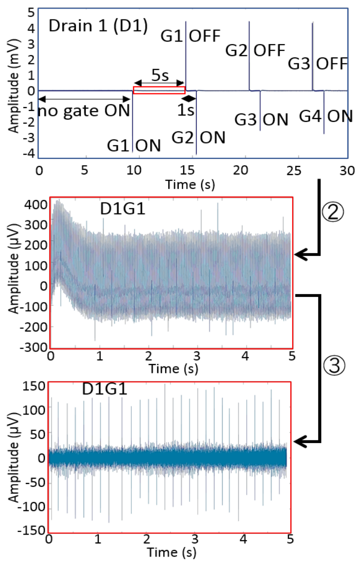

Data extraction and filtering from raw data (steps 1, 2, 3 of Matlab algorithm)

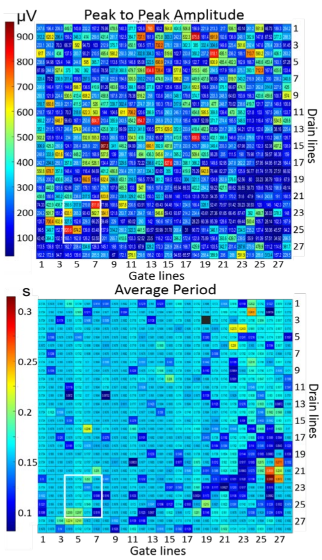

2D Cartography of the results for amplitude and period.

2. Research Achievements

2.1 Number of original journal papers: 3

2.2 International conference: 8 (including 2 invited presentation),

2.3 Domestic conference: 1 (including 0 invited presentations)

2.4 Number of patents: 0

3. List of awards

1. 19th IEEE EDS Japan Joint Chapter Student Award: Anne-Claire Eiler (Graduate School Student)
   Anne-Claire Eiler, Pierre-Marie Faure, Junichi Sugita, Satoshi Ihida, Dongchen Zhu, Yasuyuki Sakai, Katsuhito Fujiu, Kikuo Komori, Hiroshi Toshiyoshi, Agnès Tixier-Mita, "Thin-Film-Transistor Platform for Electrophysiological and Electrochemical Characterization of Cells", IEEE 66th International Electron Devices Meeting (IEDM'2020), San Francisco, US. (online) December 12-16, 2020.

4. Research Grants

4.1 Total number of research grants: 2

4.2 Number of collaboration research with industries: 1

4.3 List of major research grants (serving as Principal Investigator): 1

1. 科研費挑戦的研究（萌芽）：代表「TFT 電極アレイを応用した高時空間分解マルチバイオイメージング法の検証」、2021.10－2023.03

5. Education

5.1 Number of Ph.D. students (including current students): 1

5.2 Number of master students (including current students): 0

5.3 Number of other students: 1 (1 internship students)

6. Publication list

Journal Papers

1. Dongchen Zhu, Grant A. Cathcart, Satoshi Ihida, Hiroshi Toshiyoshi, Agnès Tixier-Mita, Yasuyuki Sakai and Kikuo Komori, "Toward the development of a label-free multiple immunosensor based on thin film transistor microelectrode arrays", Journal of Micromechanics and Microengineering, Vol. 31(11), 115002, (September 2021). DOI: 10.1088/1361-6439/ac2547

2. Wan-Ting Chiu, Tso-Fu Mark Chang, Masato Sone, Hideki Hosoda, Agnès Tixier-Mita and Hiroshi Toshiyoshi, "Developments of the Electroactive Materials for Non-Enzymatic Glucose Sensing and Their Mechanisms", Electrochem 2021, Vol. 2(2), pp. 347-389, (June 2021). DOI: 10.3390/electrochem2020025

3. Anne-Claire Eiler, Pierre-Marie Faure, Junichi Sugita, Satoshi Ihida, Dongchen Zhu, Yasuyuki Sakai, Katsuhito Fujiu, Kikuo Komori, Hiroshi Toshiyoshi, Agnès Tixier-Mita, "Application of a Thin-Film Transistor Array for Cellular-Resolution Electrophysiology and Electrochemistry",

IEEE Transactions on Electron Devices, Vol. 68(4), pp. 2041-2048, (April 2021). DOI: 10.1109/TED.2021.3050432

Conference presentations

1. Dongchen Zhu, Anne-Claire Eiler, Satoshi Ihida, Yasuyuki Sakai, Hiroshi Toshiyoshi, Agnès Tixier-Mita and Kikuo Komori, "Real-time Simultaneous Measurement of Pancreatic β Cell Electrophysiology and Fluorescent Bioimaging Based on High-resolution Thin-film Transistor Microelectrode Arrays", The 38th Sensor Symposium, Online, November 9-11 2021.

2. Agnès Tixier-Mita, Tieying Xu, Anne-Claire Eiler, Satoshi Ihida and Hiroshi Toshiyoshi, "Multi-modal Thin-Film-Transistor Biosensing Platforms for Bio-medical Investigations: Contribution to Internet-of-Medical-Things", The 10th IEEE International Components, Packaging, and Manufacturing Technology Symposium (IEEE ICSJ'2021), Kyoto, Japan, November 10-12 2021. (Invited) DOI: 10.1109/ICSJ52620.2021.9648907

3. Anne-Claire Eiler, Junichi Sugita, Satoshi Ihida, Hiroshi Toshiyoshi, Katsuhito Fujiu, and Agnès Tixier-Mita, "A thin-film-transistor active matrix array for 2D real space electrical imaging of heart cell cultures", The 31st Anniversary World Congress on Biosensors (BIOSENSORS 2020/2021), Busan Exhibition and Conference Centre, Busan, Korea, Online, July 26-29 2021.

4. Takafumi Yamaguchi, Naoto Usami, Kei Misumi, Atsushi Toyokura, Akio Higo, Shimpei Ono, Gilgueng Hwang, Guilhem Larrieu, Yoshiho Ikeuchi, Agnès Tixier-Mita, Ken Saito, Timothée Lévi and Yoshio Mita, "Self-deformable Flexible MEMS Tweezer Made of Poly(Vinylidene Fluoride)/Ionic Liquid Gel with Electrical Measurement Capability", The 21th International Conference on Solid-State Sensors, Actuators and Microsystems (Transducers'2021), Online, June 20-25 2021. DOI: 10.1109/Transducers50396.2021.9495482

5. Taku Tsuchiya, Yuki Okamoto, Frederic Marty, Ayako Mizushima, Agnès Tixier-Mita, Olivier Francais, Bruno Le Pioufle, and Yoshio Mita, "Two-Dimensionally Arrayed Double-Layer Electrode Device which, Enables Reliable and High-Thoroughput Electrorotation", The 34th International Conference on Micro Electro Mechanical Systems (IEEE MEMS'2021), Online, January 25-29 2021.

6. Agnès Tixier-Mita, Yoshio Mita, Yong Zeng, Mei He, Jonas Tegenfeldt, Christelle Prinz, "Panel discussion: Parenting in Science and Work-Life Balance", The 24th International Conference on Miniaturized Systems for Chemistry and Life Sciences (µTAS'2020), Online, October 4-9 2020. (Invited)

7. Anne-Claire Eiler, Pierre-Marie Faure, Junichi Sugita, Satoshi Ihida, Zhu Dongchen, Yasuyuki Sakai, Katsuhito Fujiu, Kikuo Komori, Hiroshi Toshiyoshi, Agnès Tixier-Mita, "Thin-Film-Transistor Platform for Electrophysiological and Electrochemical Characterization of Cells", IEEE 66th International Electron Devices Meeting (IEDM 2020), Online, December 12-16, 2020.

8. Pierre-Marie Faure, Anne-Claire Eiler, Satoshi Ihida, Junichi Sugita, Katsuhito Fujiu, Hiroshi Toshiyoshi, Agnès Tixier-Mita, "A Matlab Spiking Sorting Algorithm for Data Processing of In-Vitro Cardiomyocyte Electrophysiology with a Thin-Film-Transistor Platform", The 37th Sensor Symposium, Online, October 26-28 2020.

Application of a Thin-Film Transistor Array for Cellular-Resolution Electrophysiology and Electrochemistry

Anne-Claire Eiler, Pierre-Marie Faure, Junichi Sugita, Satoshi Ihida, Dongchen Zhu, Yasuyuki Sakai, Katsuhito Fujiu, Kikuo Komori, Hiroshi Toshiyoshi, *Member, IEEE*, and Agnès Tixier-Mita, *Member, IEEE*

***Abstract*—The constant development and improvement of microelectromechanical systems (MEMS) have been given a great opportunity to develop new reliable microsystems devices for biomedical research. This article presents a locally addressable 2-D arrayed indium–tin oxide microelectrode platform with integrated thin-film transistors (TFTs) for biological and chemical sensing. Microelectrode arrays (MEAs) using TFT have the advantage of being transparent with a high density of microelectrodes on a large surface. *In vitro* 2-D electrical measurements on 28 parallel-connected lines selected from a 22 500 MEA were successfully performed with heart cells for the first time. Observation of cell contraction was performed simultaneously with an inverted microscope. Voltammetry and amperometry measurements were also demonstrated using the transparent microelectrodes as working electrodes and an integrated Ag/AgCl reference electrode. Due to its unique features, we believe that the TFT platform can provide more understanding of the key communication between heart cells, and large-scale cardiovascular and nervous systems. As a result, the platform offers unique access to versatile lab-on-a-chip devices that integrate many measurement techniques on one chip for the study of cell cultures, tissues, and organoids.**

***Index Terms*—Cardiomyocytes, electrochemistry, electrophysiology, indium–tin oxide (ITO), microelectrode array (MEA), sensors, thin-film transistors (TFTs), tyramine.**

Manuscript received November 24, 2020; revised December 22, 2020; accepted January 3, 2021. Date of publication January 22, 2021; date of current version March 24, 2021. This work was supported in part by the Japan Society for the Promotion of Science (JSPS) Grant Kakenhi Kiban B16H04344, in part by the Institute of Industrial Sciences 2019 Grant Senteikenkyu, and in part by the Laboratory for Integrated Micro Mechatronic Systems (LIMMS) Internal Project 2019 Grant. This article is an extended version of a paper presented at IEDM 2020. The review of this article was arranged by Editor D. Triyoso. *(Corresponding author: Anne-Claire Eiler.)*

Anne-Claire Eiler is with the Department of Advanced Interdisciplinary Studies, The University of Tokyo, Tokyo 153-8505, Japan (e-mail: anne@iis.u-tokyo.ac.jp).

Pierre-Marie Faure is with ENSEIRB-MATMECA, 33400 Bordeaux, France (e-mail: pierre-marie.faure@bordeaux-inp.fr).

Junichi Sugita and Katsuhito Fujiu are with the Department of Cardiovascular Medicine, The University of Tokyo, Tokyo 113-8654, Japan (e-mail: jsugita-tky@umin.ac.jp; fujiu-tky@umin.ac.jp).

Satoshi Ihida, Hiroshi Toshiyoshi, and Agnès Tixier-Mita are with the Institute of Industrial Science, The University of Tokyo, Tokyo 153-8505, Japan (e-mail: ihida@iis.u-tokyo.ac.jp; hiro@iis.u-tokyo.ac.jp; agnes@iis.u-tokyo.ac.jp).

Dongchen Zhu and Yasuyuki Sakai are with the Department of Chemical System Engineering, The University of Tokyo, Tokyo 113-8654, Japan (e-mail: dongchenzhu1996@g.ecc.u-tokyo.ac.jp; sakaiyasu@chemsys.t.u-tokyo.ac.jp).

Kikuo Komori is with the Department of Biotechnology and Chemistry, Kindai University, Hiroshima 739-2116, Japan (e-mail: komori@hiro.kindai.ac.jp).

Color versions of one or more figures in this article are available at https://doi.org/10.1109/TED.2021.3050432.

Digital Object Identifier 10.1109/TED.2021.3050432

Nomenclature

MEMS	Microelectromechanical systems.
MEA	Microelectrode array.
CMOS	Complementary metal–oxide–semiconductors.
IEDM	International Electron Devices Meeting.
TFT	Thin-film transistor.
LCD TVs	Liquid crystal display televisions.
ITO	Indium–tin oxide.
PCB	Printed circuit board.
PDMS	Polydimethylsiloxane.
V_{TH}	Threshold voltage.
IV	Current–voltage.
I_d	Drain current.
V_g	Gate voltage.
V_d	Drain voltage.
V_{gs}	Gate–source voltage.
V_{ds}	Drain–source voltage.
$I_d - V_g$	Drain current–gate voltage.
$g_m - V_g$	Transconductance-gate voltage.
$I_d - V_d$	Drain current–drain voltage.
$I_d$sat	Drain current saturation.
MCS	Multichannel system.
FIR	Finite impulse response.
CE	Counter electrode.
WE	Working electrode.
RE	Reference electrode.
PBS	Phosphate-buffered saline.
pk-pk	Peak-to-peak.
SNR	Signal-to-noise ratio.

I. Introduction

THE wealth of recent research on applications of MEMS in the biomedical field is leading to a new generation of microsystems that give the opportunity to revolutionize

2021 IEEE CPMT Symposium Japan (ICSJ) | 978-1-6654-4079-0/21/$31.00 ©2021 IEEE | DOI: 10.1109/ICSJ52620.2021.9648907

Multi-modal Thin-Film-Transistor Biosensing Platforms for Bio-medical Investigations: Contribution to Internet-of-Medical-Things

Agnès Tixier-Mita
Institute of Industrial Sciences
The University of Tokyo
Tokyo, Japan
agnes@iis.u-tokyo.ac.jp

Tieying Xu
LIMMS/CNRS (IRL 2820)-Institute of Industrial Sciences
The University of Tokyo
Tokyo, Japan
tieying@iis.u-tokyo.ac.jp

Anne-Claire Eiler
Institute of Industrial Sciences
The University of Tokyo
Tokyo, Japan
anne@iis.u-tokyo.ac.jp

Satoshi Ihida
Institute of Industrial Sciences
The University of Tokyo
Tokyo, Japan
ihida@iis.u-tokyo.ac.jp

Hiroshi Toshiyoshi
Institute of Industrial Sciences
The University of Tokyo
Tokyo, Japan
agnes@iis.u-tokyo.ac.jp

Abstract— **The great evolution of device technology, wireless systems, and artificial intelligence is bringing tremendous and deep change in the field of biomedical. This transformation is participating to the Internet of Medical Things revolution. But, biomedical analyses devices are still limited to not portable devices, single analyses technique or poor spatial sensing. In our research, we used Thin-Film-Transistor technology to realize devices with multi-modal sensing possibility, and with high spatial sensing. We report the results obtained with these devices applied to various sensing and manipulation techniques on biological cells, like dielectrophoresis, electrophysiology, bioimpedance, or electrochemistry. It is expected that they participate to development of digital health.**

Keywords—Thin-Film-Transistor Technology, Biosensor, IoMT, Digital health, Multi-modal sensing, Active matrix, Multi-cells culture, Multi-organoid culture.

I. Introduction

The XXIst century is seeing a revolution in the biomedical field in term of diagnostic and investigation tools which will hasten the development of personalized medicine, wearable health devices, homecare and connected health devices [1]. This revolution is first the consequence of the evolution of device technology characterized by miniaturization and integration with electronics for portable and autonomous functioning. Secondly, integration with miniature communication devices is carrying out wireless systems. Thirdly, the progression of artificial intelligence is generating smart systems. In other words, biomedical tools are modernizing based on the maturation of all these elements letting them rush towards the Internet of Medical Things (IoMT) area [2], which is IoT applied to biomedical. The consequence will be faster treatment of the medical information, data exchange easiness, more prevention, and higher flexibility in the investigations (Fig. 1).

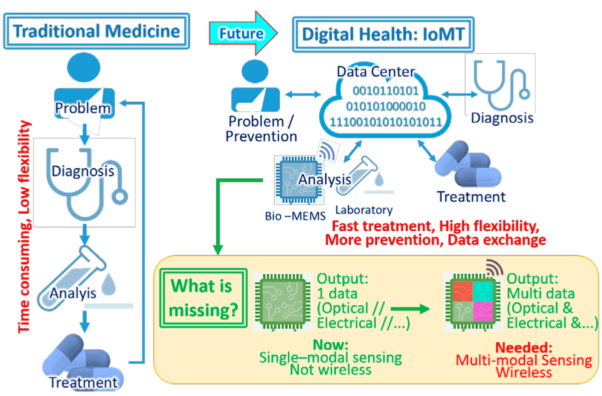

Fig. 1: Evolution of medical procedure: from traditional "water fall" model medicine to IoMT "agile" model medicine. With IoMT, all the elements communicate between them via data center, which stocks commands and data. Wireless multi-modal sensing devices are needed for more efficiency.

This work was supported by the JSPS Core-to-Core Program (A. Advanced Research Network). This work was also supported by the JSPS Challenging Research (Pioneering) no. 21K18869.

The advancement of efficient IoMT devices goes with the evolution of the devices towards multi-modal possibilities, for complex investigations. In that aspect, the platforms developed by Berkley Lights, Inc. are among the most advanced automatic in-vitro analysis and drug discovery tool [3]. However, analyses is performed optically, which prevent the possibility to have accurate sensing and portable tools. As for electrical devices, a great number is already available. But most of them are usually very specific to single application, like glucometers, wearable heart rate sensors or specific disease diagnosis with PCR. It means that systems which combine multi-modal sensing, despite their very attracting possibilities to perform complex analyses, are still in the research phase. Actually, it is still challenging to integrate several sensing elements on the same device due to device spatial limitation, resolution, or incompatibility in the fabrication or analyses techniques. This is particularly true for devices for in-vitro analyses on cell culture.

Our group is using Thin-Film-Transistor (TFT) technology, originally used for Liquid-Crystal-Display (LCD) fabrication, to develop multi-modal devices for in-vitro application,. Substrates with a large area (several centimeter square) covered with high resolution and high density transparent sensors can be obtained with that technology. These thousands of sensors can be specifically dedicated to various sensing applications. We have already demonstrated the possibility to perform: electrophysiology, bio-impedance sensing, electrochemical sensing, and dielectrophysiology on neurons, cardiomyocytes and pancreas cells. These results were obtained with the same TFT-device platform with dedicated instrumentation for each technique.

II. The Thin-Film-Transistor Device Platform

TFT technology has more than 50 years history and has been mainly used until now in the fabrication of LCD. With

978-1-6654-4079-0/21/$31.00 ©2021 IEEE

IOP Publishing
Journal of Micromechanics and Microengineering
J. Micromech. Microeng. **31** (2021) 115002 (7pp)
https://doi.org/10.1088/1361-6439/ac2547

Toward the development of a label-free multiple immunosensor based on thin film transistor microelectrode arrays

Dongchen Zhu[1], Grant A Cathcart[2], Satoshi Ihida[2], Hiroshi Toshiyoshi[2], Agnès Tixier-Mita[2], Yasuyuki Sakai[1] and Kikuo Komori[1,3,*]

[1] Chemical System Engineering, The University of Tokyo, Hongo, Bunkyo-ku, Tokyo 113-8656, Japan
[2] Institute of Industrial Science, The University of Tokyo, Komaba, Meguro-ku, Tokyo 153-8505, Japan
[3] Department of Biotechnology and Chemistry, Kindai University, Takaya-Umenobe, Higashi-Hiroshima 739-2116, Japan

E-mail: komori@hiro.kindai.ac.jp

Received 19 June 2021, revised 12 August 2021
Accepted for publication 9 September 2021
Published 28 September 2021

Abstract

A label-free immunosensor using thin film transistor microelectrode arrays (TFT-μEAs) derived from flat-panel technology has been developed for the first time. The TFT-μEAs used here incorporate a large sensing area of 15 mm $\times$ 15 mm with a 150 $\times$ 150 array of transparent indium tin oxide (ITO) electrodes placed at a 100 μm pixel pitch. Anti-human serum albumin (HSA) IgG was characterized to be immobilized on functionalized ITO electrodes. HSA, which is one of the indexes for liver functions, was successfully detected by recording the change of real-time current based on the change in the electric double layer capacitance before and after conjugation of HSA with anti-HSA IgG. Ionic strength and pH value of HSA solution were optimized. In 0.01 mM phosphate buffered saline with pH 6.0, linear range of HSA was determined as 0.3–300 pM. The present TFT-μEAs are applicable to a label-free multiple immunosensing by patterning antibodies on its surface.

Keywords: thin film transistor, microelectrode array, immunosensor, biosensing

(Some figures may appear in color only in the online journal)

1. Introduction

Nowadays, thin film transistor (TFT) technology is broadly applied in manufacturing liquid crystal displays (LCDs), such as computers and smart phones. TFT microelectrode arrays (TFT-μEAs) can therefore be fabricated on various substrates including glass and plastic ranging in the size from mm^2 to m^2 [1]. Additionally, TFT-μEAs is superior to complementary metal oxide semiconductor (CMOS) electrode arrays in terms of large surface area and transparency [2], where the former is essential to multi-analyte detection and the latter is useful for precise optical observation [1].

Recently, the research group of the authors has got interest in using the TFT technology for biological applications, such as electrophysiology, cells culture monitoring by impedance sensing and bio-sensing [3–5]. Actually, when compared to commercial MEAs with 64 electrodes per chip in general, TFT-μEAs are advantageous in higher electrode density with about 1.2 $\times$ 10^4 electrodes cm^{-2} (50–100 μm pitches and ~5 μm spacing between neighboring electrodes) to avoid misaligning with cells, size of which is about 10–20 μm in diameter [6, 7]. Taking the advantage of large surface area, higher electrode density and optical transparency, Tixier-Mita *et al* have successfully detected the presence of living yeast cells on the TFT-μEAs by measuring impedance variation and microphotographs simultaneously [1]. Moreover, Bakkum *et al* have conducted a two-dimensional mapping

[*] Author to whom any correspondence should be addressed.

Real-time Simultaneous Measurement of Pancreatic β Cell Electrophysiology and Fluorescent Bioimaging Based on High-resolution Thin-film Transistor Microelectrode Arrays

——薄膜トランジスタアレイを用いた膵β細胞の電気生理学マッピングと蛍光バイオイメージングのリアルタイム同時計測——

Dongchen Zhu* (The University of Tokyo), Anne-Claire Eiler (The University of Tokyo), Satoshi Ihida (The University of Tokyo), Yasuyuki Sakai (The University of Tokyo), Hiroshi Toshiyoshi (The University of Tokyo), Agnès Tixier-Mita (The University of Tokyo) and Kikuo Komori (Kindai University)

Abstract Real-time electrophysiological monitoring and simultaneous fluorescent bioimaging for glucose-stimulated insulin secretion dynamics of pancreatic β cells were presented, for the first time, using Thin-Film-Transistor-microelectrode arrays (TFT-μEAs). TFT-μEAs employed in this work are designed based on the switch matrix architecture, which incorporates a large sensing area (15.6 mm × 15.6 mm) with a 150 × 150 array of indium-tin-oxide (ITO) microelectrodes placed at a 100 μm pixel pitch. Pancreatic β cells were cultured on functionalized ITO microelectrodes then characterized. Real-time action potentials of pancreatic β cells stimulated by 15 mM glucose were successfully monitored. Our biosensor exhibited similarity to those exploiting multielectrode array (MEA) in recording extracellular voltage. These results are the first step towards the development of a multimodal TFT-μEAs device for simultaneous electrophysiology, biochemical and optical analyses of pancreas islets. TFT-μEAs are extremely promising platforms in the biosensor research field for the development of multi-modal sensing and analyses of multi-organ-on-chip.

Keywords: Thin film transistor, Microelectrode array, Pancreatic β cell.

1. INTRODUCTION

As the functional unit of the pancreas, islets of Langerhans play an vital role in regulating glycaemia by secreting insulin at the right moment and in appropriate amounts. Dysfunction of the insulin-secreting β cells perturbs glucose homeostasis, leading to life-threatening hypoglycaemia due to excessive insulin secretion or to damaging hyperglycaemia owing to insufficient insulin secretion [1][2]. To elucidate the pathophysiology of islet-related diseases, new approaches are being employed to study islets at the cellular level.

The electrophysiology of pancreatic β cells has been investigated using a patch-clamp technique [3]. Kanno et.al have investigated the relugation of K^+ current in the presence of 10 mM glucose by applying perforated patch-clamp to mouse pancreatic iselets [4]. However, patch-clamp technique is invasive to cells with complex operation. Moreover, it is difficult to record long-term electrophysiology of pancreatic β cells for hours using patch clamp technique [5]. Multielectrode array (MEA), on the other hand, have been employed to record electrical activities of islets during insulin secretion [6]. Pfeiffer et.al have detected burst and interbusrt phase of membrane potential oscillations using MEAs and correlated length of burst phase with the amount of insulin release [7]. Owing to low density and numbers of electrodes, two-dimensional analysis of tissues with larger diameter using MEAs is difficult.

Thin-film-transistor microelectrode arrays (TFT-μEAs), as a microelectromechanical system originating from flat panel display technology, offer an new category of transducers with much wider sensing possibilities. Taking the advantage of large surface area, higher electrode density and optical transparency, Tixier-Mita et al. have successfully detected the presence of living yeast cells on the TFT-μEAs by measuring impedance variation and microphotographs simultaneously [8]. Moreover, Cathcart et al. have conducted a two-dimensional mapping analysis for cell viability and function using human-derived cells, such as human hepatocarcinoma cell line Hep G2, by impedance variation simultaneously with microscopic observation of fluorescent imaging on the transparent TFT-μEAs [9]. Furthermore, real-time extracellular potential measurement for cardiomyocytes and neural cells was also performed with similar devices toward the application to electrophysiological research [10][11]. It offers an alternative to MEA and complementary metal oxide semiconductor (CMOS) for characterizing two-dimensional analyses of cardiomyocytes and neural cells on a large surface, with using high resolution and a dimension of pixels is as small as few cells. Therefore, the TFT-μEAs can serve as one of the powerful biosensing devices. However, pancreatic β cell-based biosensors using TFT-μEAs have never been investigated regardless of their fruitful future in high-resolution electrophysiological measurement simultaneous with biological assays.

In this work, we present for the first time real-time electrophysiological monitoring and simultaneous fluorescent bioimaging for glucose-stimulated insulin secretion dynamics of pancreatic β cells using Thin-Film-Transistor-microelectrode arrays

A Matlab Spiking Sorting Algorithm for Data Processing of In-Vitro Cardiomyocyte Electrophysiology with a Thin-Film-Transistor Platform

Pierre-Marie Faure*, Anne-Claire Eiler**, Satoshi Ihida**, Junichi Sugita**, Katsuhito Fujiu**, Hiroshi Toshiyoshi**, Agnès Tixier-Mita**

*ENSEIRB-MATMECA, Bordeaux, France, ** The University of Tokyo, Tokyo, Japan

Abstract:

The paper presents a Matlab Spiking Sorting Algorithm which was developed to process data of cardiomyocyte cells electrophysiology activity, cultured on a locally-addressable 2-dimensional arrayed transparent electrode platform with integrated Thin-Film-Transistor. An array of 28x28 microelectrodes was selected from the 22,500 (150x150) microelectrodes of the platform for measurement. Such large data cannot be processed using available software of the data acquisition system used. This algorithm includes specific functions adapted to the TFT platform functioning and can be applied also to larger TFT electrode arrays.

TFT platform description:

For in-vitro electrophysiology area, Multi-Electrode Array (MEAs) still remains the device of reference [1]. However, it is essentially dedicated to mono-cells culture, because the sensing area is small (mm size). Our research group proposes to use Thin-Film-Transistors technology, already employed to fabricate Liquid-Crystal display (Fig. 1), to develop devices with large surface (cm size) and fine resolution of microelectrodes for biological application [2]. In-vitro culture of multi-cells, tissues or organoids can then be performed and applied to investigate cellular communication [3].

The TFT platform consists in a transparent TFT array substrate mounted on a hollowed PBC for simultaneous observation with an inverted microscope. The TFT array substrate consists in a large and dense array of transparent Indium Tin Oxide (ITO) microelectrodes fabricated on top of a glass substrate. The ITO microelectrode array is individually addressable integrated TFT switch. The source terminal of each TFT is connected to an ITO electrode. Gate terminals are column-parallel connected, and Drain terminals are row-parallel connected. By applying a potential (12V) to one Gate column, all transistors connected to that column are turned on. When a data acquisition system is connected to a perpendicular drain line, the signal at the intersection electrode can be measured. For 2D measurement, the gate lines are scanned successively. The data obtained at each drain line include then the data of all electrodes of that drain line, concatenated successively, for each gate line switch.

Algorithm description and results:

The 3 first steps of the program algorithm (Fig. 3) consist in: 1) reading the raw data file containing the data of all 28x28 microelectrodes measured during 5s; 2) separate in different files the data for each drain line; 3) extract the information for each electrode in each drain line. The data of each electrode can be easily recognized as they are placed in between the two commutation peaks when gates switch ON then OFF. Then the data are filtered with a band-pass digital FIR filter. This filter has symmetrical coefficients which do not disturb too much the signal thanks to a constant group delay. Then the spikes are recognized and their amplitude, type (positive, negative, both) and period are characterized. At the end, the results are both stored in an Excel file and displayed by heat-map graphs as on Fig. 4. Fig. 5 presents a close view result: on the right the raw data are overlaid on a microscope photo of the culture (10x lens), and the results obtained with the algorithm are on the right. All these data are very coherent together showing the efficiency of that algorithm